



Visible light emission and metal-semiconductor transition in single walled carbon nanotube-noble metal nanoparticle composites

T. Pradeep

Department of Chemistry and Sophisticated Analytical Instrument Facility
Indian Institute of Technology Madras
Chennai 600 036

<http://www.chem.iitm.ac.in/professordetails/profpradeep/index.php>

ICONSAT 2008, February 27-29, Chennai



Acknowledgements

C. Subramaniam

Collaborators

T. Ogawa, Institute of Molecular Science, Okazaki

J. Chakrabarti, SN Bose Centre, Kolkata

Chandrabhas Narayana, JNCASR, Bangalore

Nanoscience and Nanotechnology Initiative of the DST



**Confocal Raman
Microscope**



Transmission Electron Microscope



MALDI TOF MS

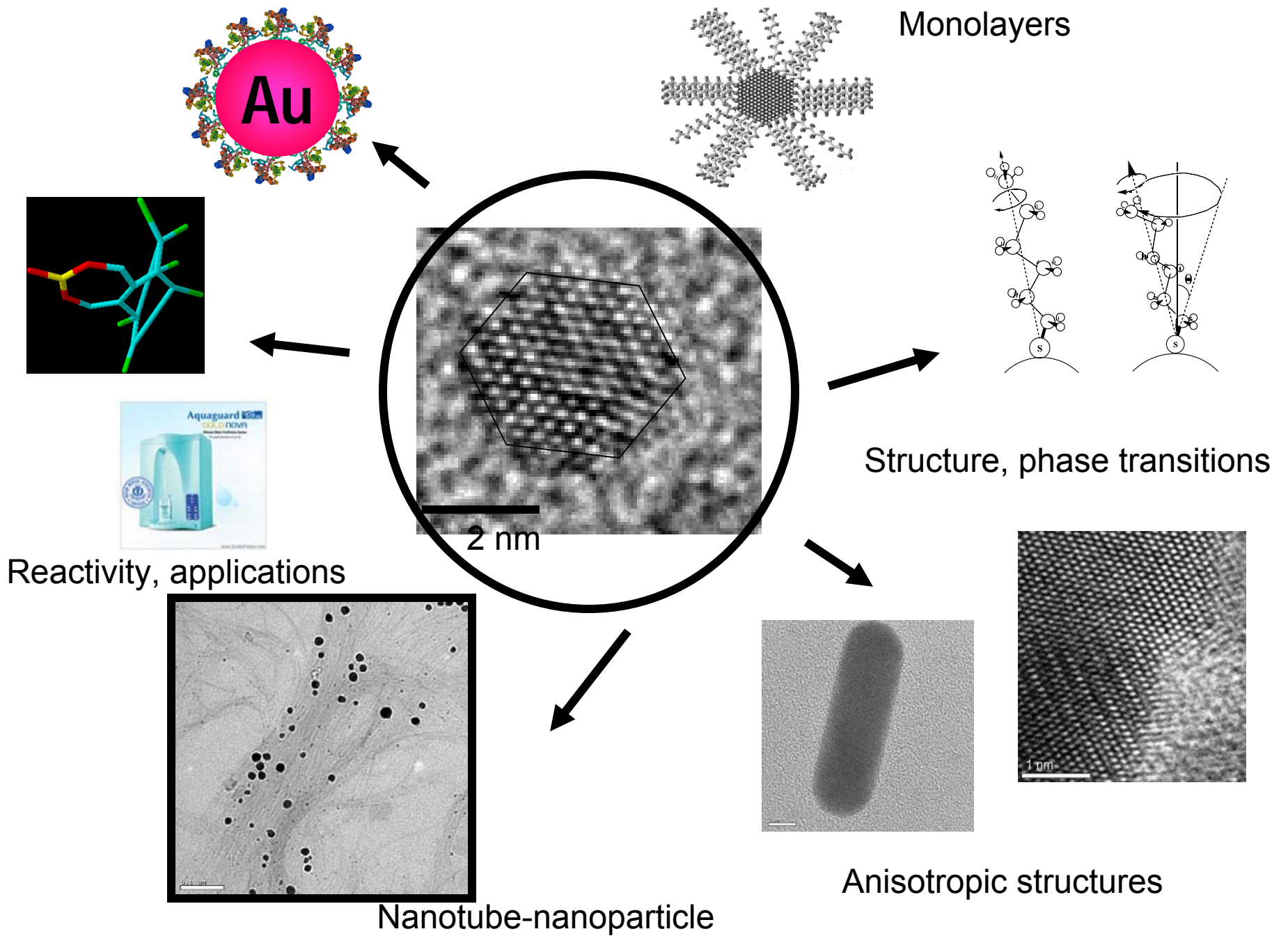


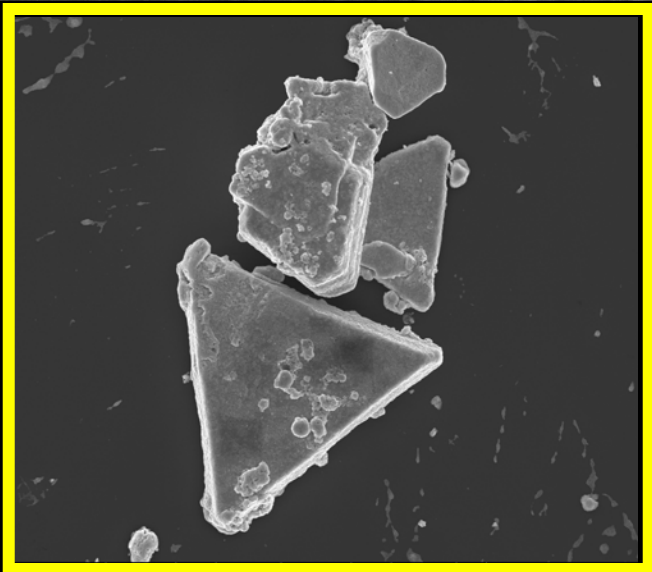
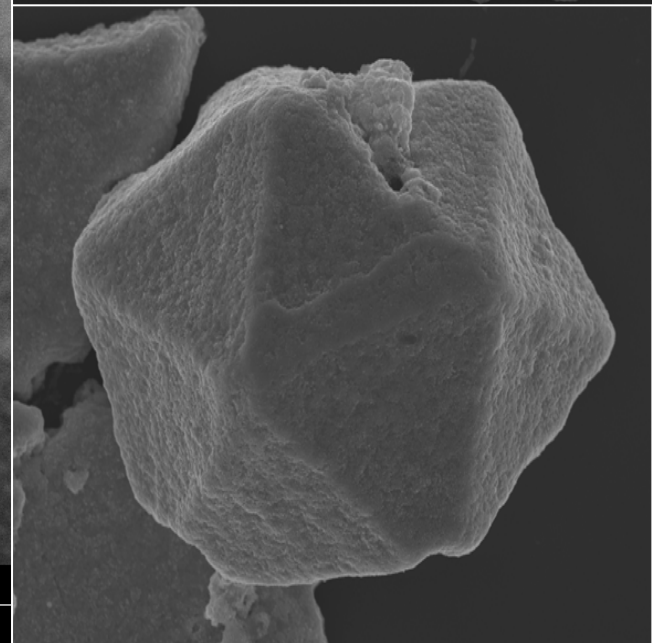
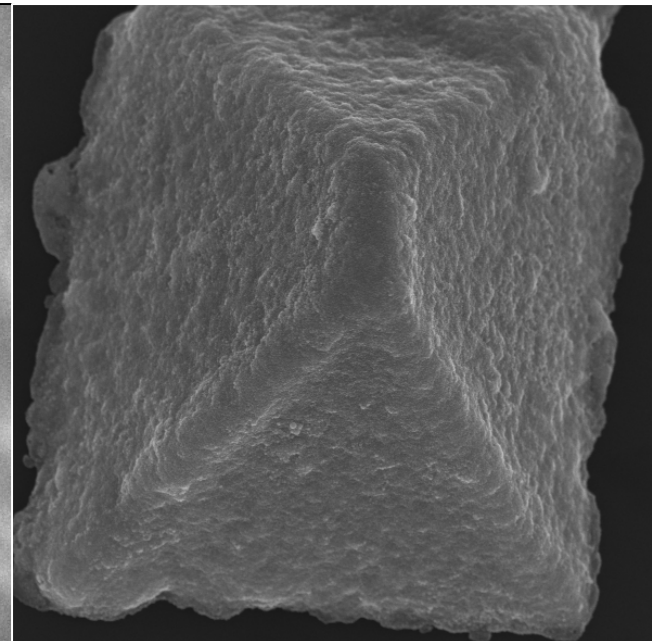
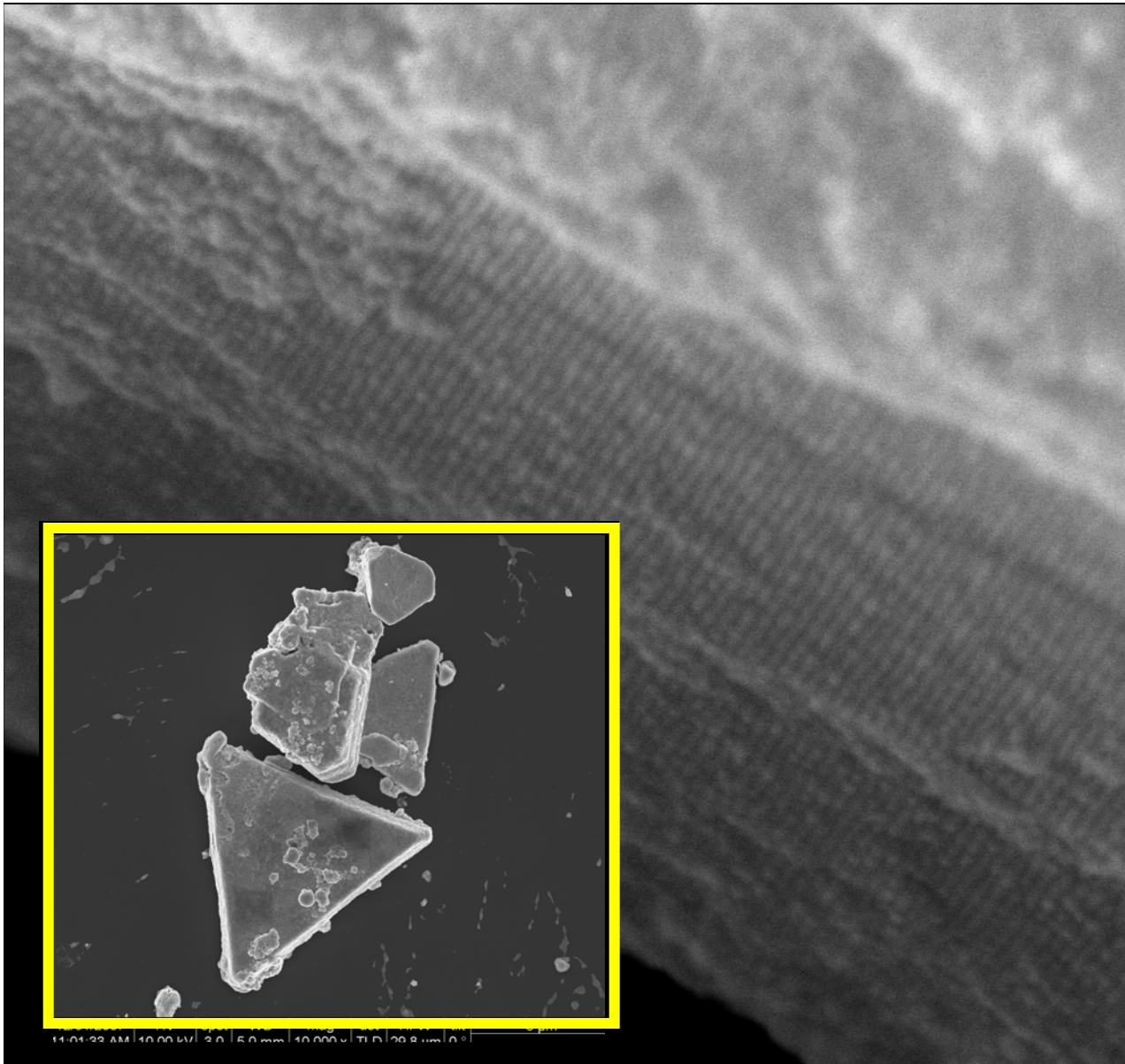
QTrap MS



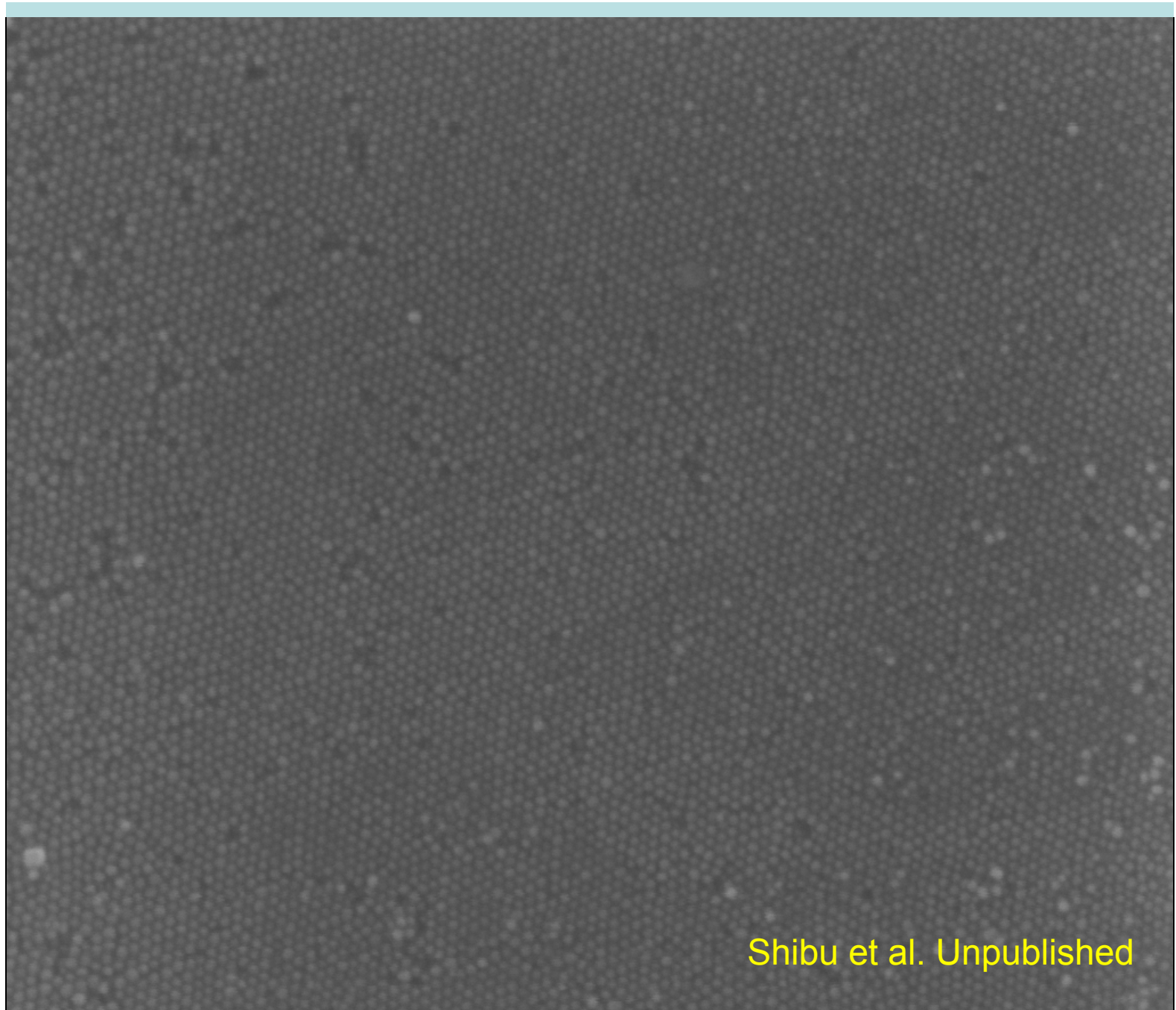
Ultramicrotome

Nanoscience and Nanotechnology Initiative of the DST



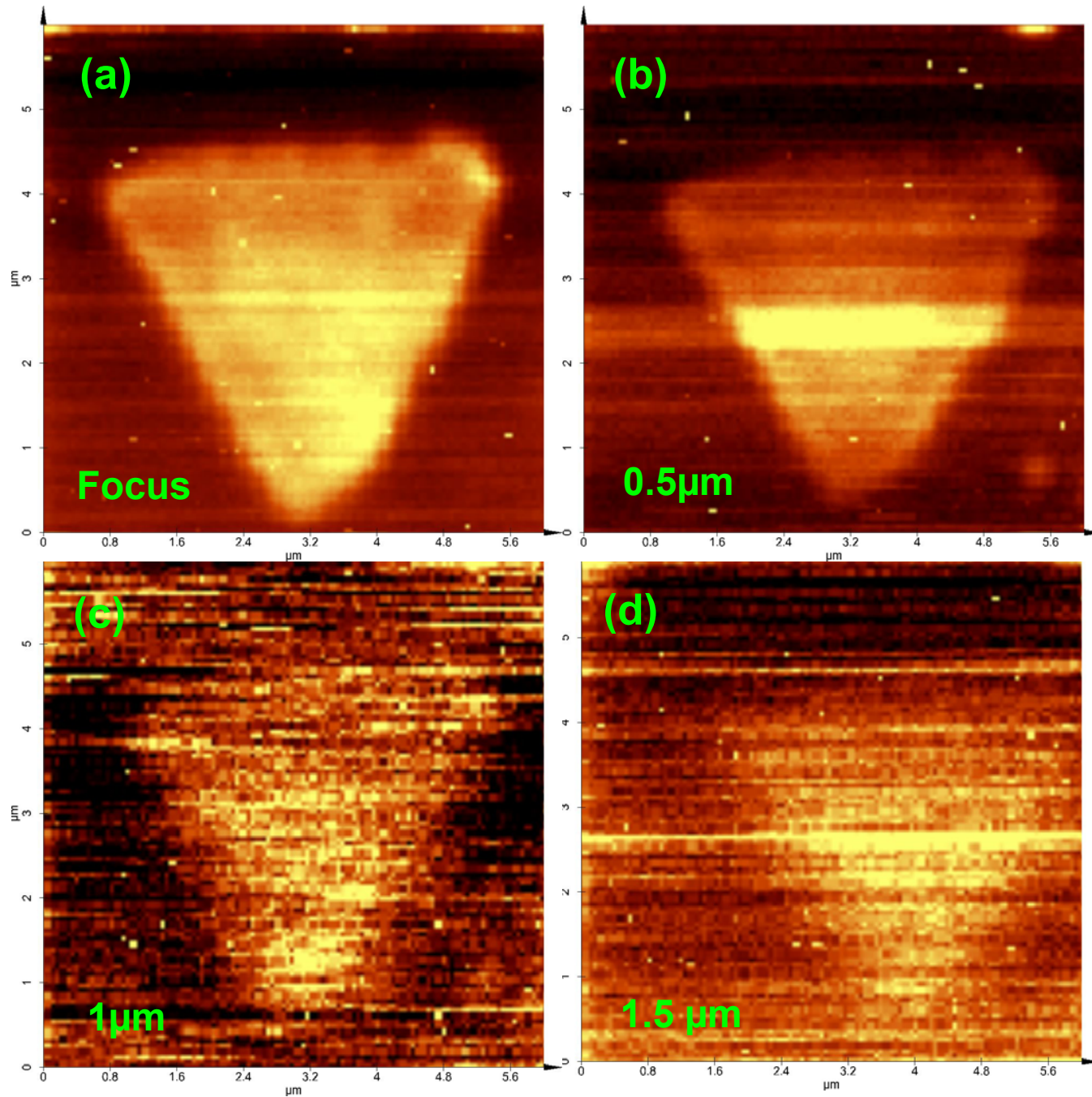


12/31/2007 | HV | spot | WD | mag | det | HFW | tilt | — 100 nm —
10:46:27 AM | 15.00 kV | 3.0 | 5.0 mm | 400 000 x | TLD | 746 nm | 45 °

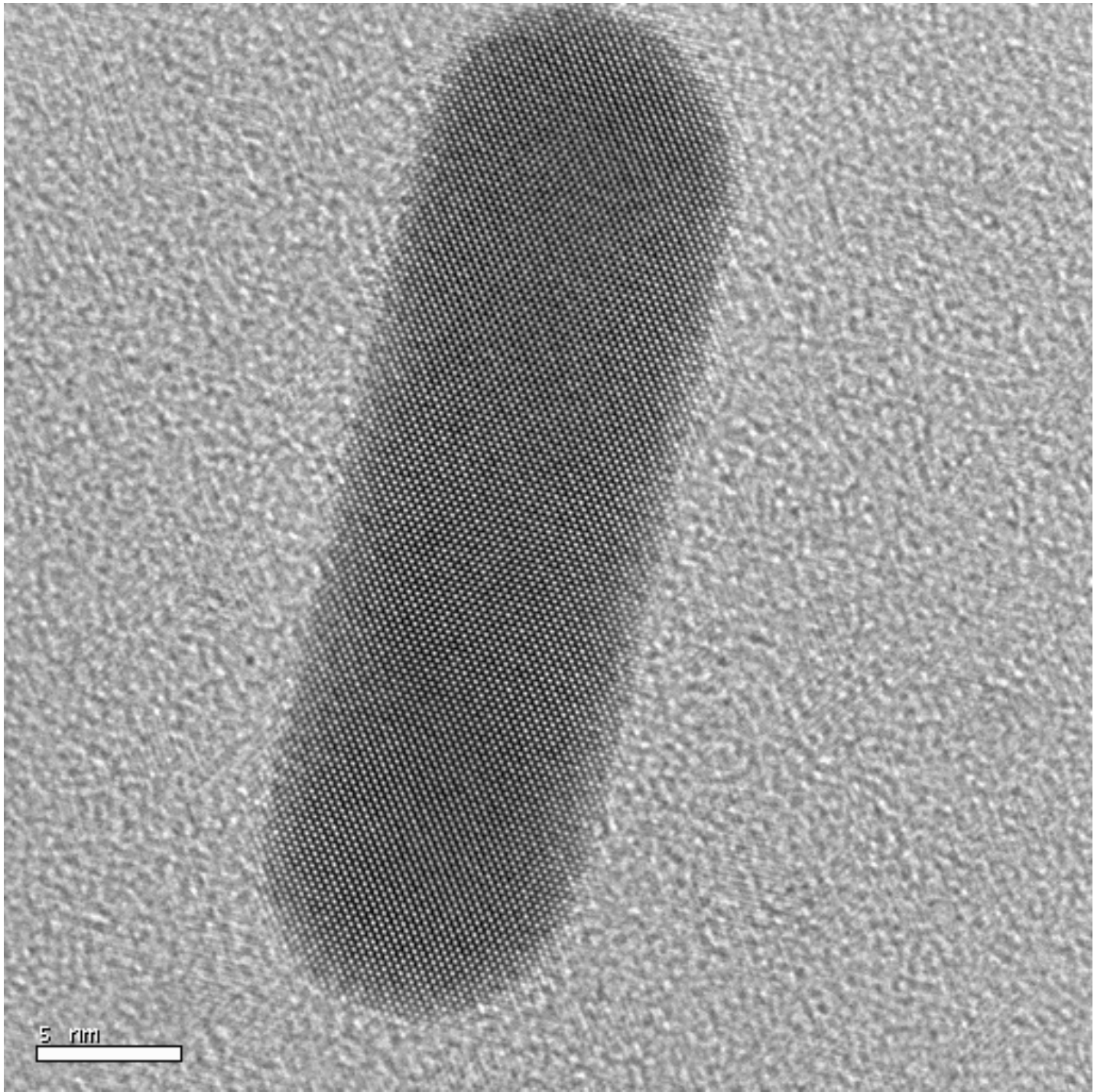


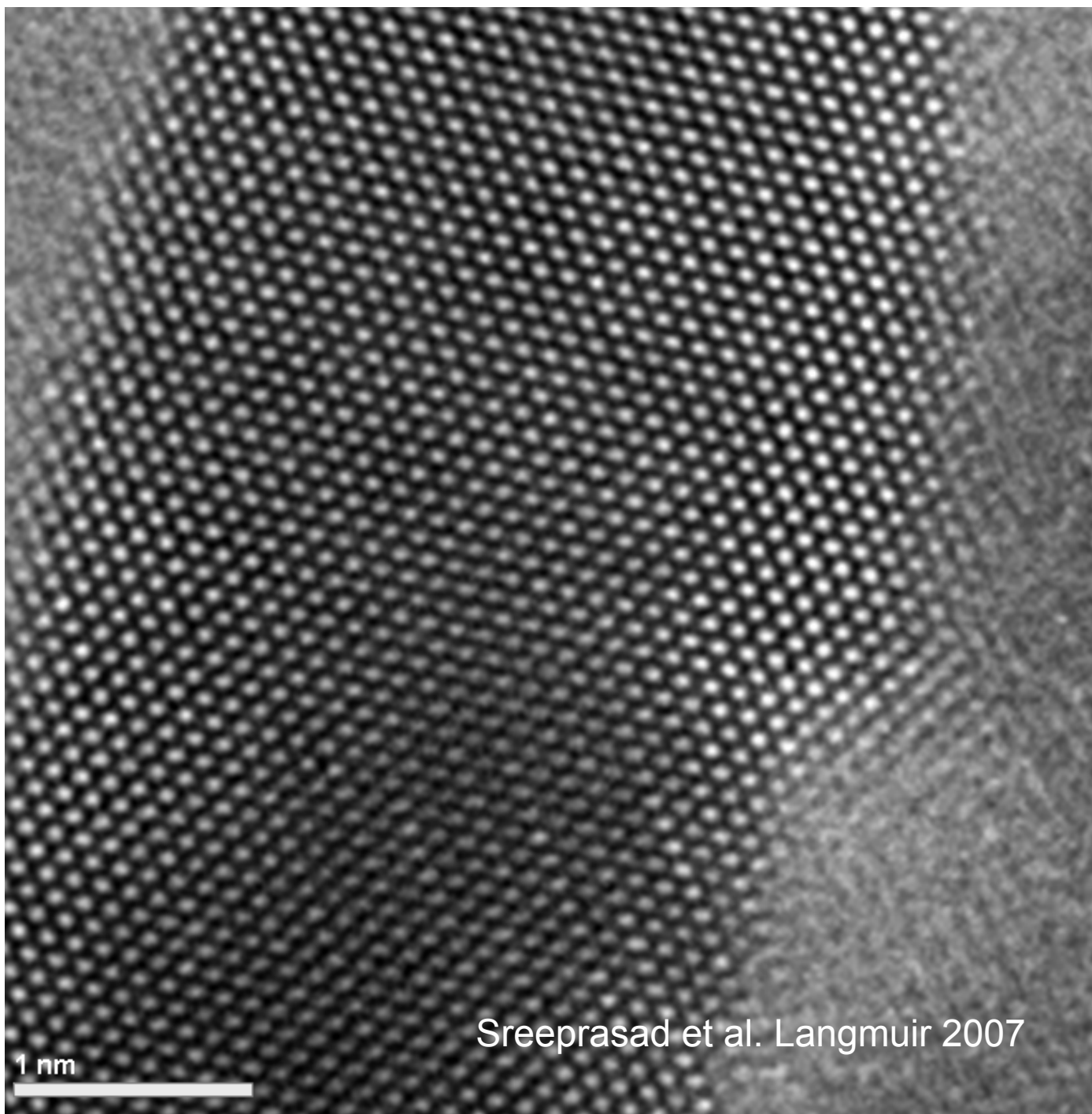
Shibu et al. Unpublished

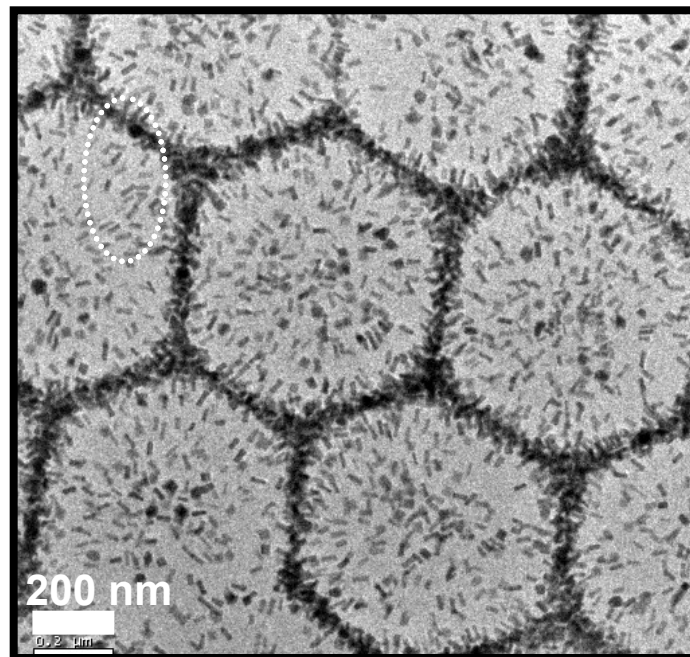
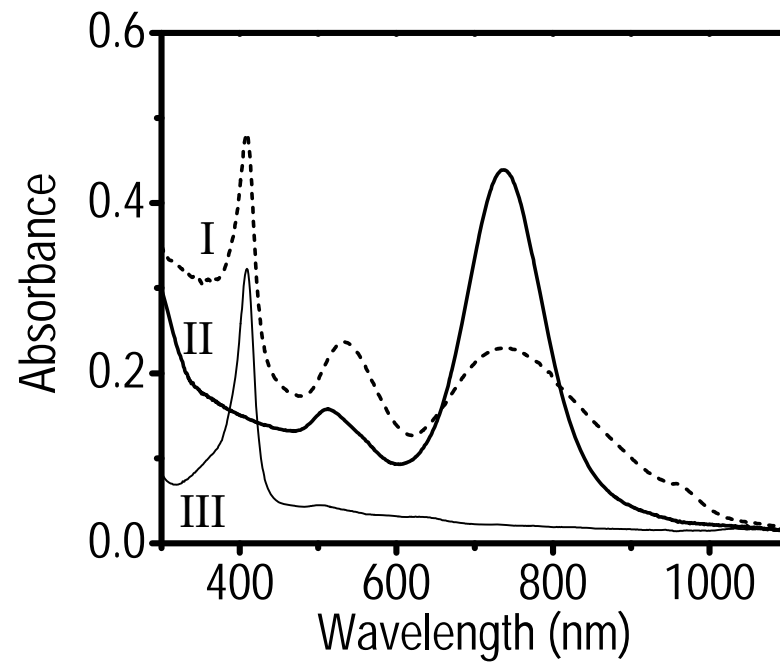
1/17/2008	HV	spot	WD	mag	det	HFW	tilt	← 200 nm →
3:54:06 PM	14.00 kV	3.5	4.5 mm	290 000 x	TLD	1.03 μ m	10 $^\circ$	

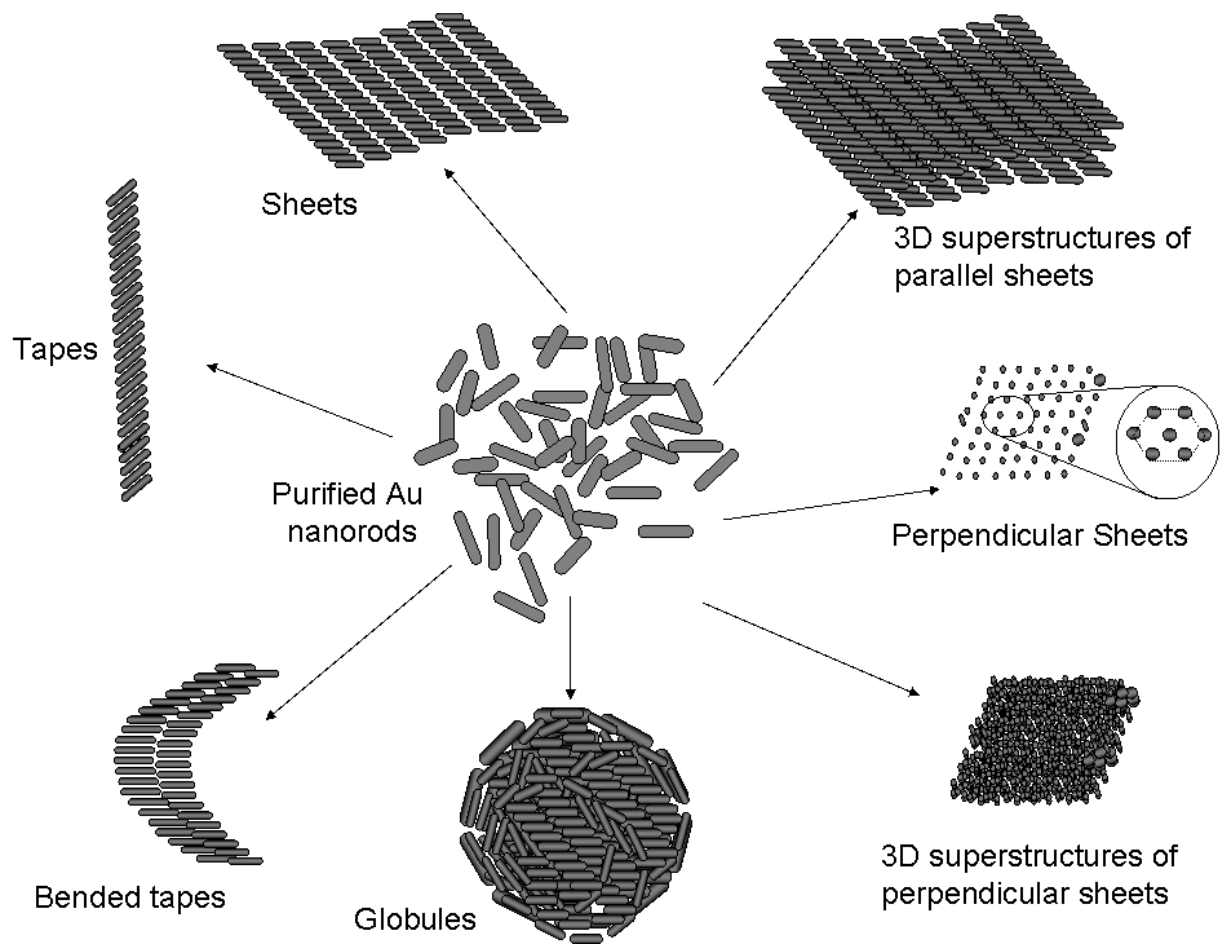


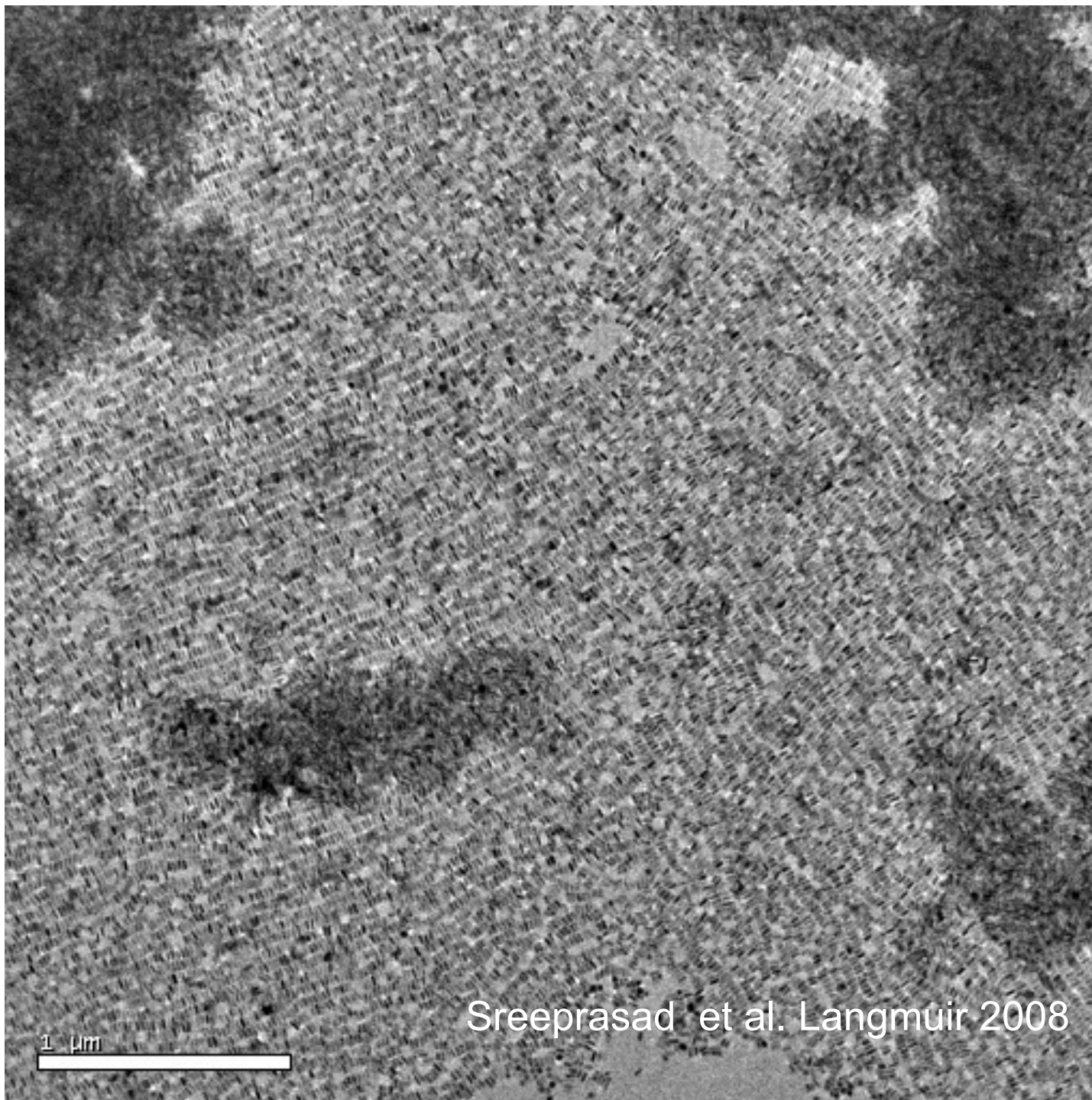
With K. Kimura, Hyogo University ⁷



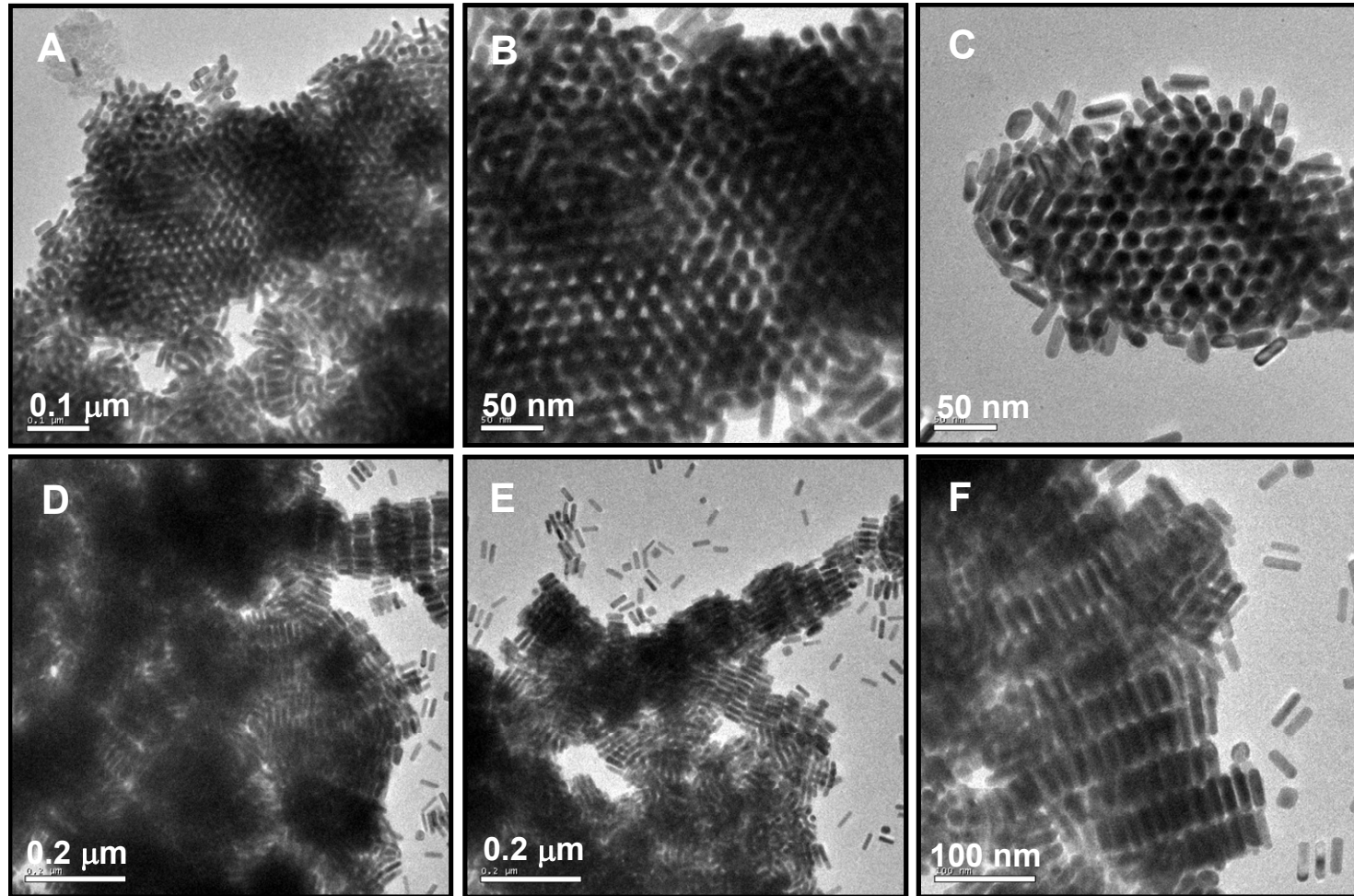


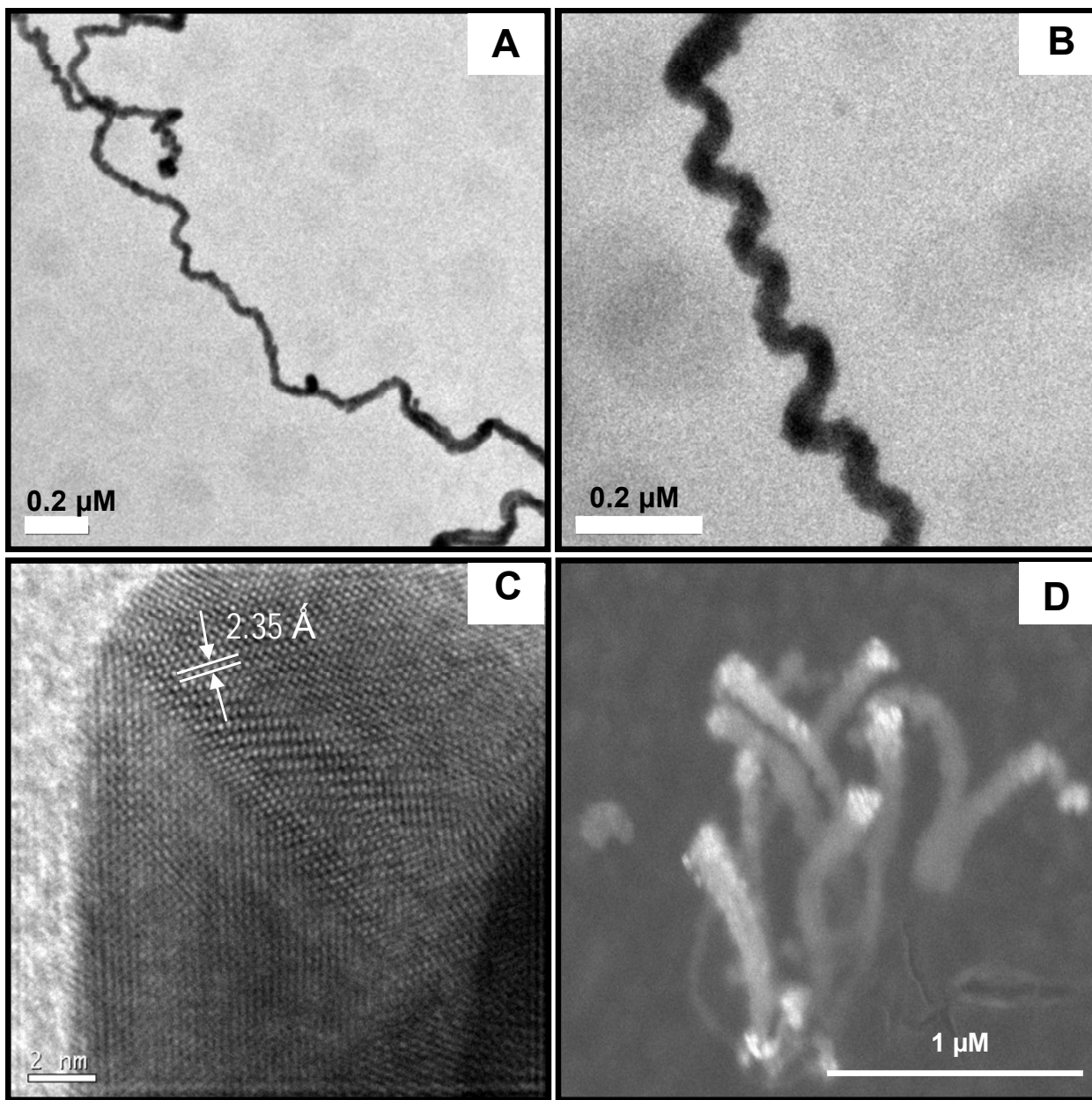


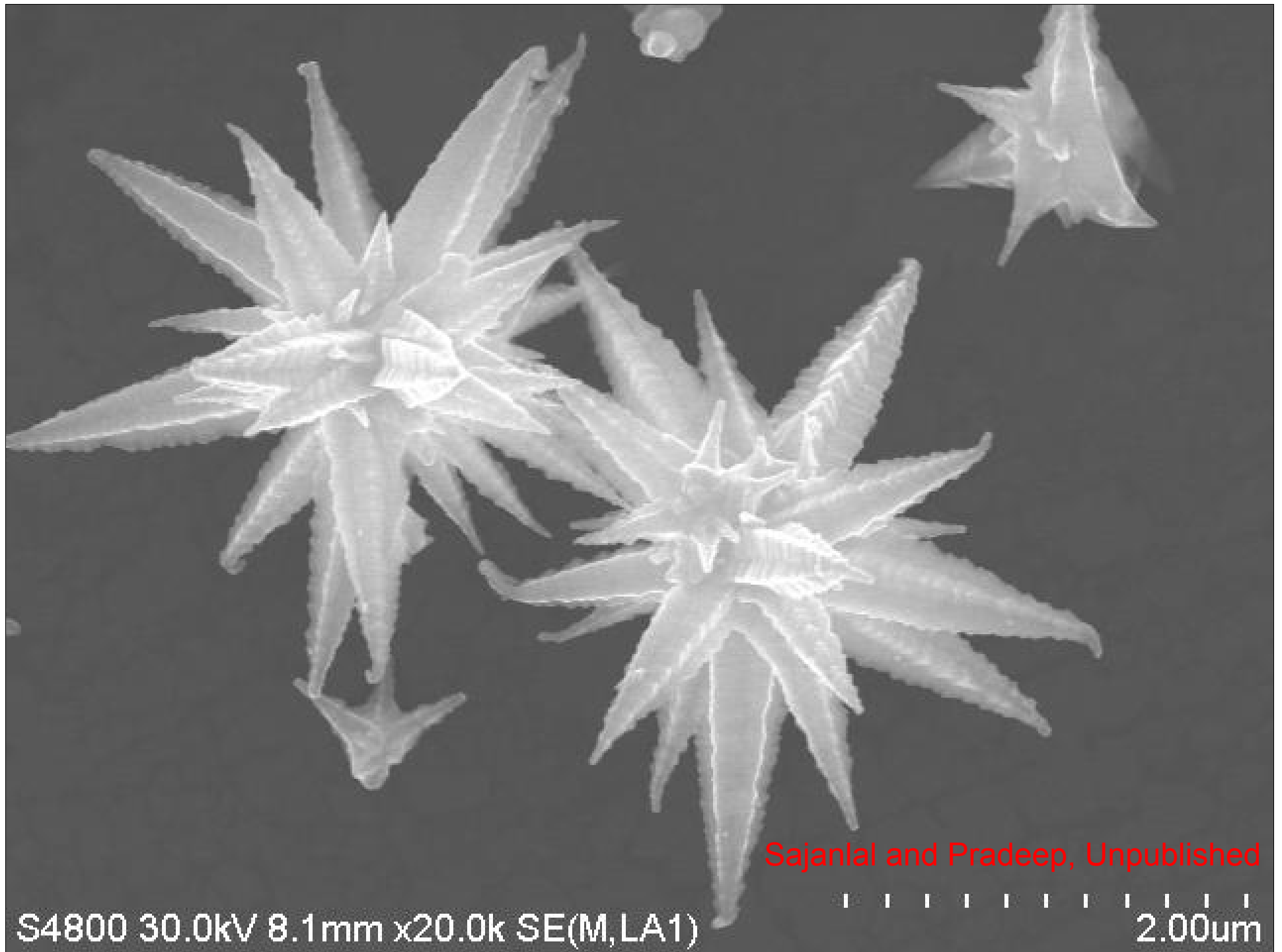




Sreeprasad et al. Langmuir 2008



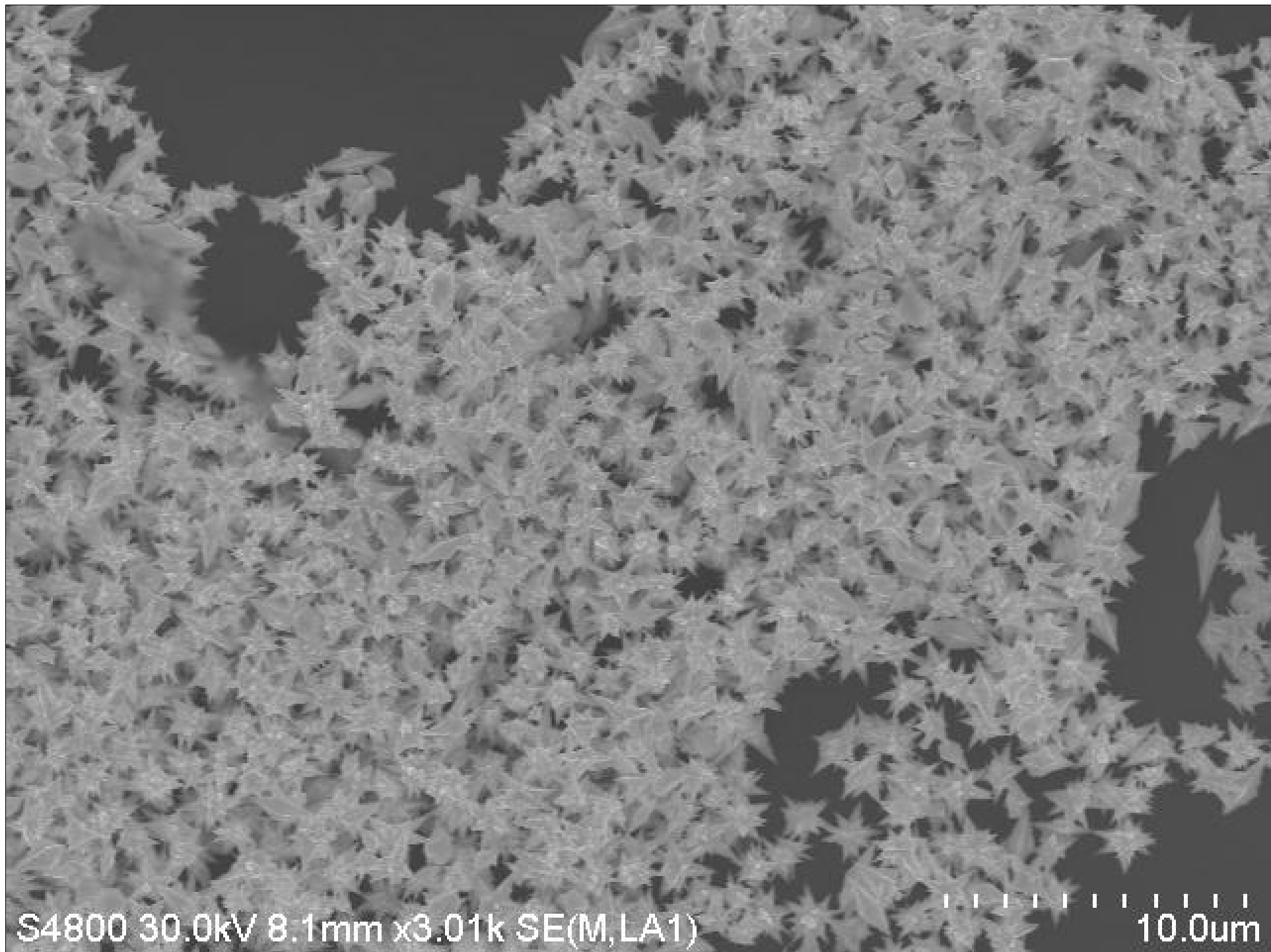


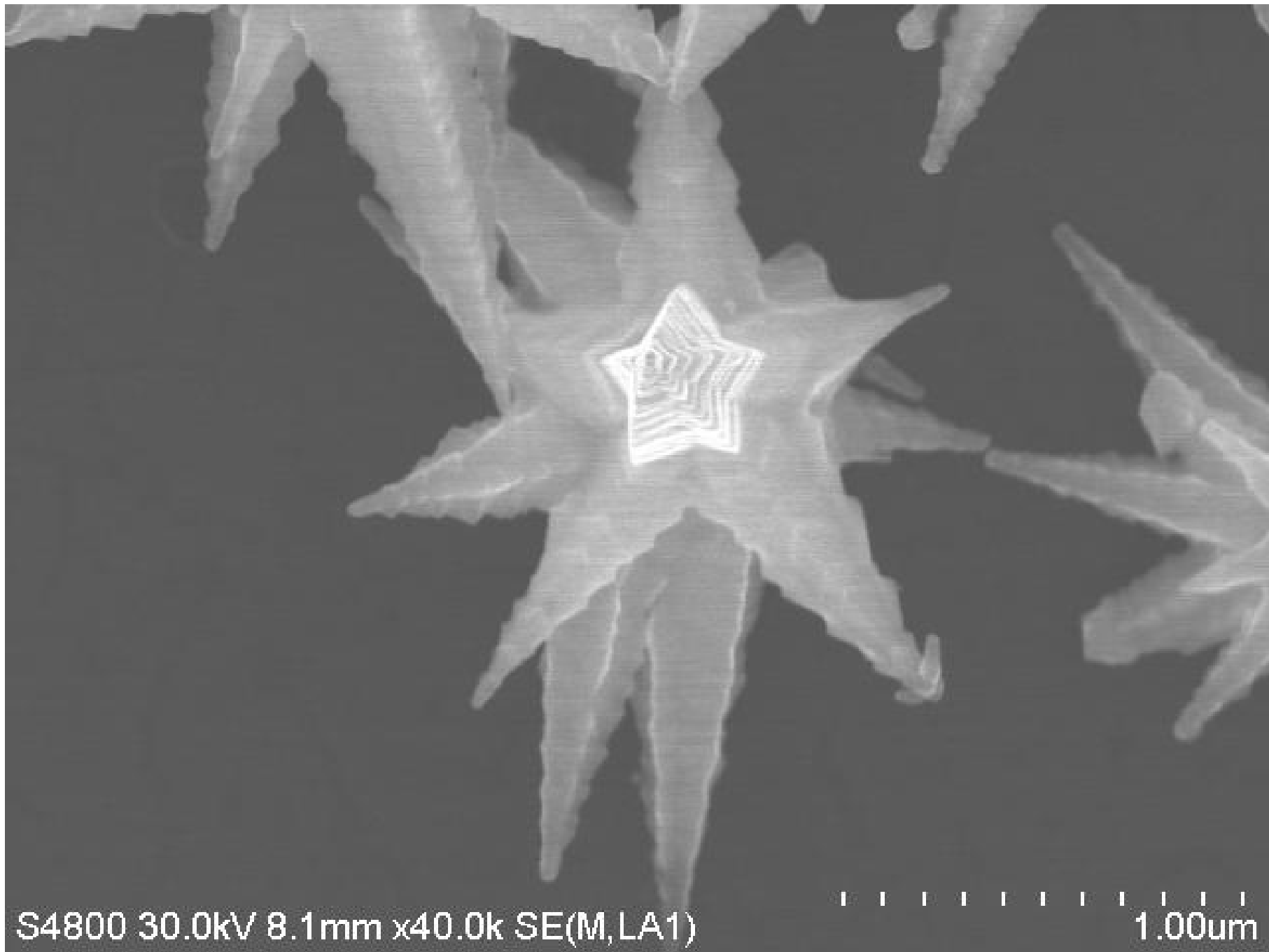


Sajanlal and Pradeep, Unpublished

S4800 30.0kV 8.1mm x20.0k SE(M,LA1)

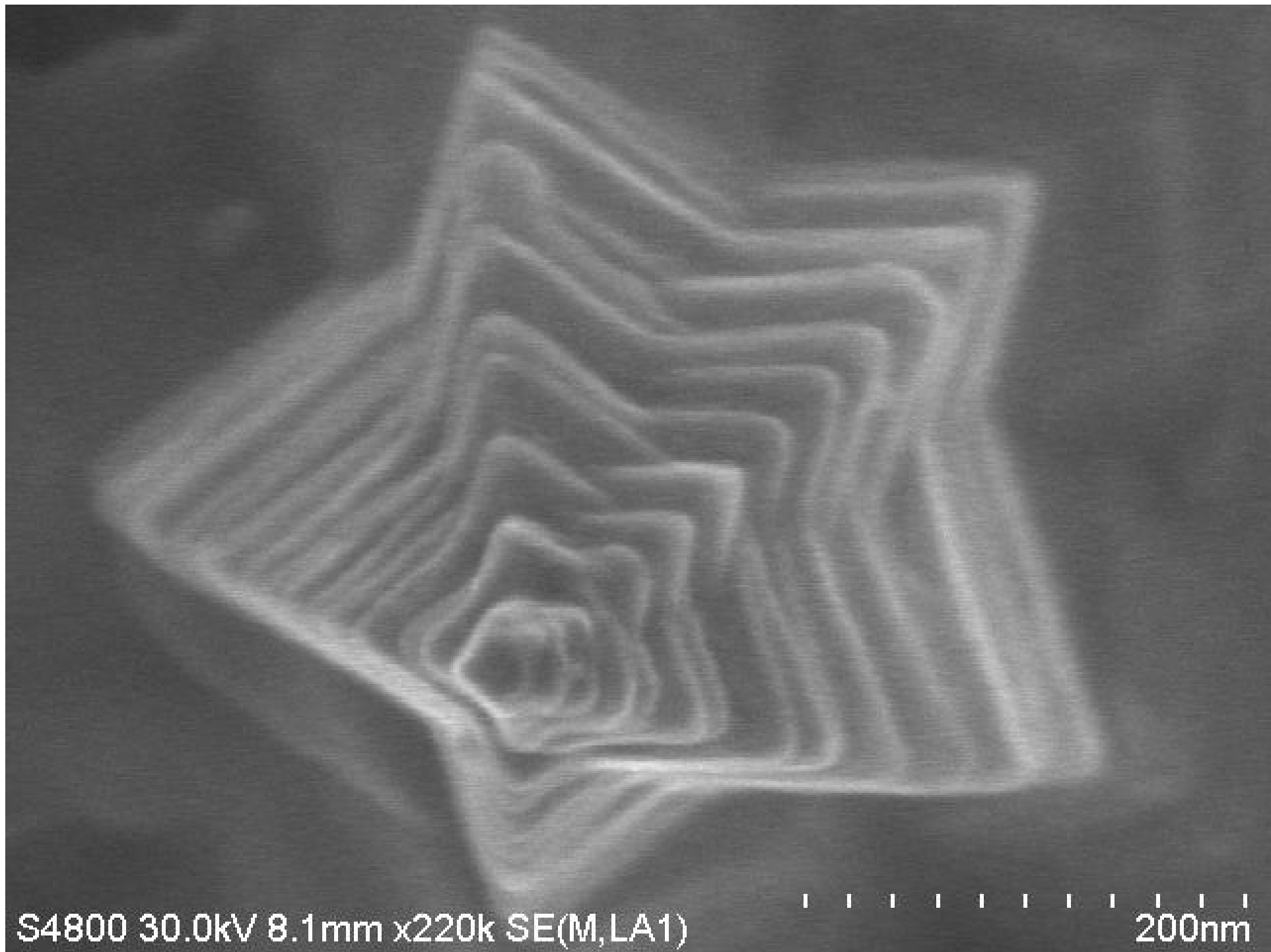
2.00um





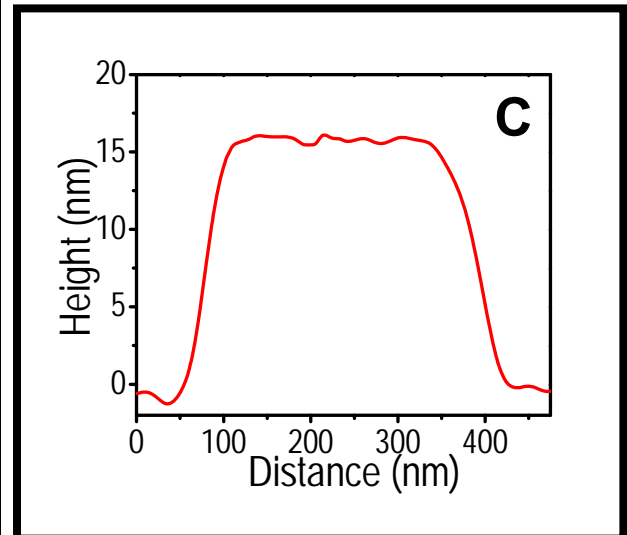
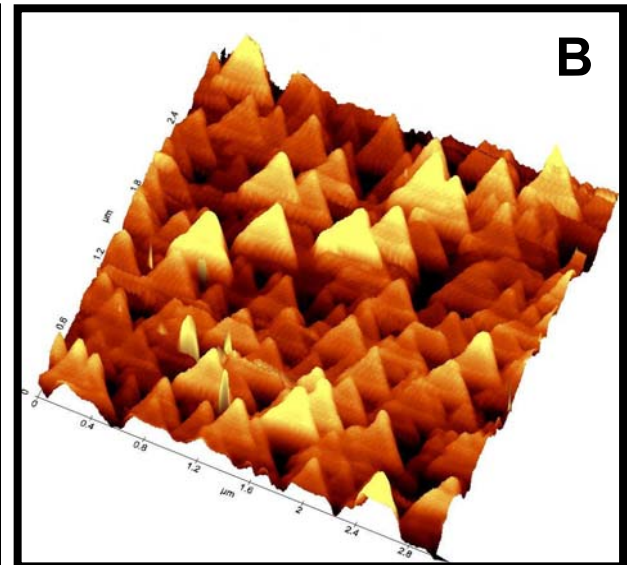
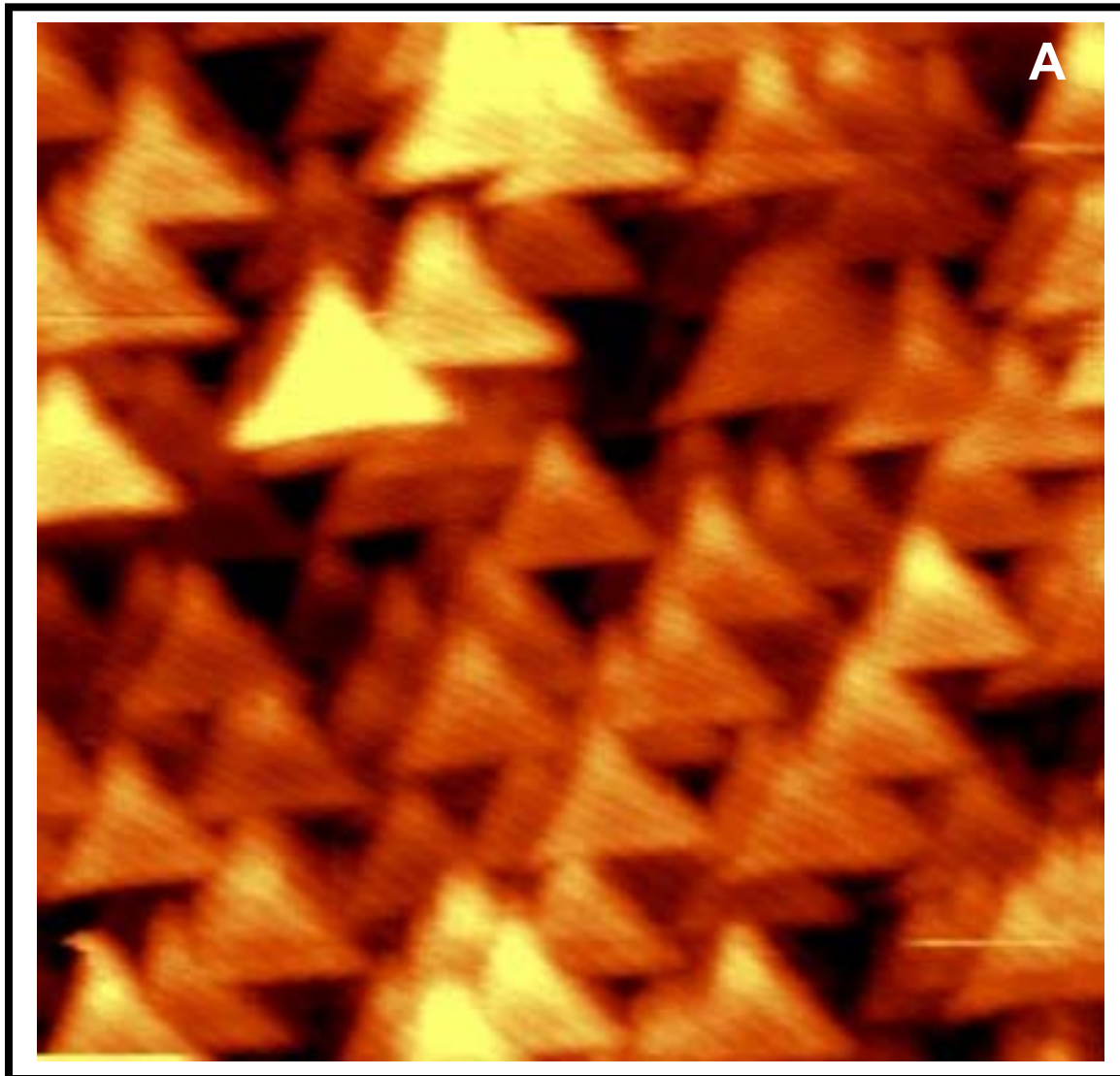
S4800 30.0kV 8.1mm x40.0k SE(M, LA1)

1.00um

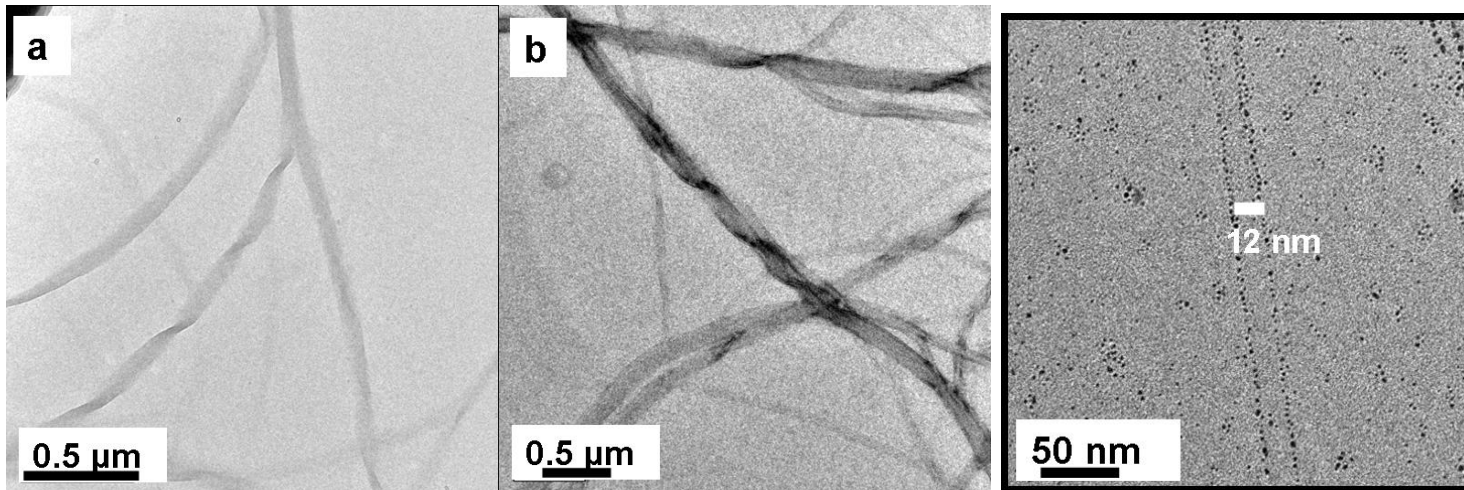
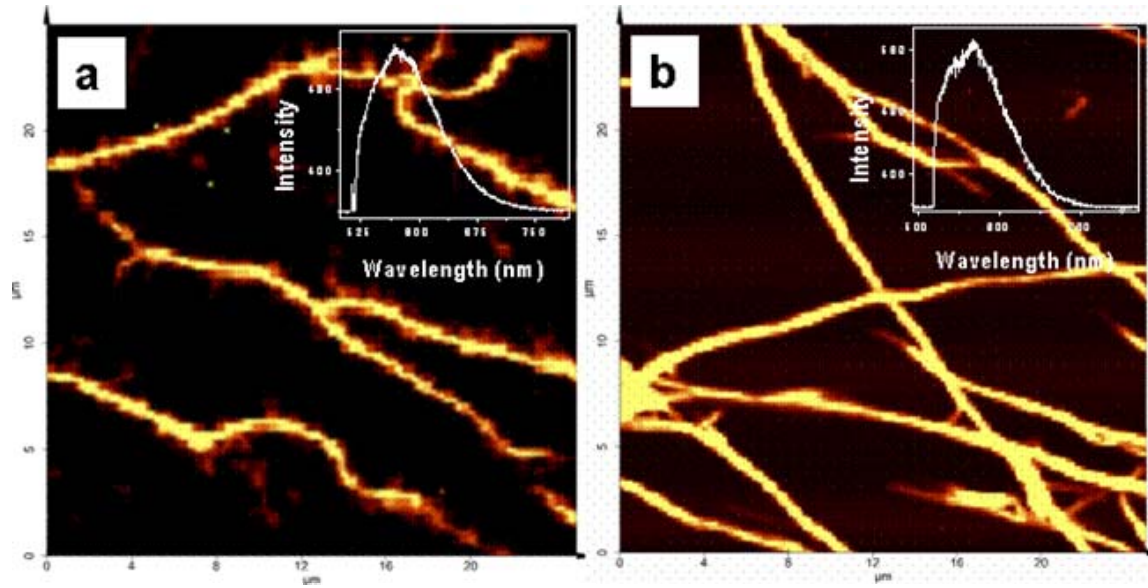


S4800 30.0kV 8.1mm x220k SE(M,LA1)

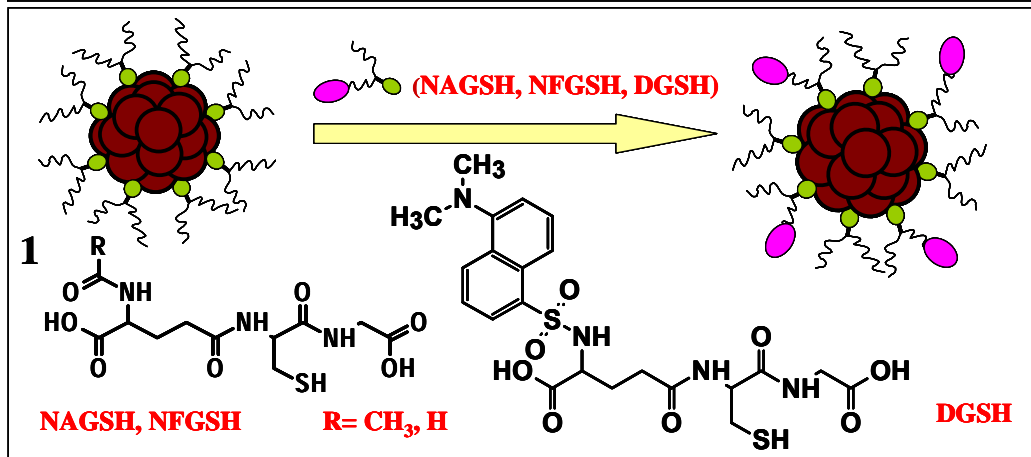
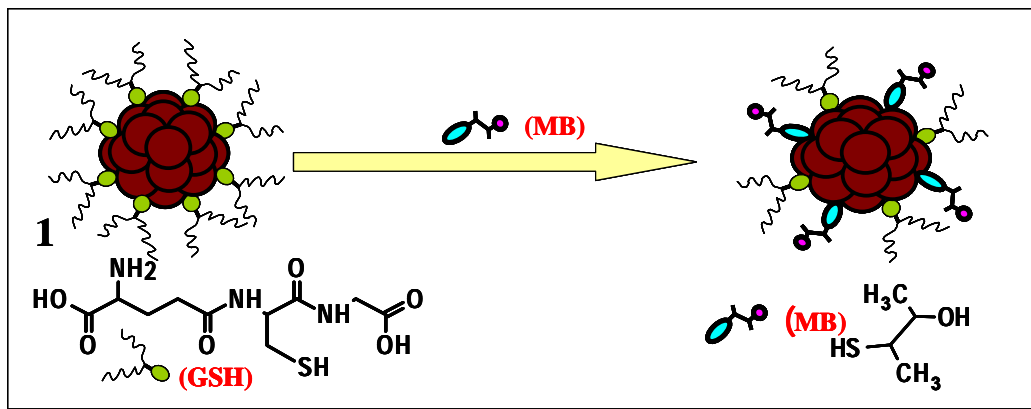
200nm

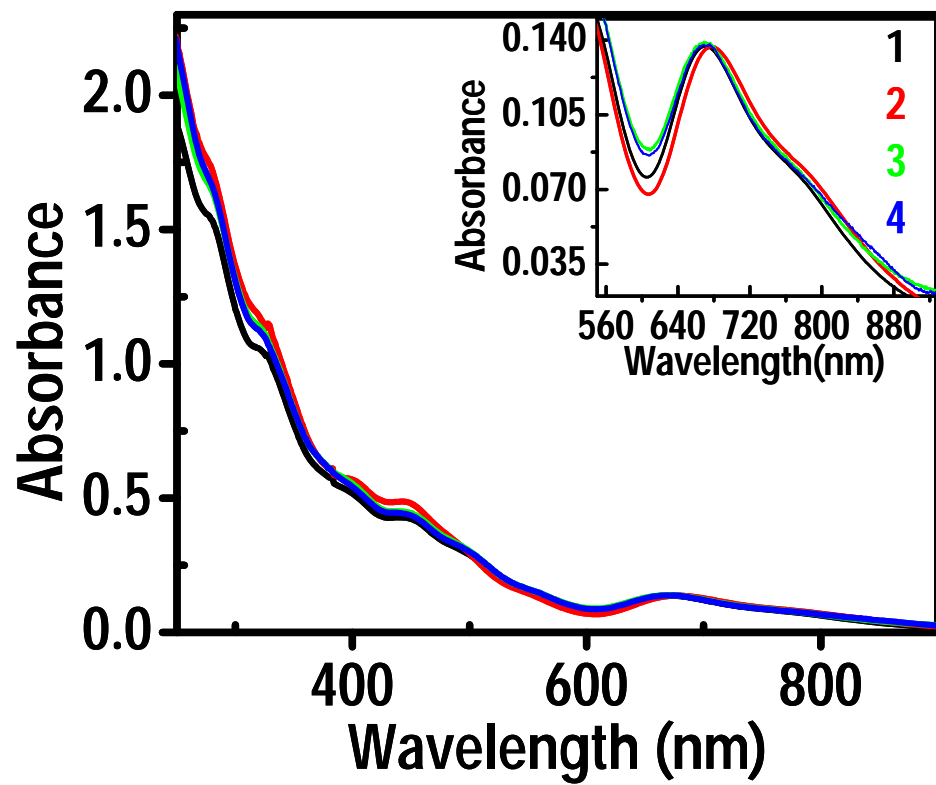


Sajanlal *et al* Adv. Mat. (2008)

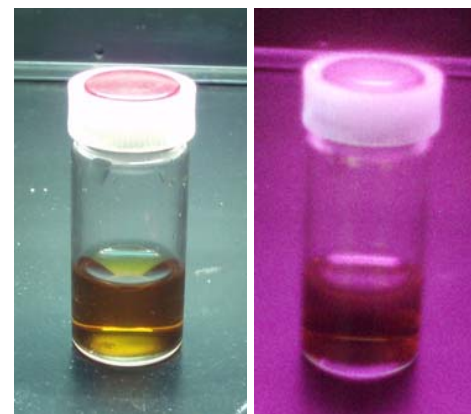


With Ajayaghosh 2008

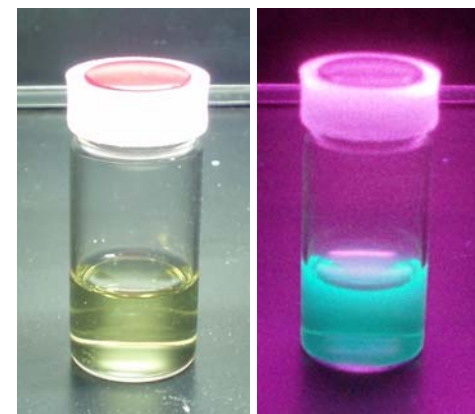




Au_{25}



Au_8



Shibu et al. J. Phys. Chem. C. 2008

Habeeb et al. Unpublished

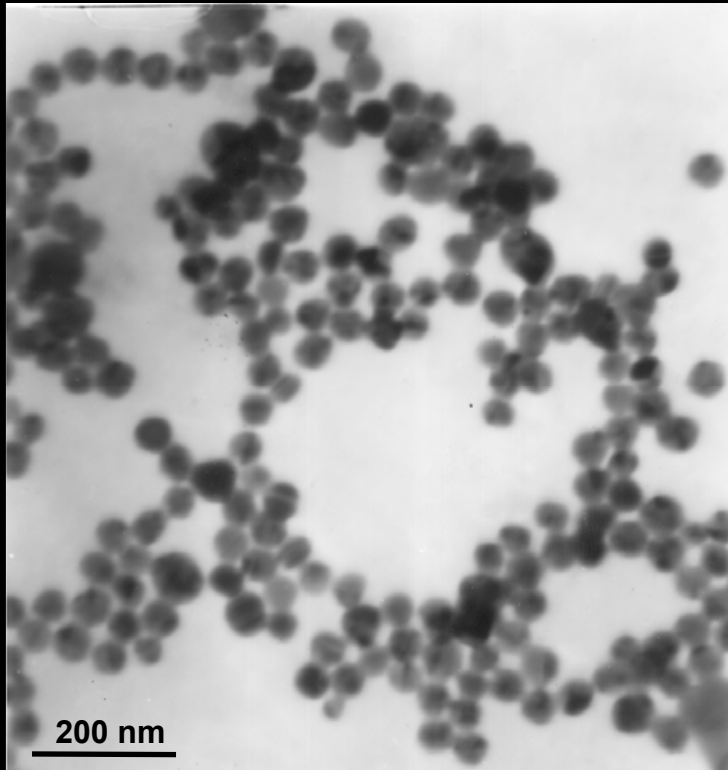


Reactions with the metal core

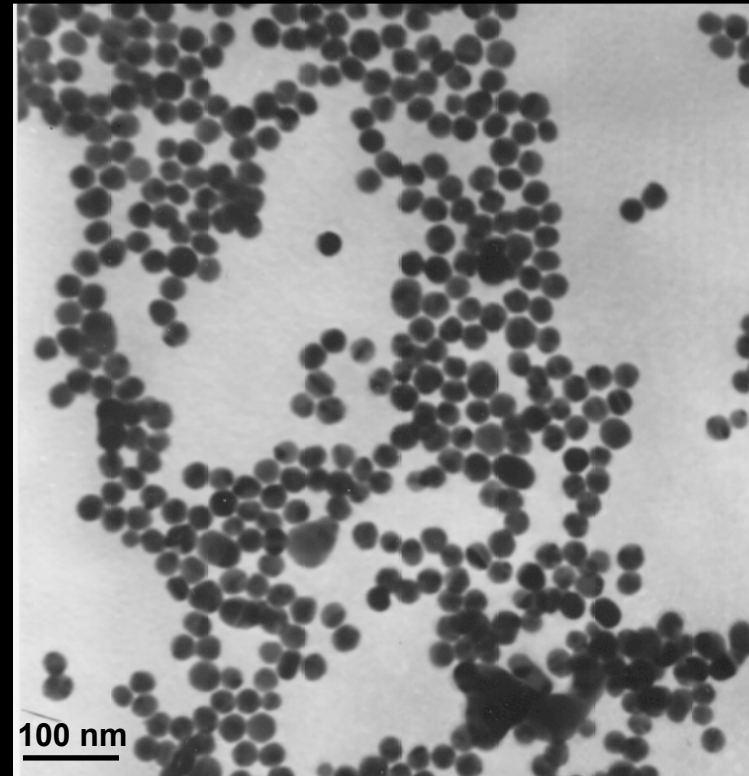


Nanoparticles of silver disappear in a chemical reaction.

Nair and Pradeep 2003



Silver nano-particles ~70 nm

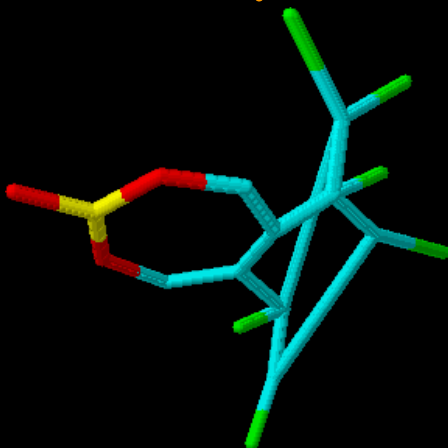


Gold nanoparticles ~15-20 nm

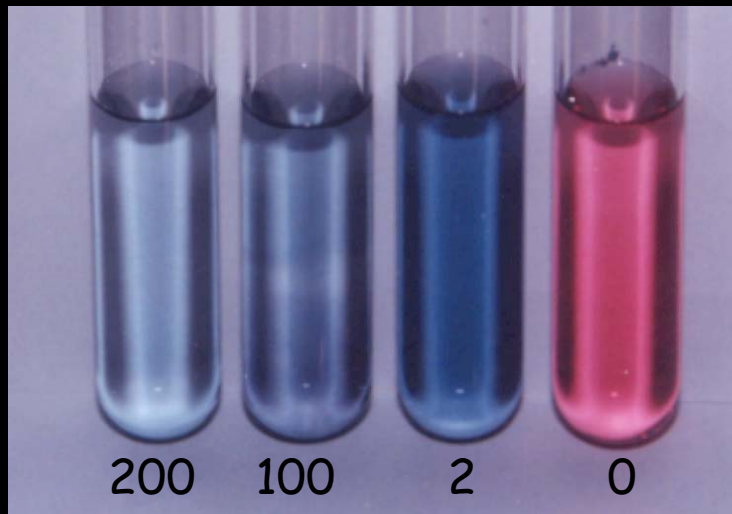
Reactions with pesticides

Color of gold nanoparticles with endosulfan

Example



Endosulfan



Endosulfan concentration in ppm

Color changes with pesticide concentration

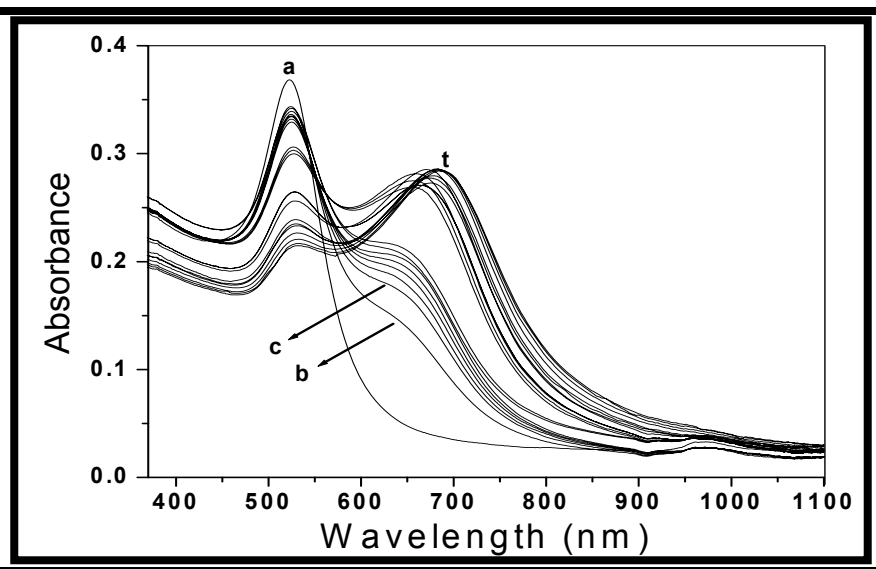
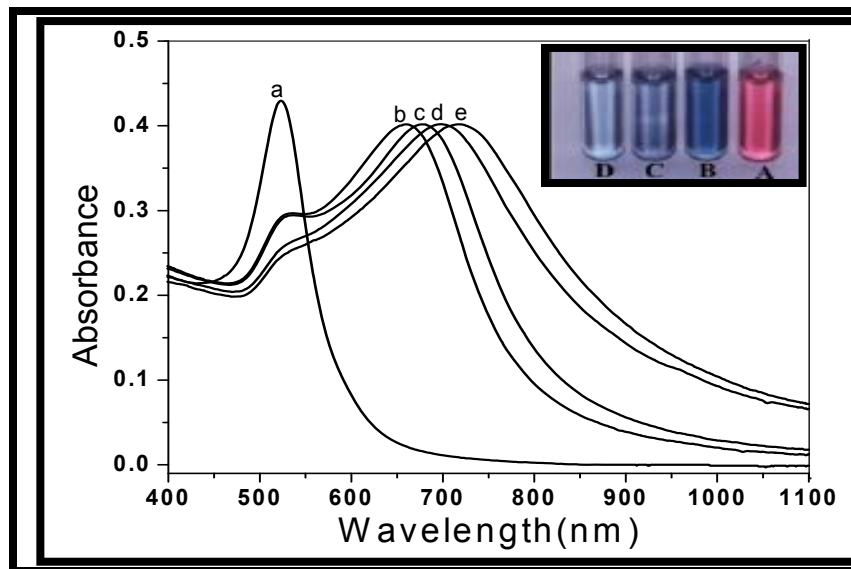
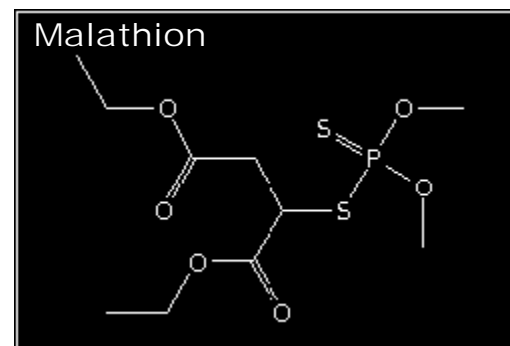
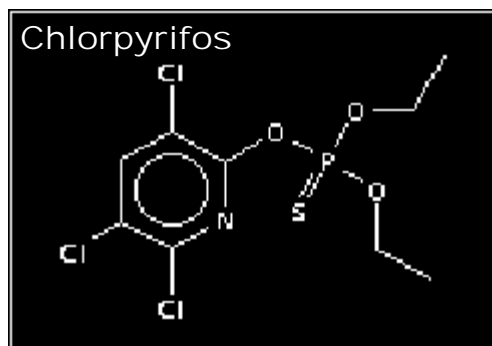
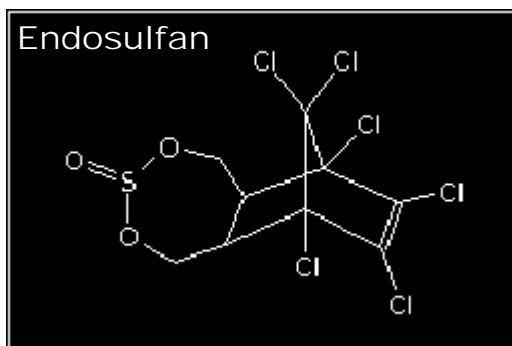
Good response at lower concentrations

Down to 0.1 ppm

Absorbed pesticides can be removed from solution

Pesticide removal
Indian Patent granted
International patent filed
Technology commercialized

Some of the pesticides contain halocarbons whereas others have P or S, which can bind metal nanoparticles which is used for pesticide detection and extraction.

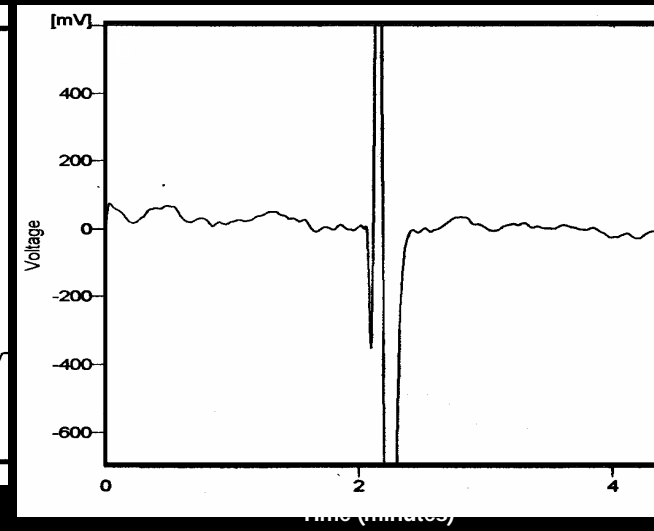
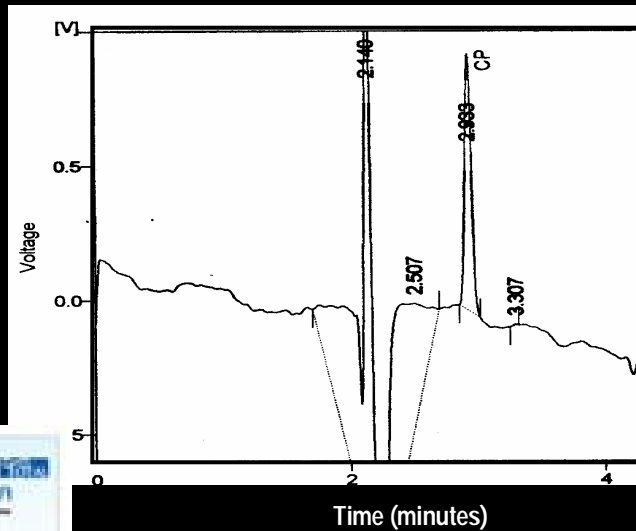


UV-visible spectra of gold nanoparticles showing the detection of endosulfan at different concentrations (b.2, c.10, d.100 and e. 250 ppm). Inset (A-D): Color changes of the solutions corresponding to traces a, b, c and d, respectively.

Time dependent adsorption of endosulfan on gold nanoparticles and the corresponding spectral changes (a-t). The shifts in the plasmon band are due to the binding of the pesticide on the nanoparticle surface.



Pesticide removal from drinking water



Product is marketed now

A pesticide test kit has been developed > 25 ppb

In this talk.....

Visible emission from single walled carbon nanotubes

Background

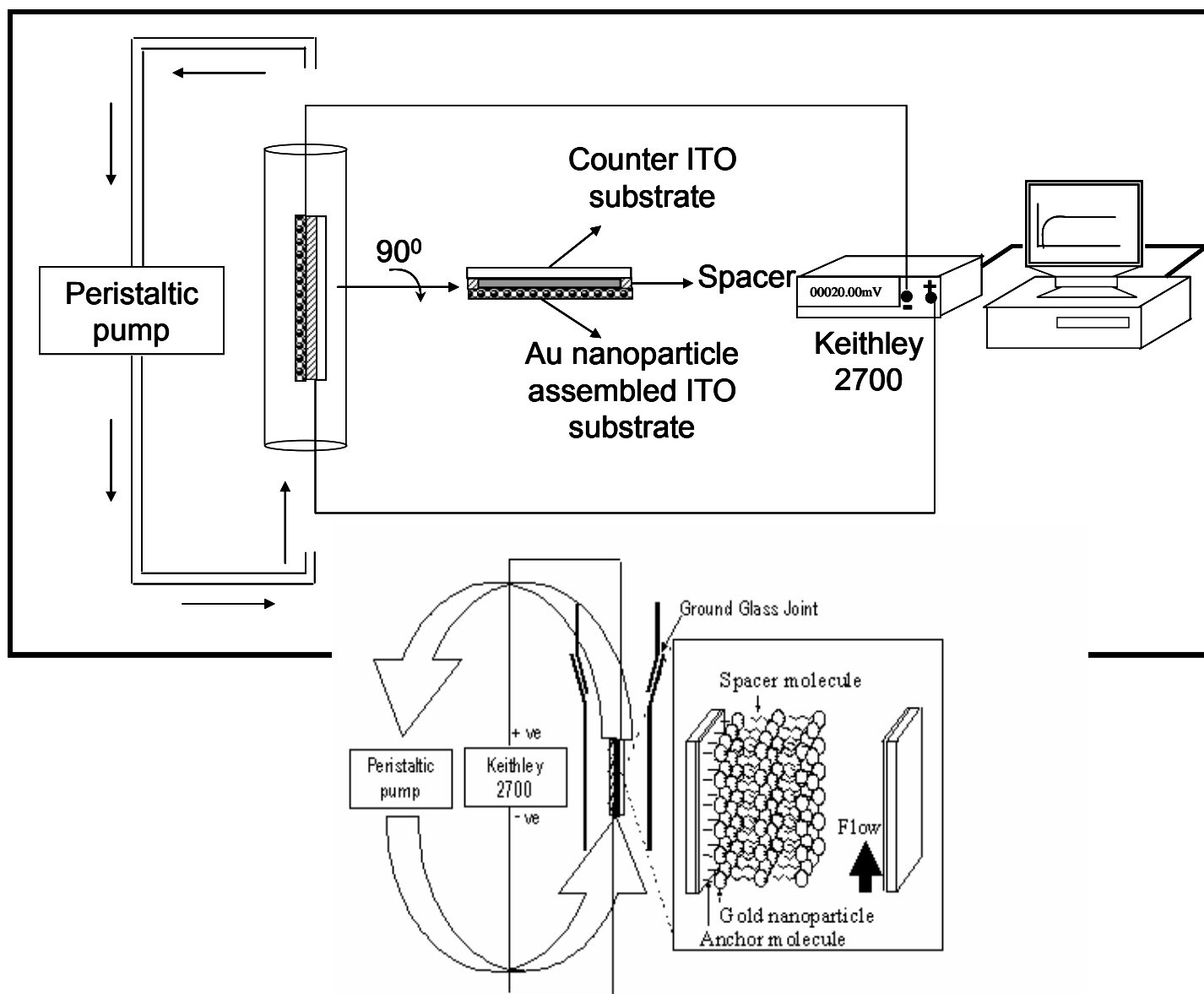
Experiment

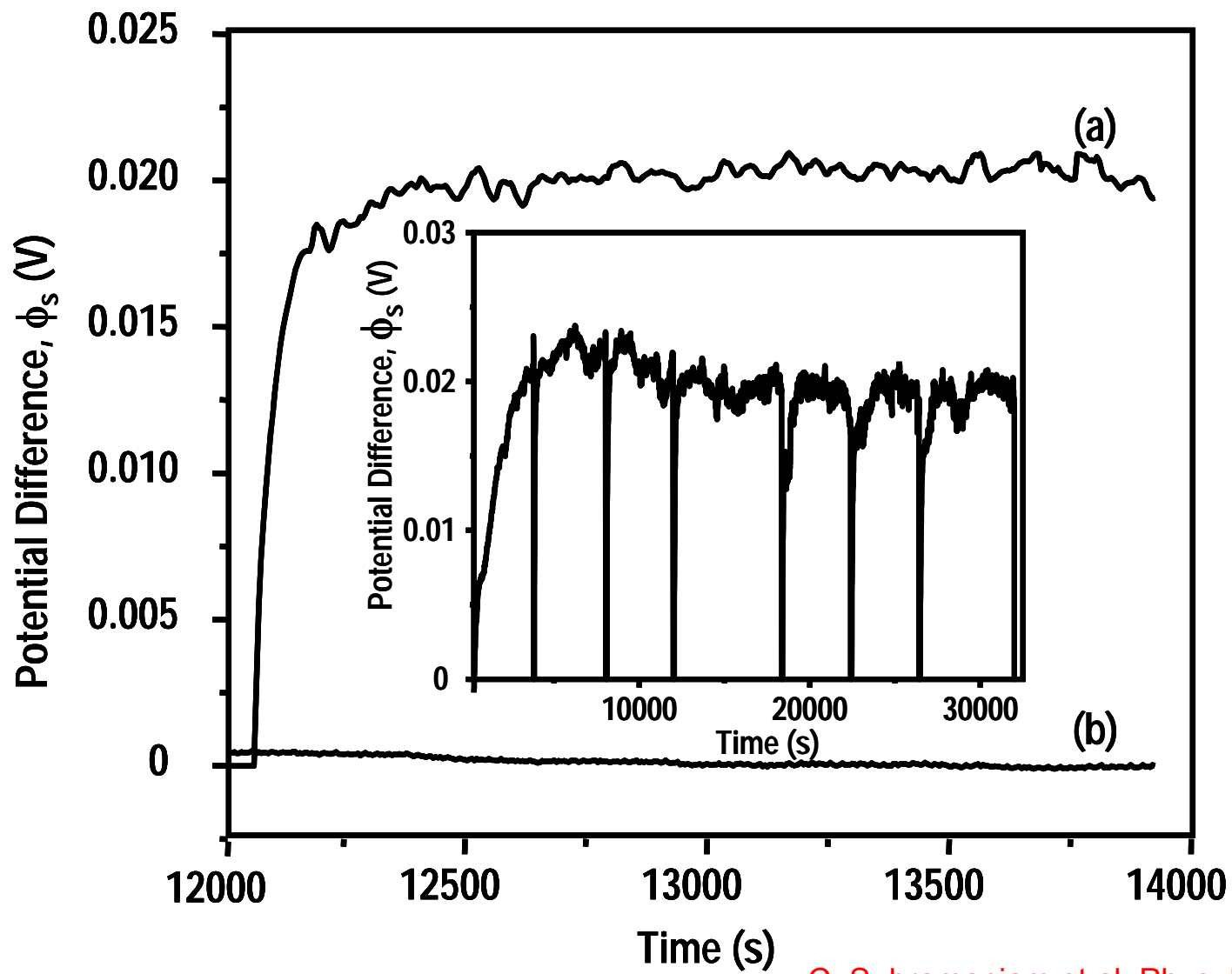
Control experiments

What next...

Chemical interactions leading to devices

Flow induced potential in nanoparticle assemblies



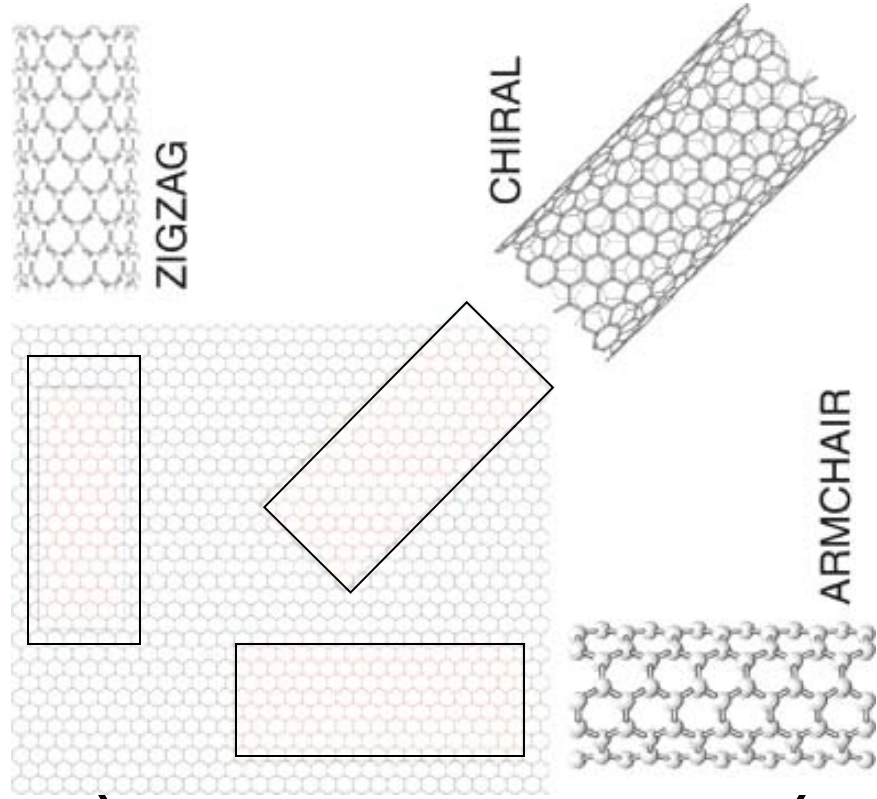


C. Subramaniam et al. Phys. Rev.Lett.2005

J. Phys. Chem. C 2007

34

Indian Patent application 2005



(n,m) indices

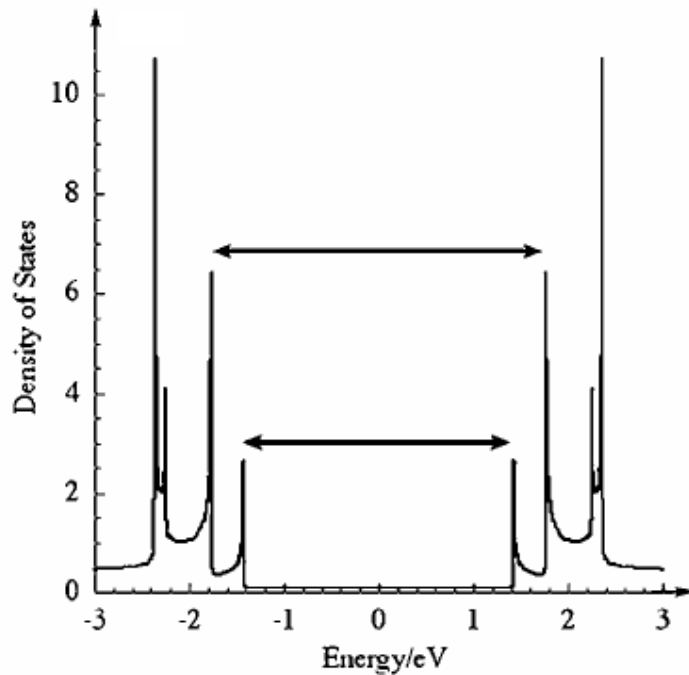
Metallic

Semiconducting

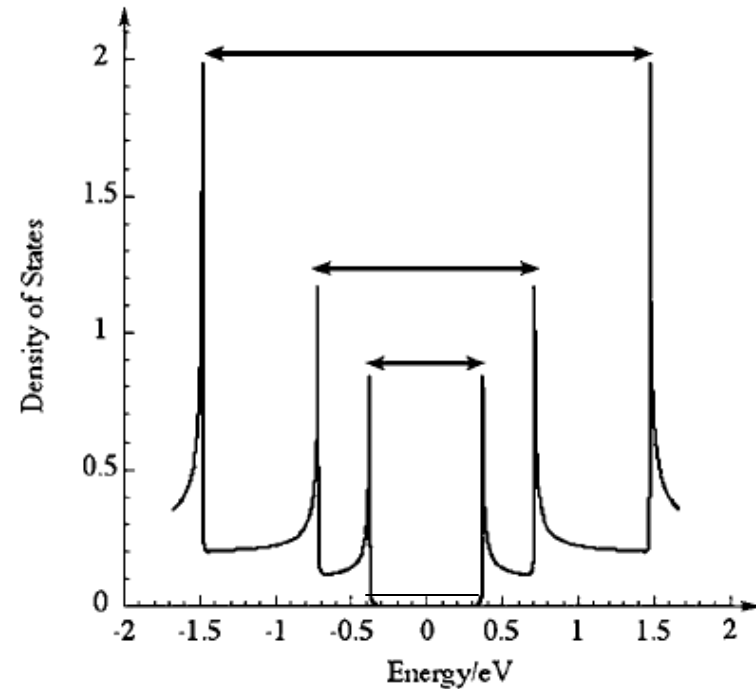
Electrical transport properties

📖 Semiconducting : $(n-m) \neq 3!$. $E_g = 1.7 - 2.0$ eV

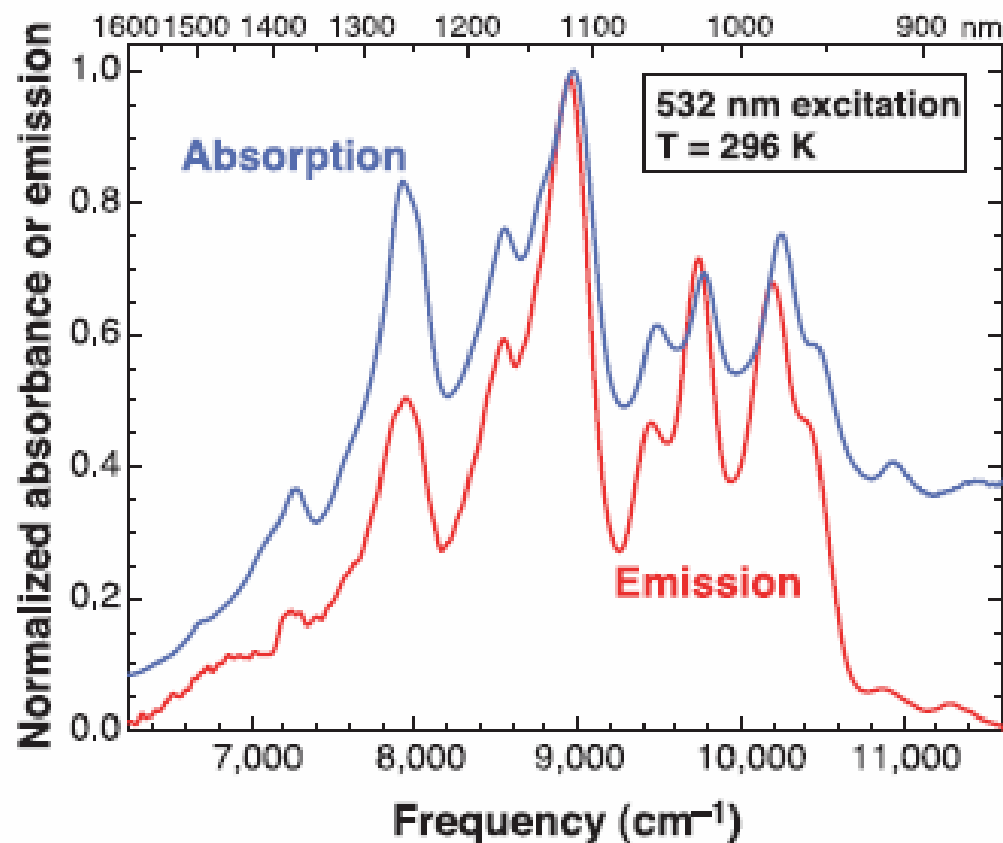
📖 Metallic : $(n-m) = 3!$. $E_g = 0.0 - 0.5$ eV



Semiconducting



Metallic

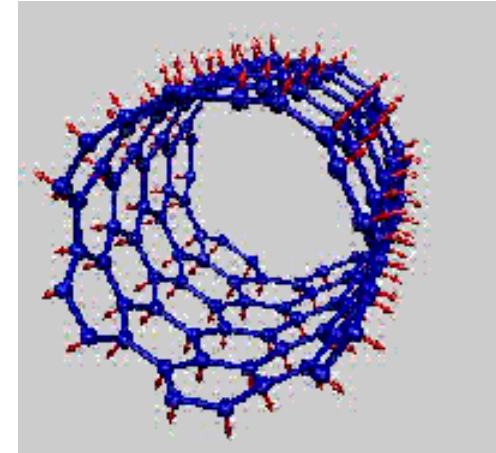


Emission spectrum (red) of individual fullerene nanotubes suspended in SDS micelles in D₂O excited by 8 ns, 532-nm laser pulses, overlaid with the absorption spectrum (blue) of the sample in this region of first van Hove band gap transitions.

Vibrational Properties

(A) Radial Breathing Mode (RBM)
Diameter dependent

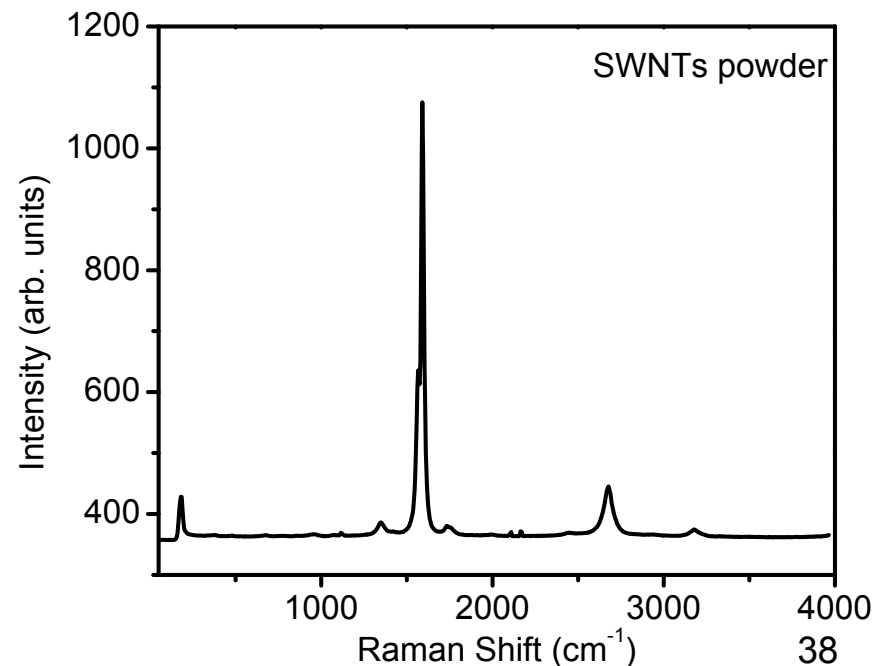
$$\omega_{RBM} (cm^{-1}) = \frac{224.8}{d_t (nm)} + 12.5$$



(B) Tangential G band
In-plane vibrations

(C) D-band
Defect centered

(D) G' band
Occurs at $2\omega_D$



Vibrational properties of single walled carbon nanotubes (SWNTs)

Experimental methods

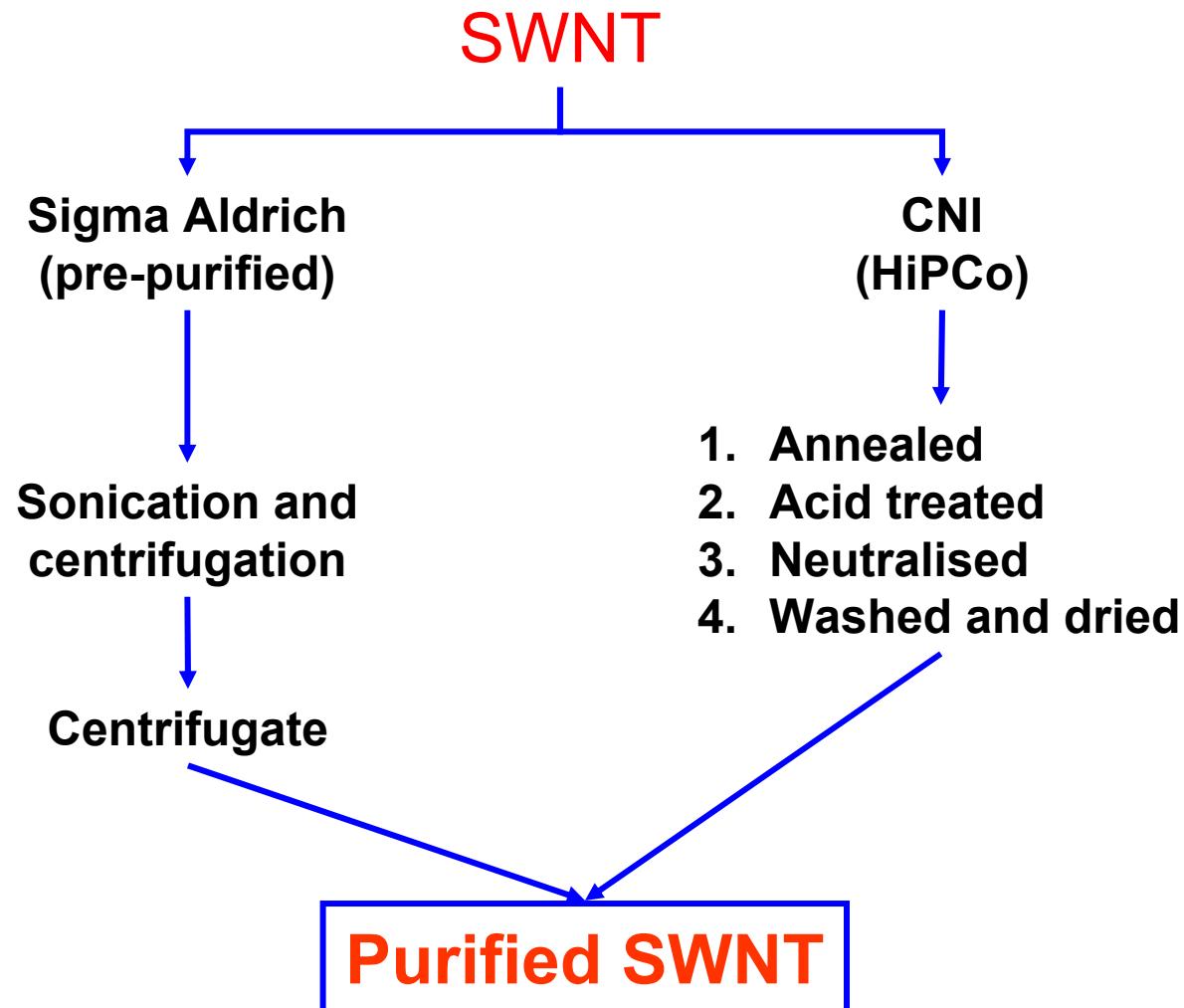
Confocal Raman spectral analysis and imaging

Scanning near field optical microscopy (SNOM)

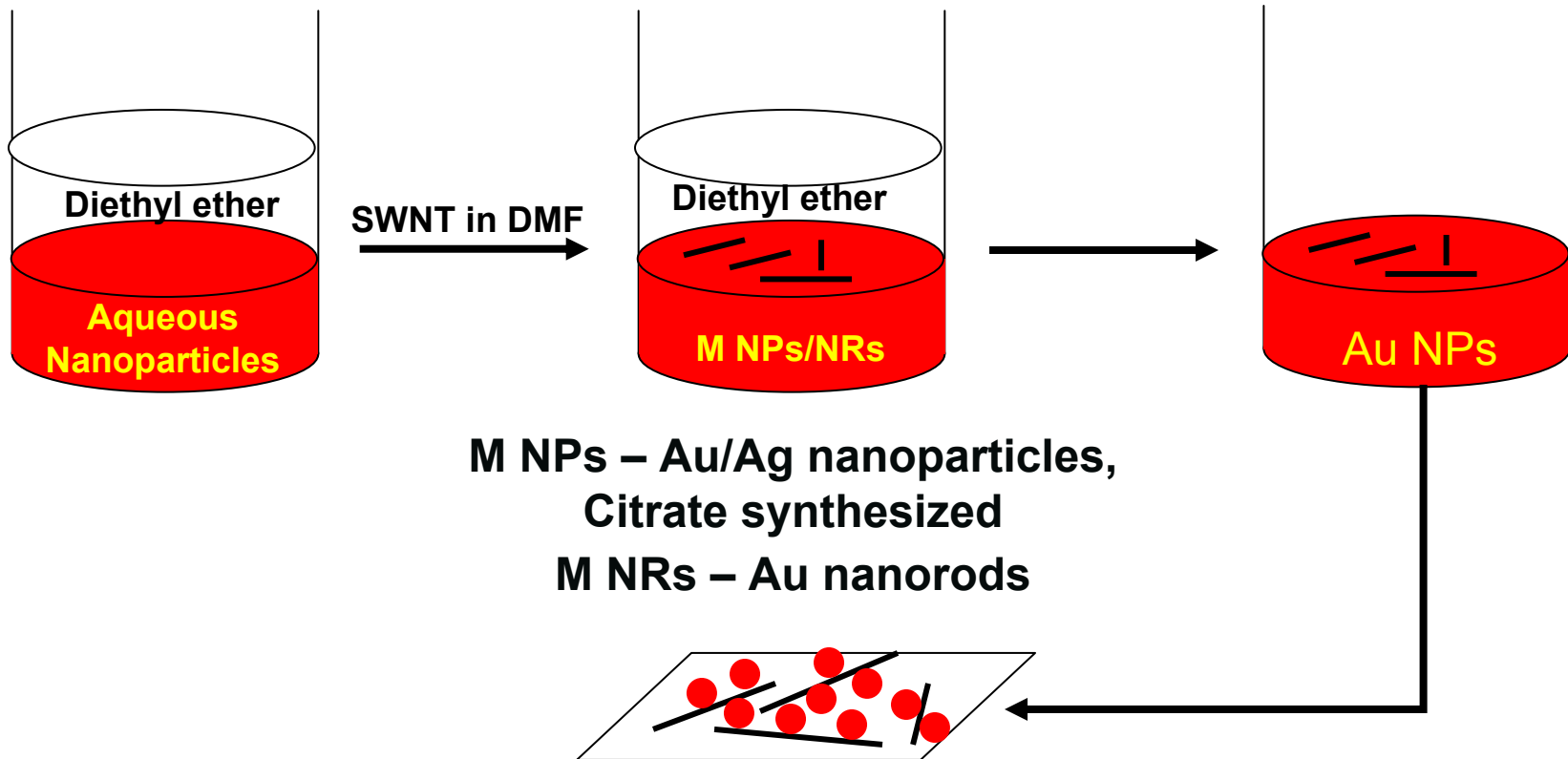
Point-contact current image Atomic force microscopy (PCI-AFM).

Other supporting experiments

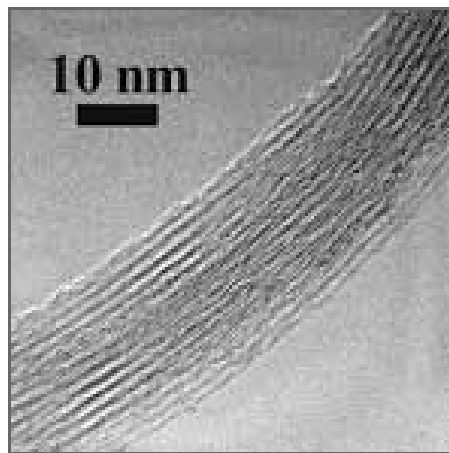
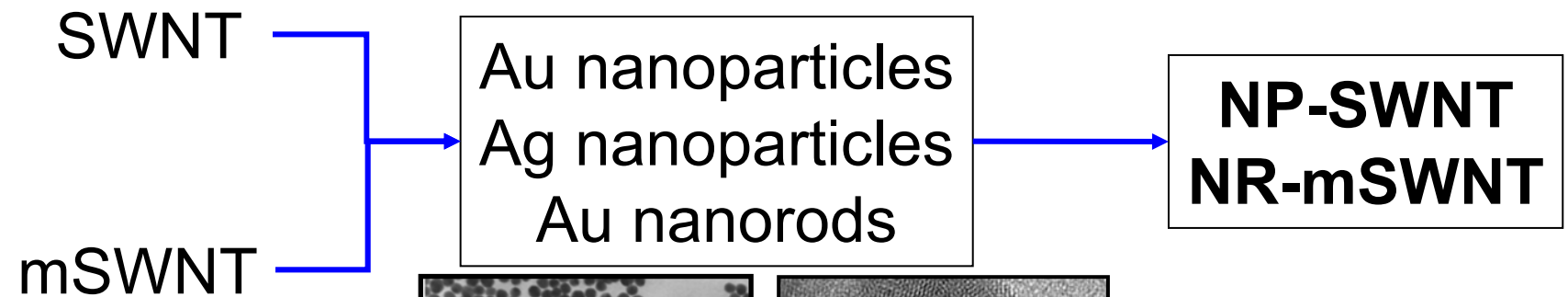
Purification of SWNT



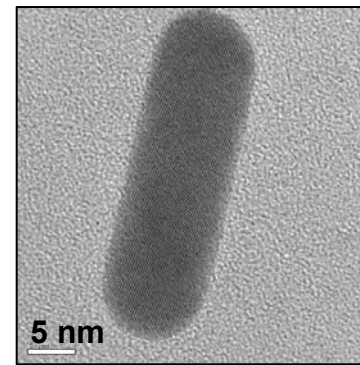
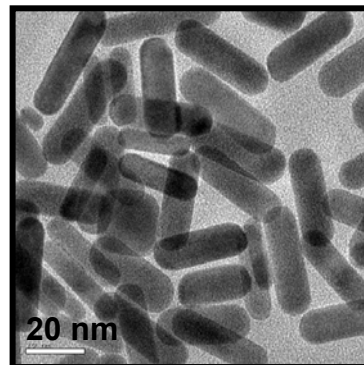
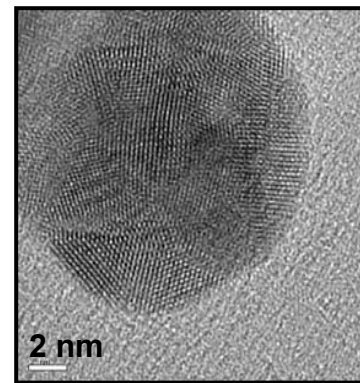
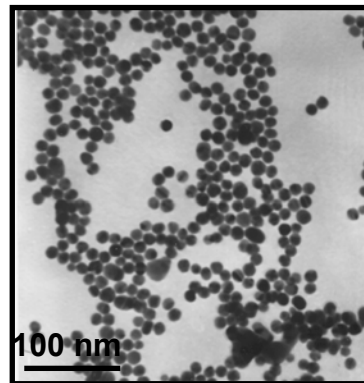
Preparation of composite



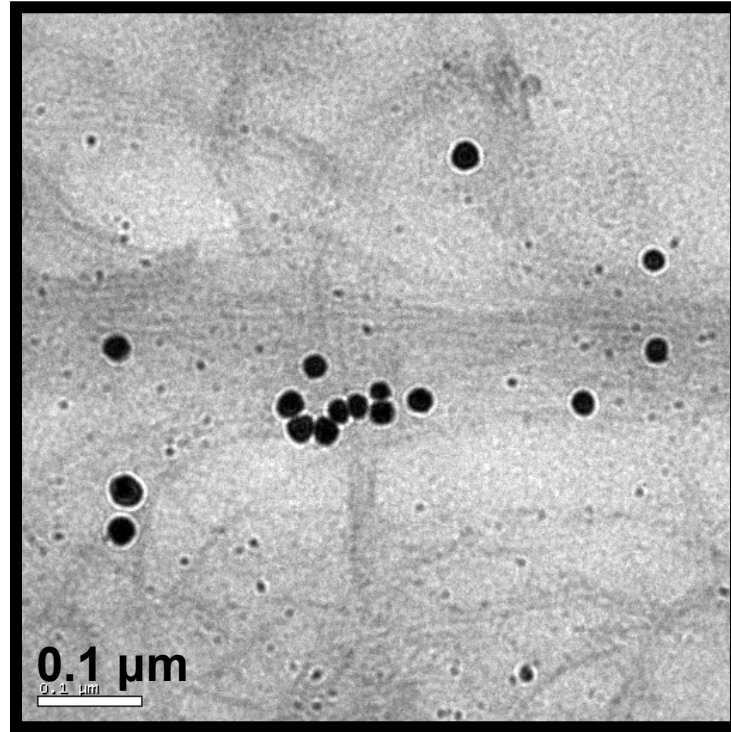
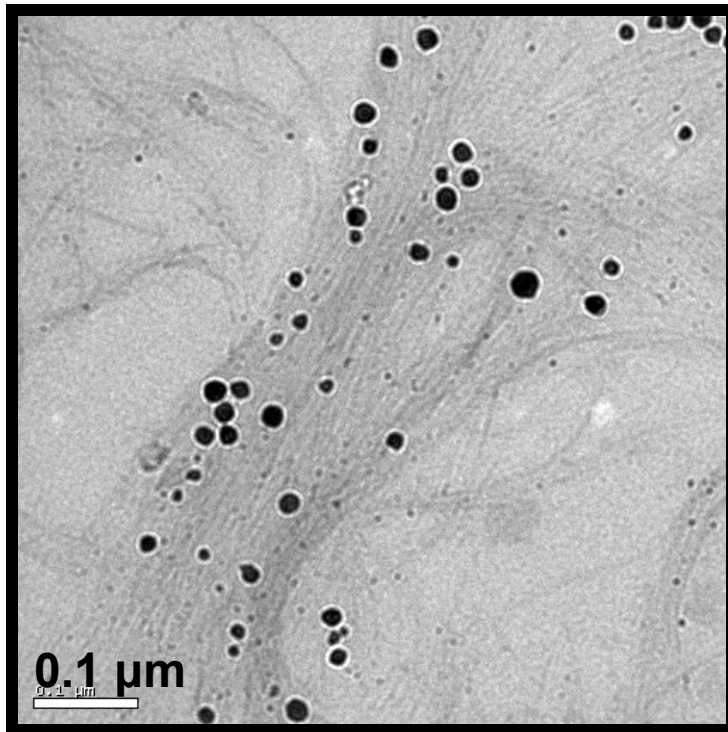
Types of systems investigated



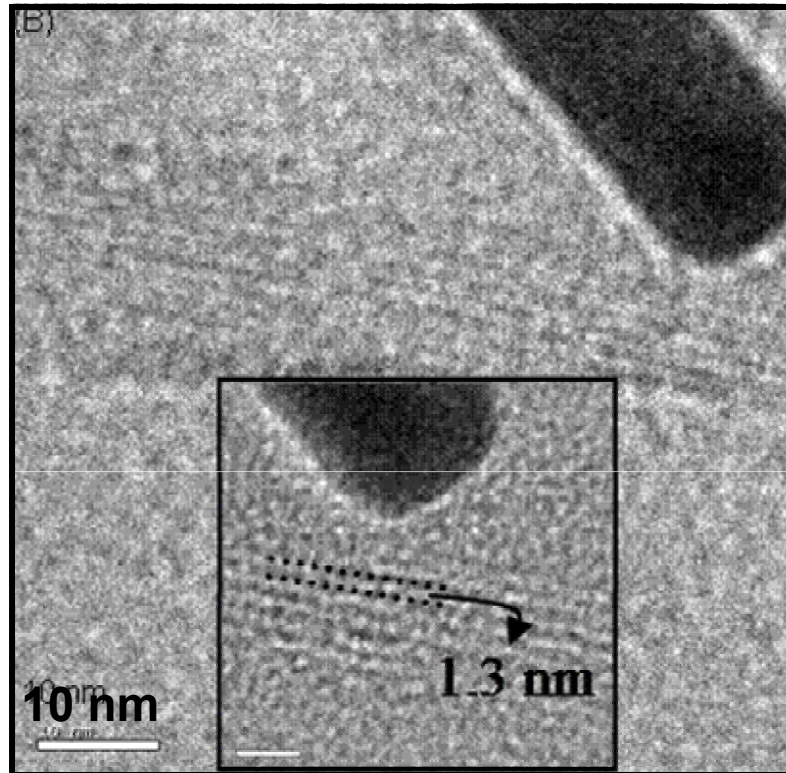
www1.eere.energy.gov



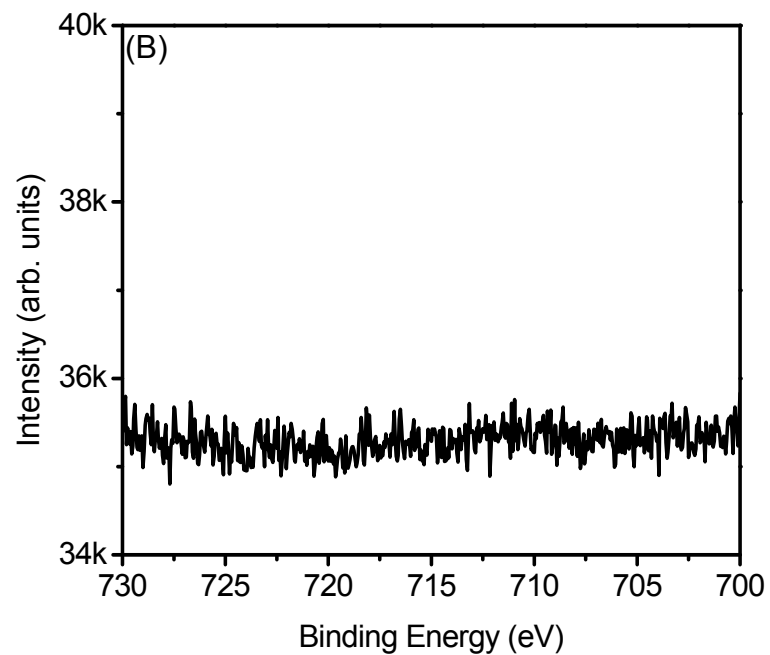
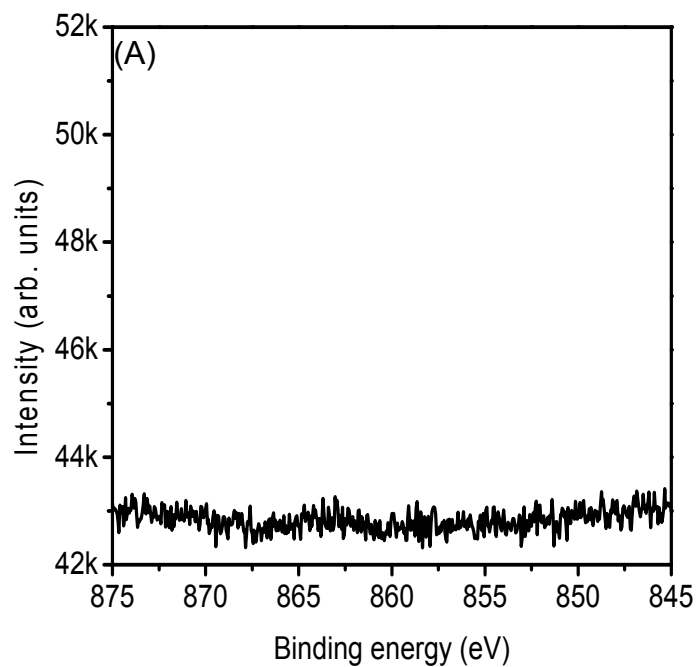
Transmission Electron Microscopy



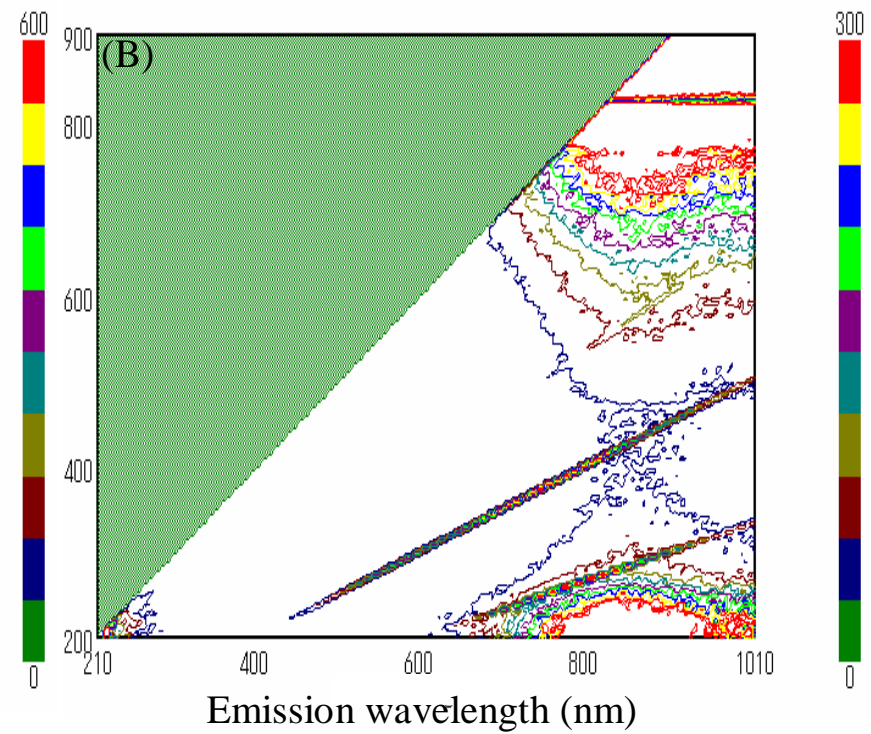
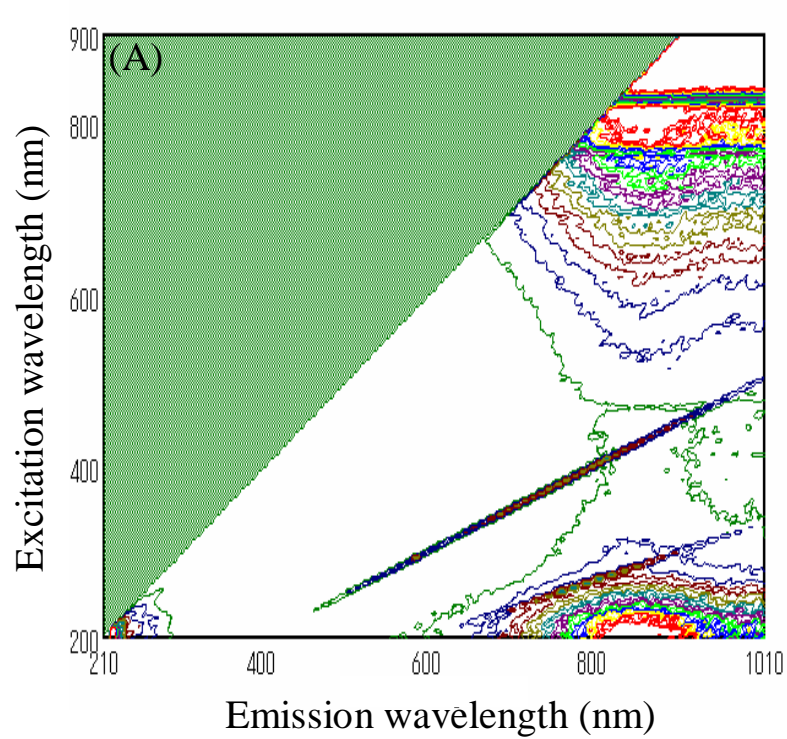
TEM images of Au-SWNTs composite acquired at 100 keV.



TEM images of (A) AuNRs-SWNTs composite acquired at 300 keV.

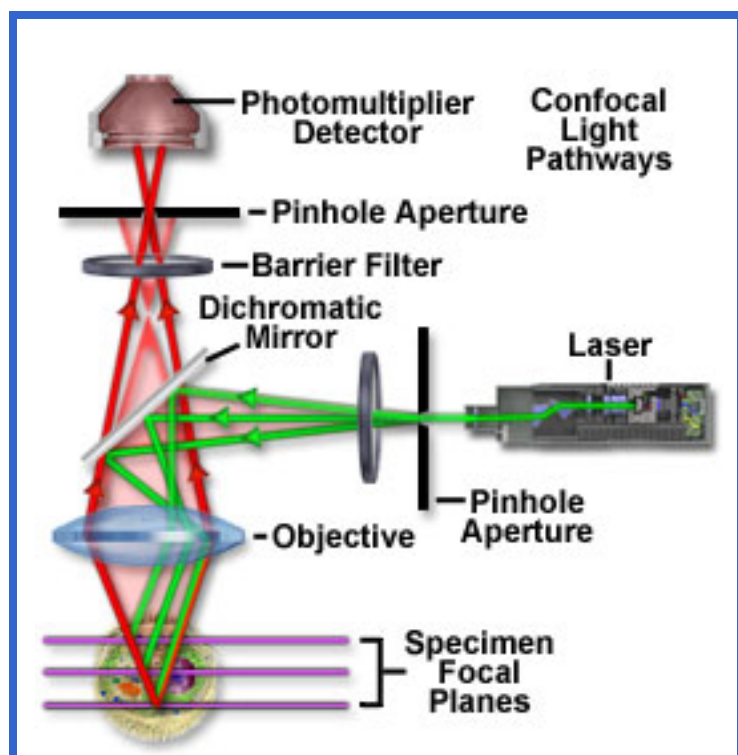


XPS spectra of Au-SWNT composite in the (A) Ni 2p and (B) Fe 2p regions.
ICP - MS

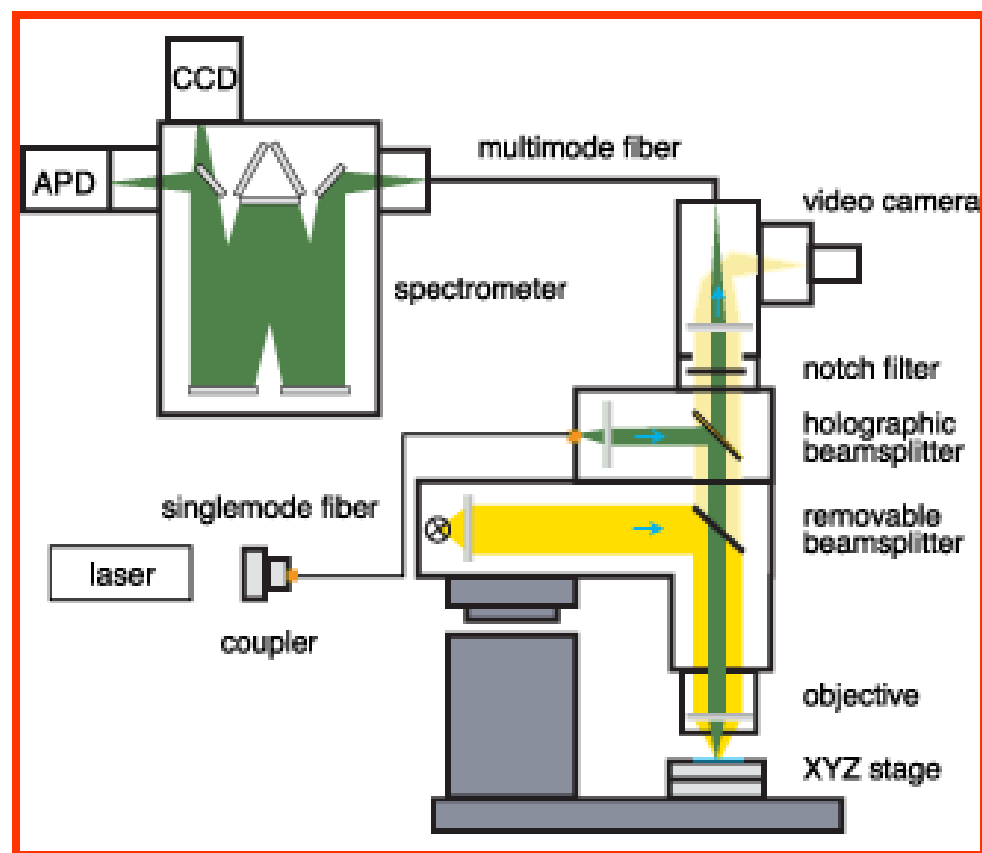


Fluorescence contour plots of (A) supernatant solution and (B) blank water at pH 7.12.

Instrumentation – Confocal Raman



Concept of confocality



Raman Instrument

Key instrument specifications

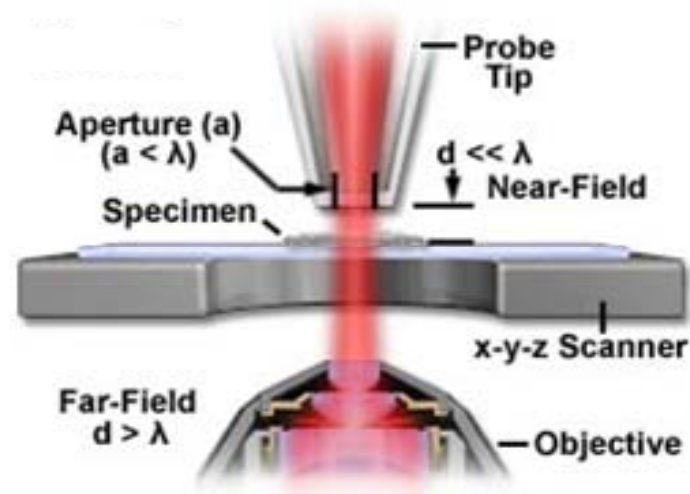
- ✚ Argon Ion laser : 514.5 nm
- ✚ Back scattering geometry
- ✚ Super notch filter



Scanning Near-field Optical Microscopy

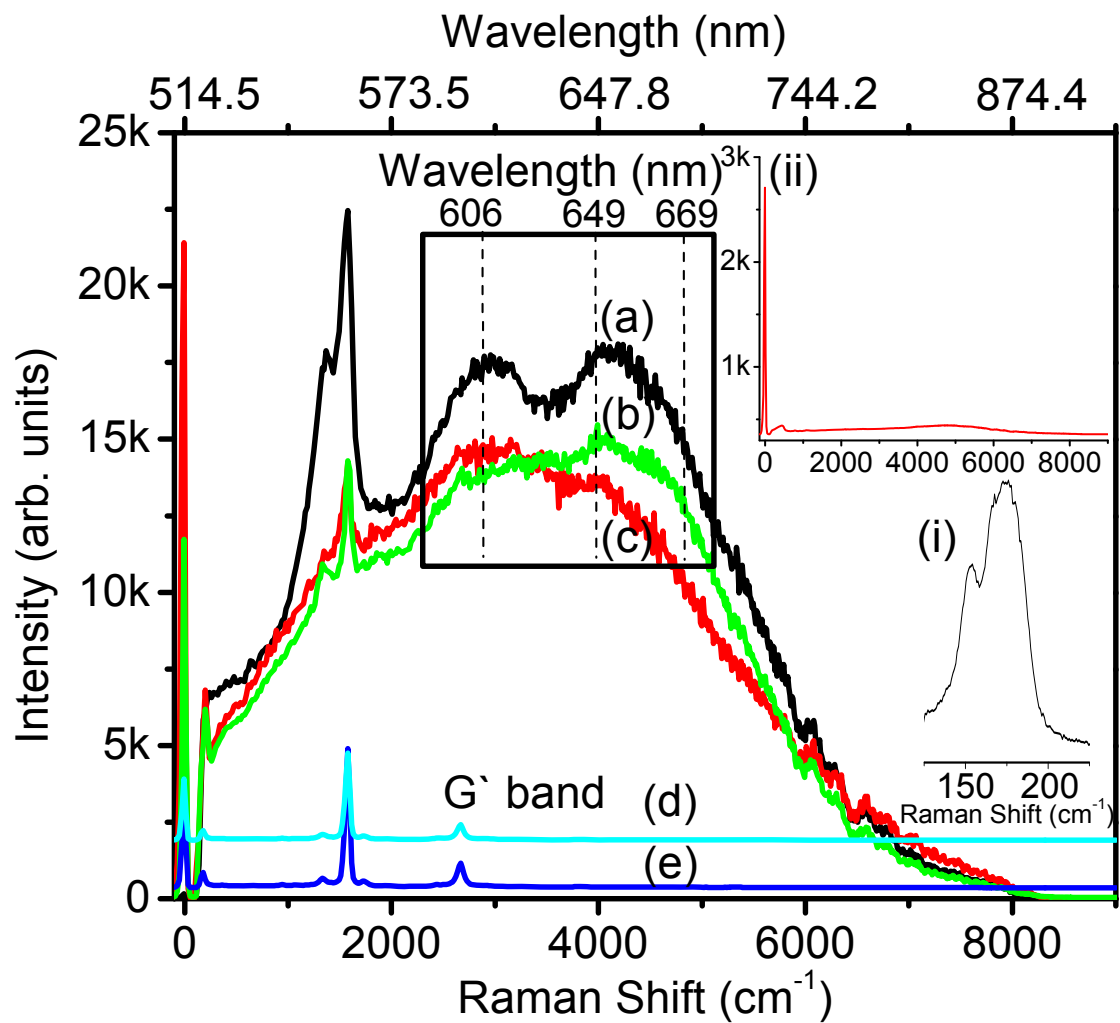
- Resolution is limited by wavelength of light used.
- Near-field microscopy was first proposed by Synge in 1928.

“Resolutions below the diffraction limit can be obtained when the tip-sample distance is smaller than the aperture diameter. In such a case, the aperture diameter controls the resolution and not the wavelength of light used²”



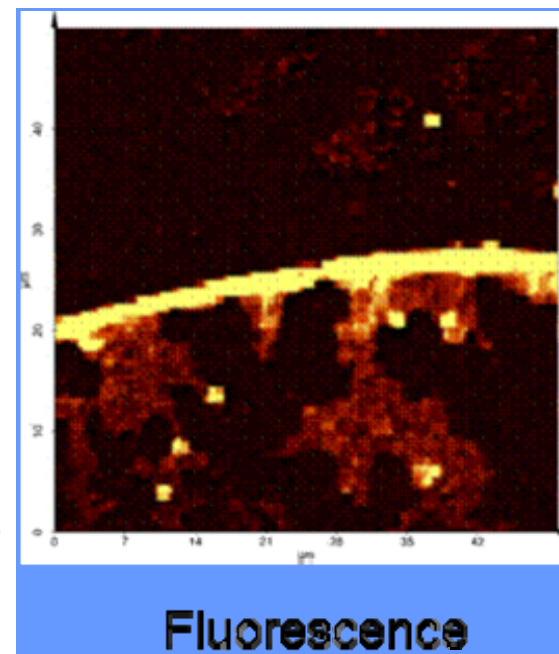
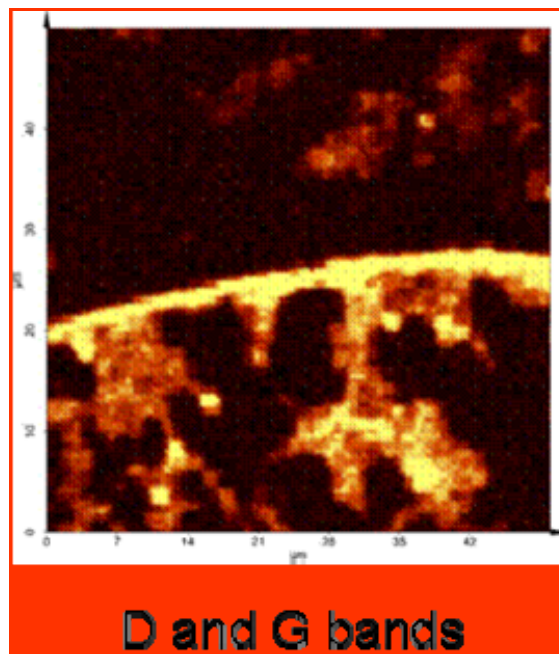
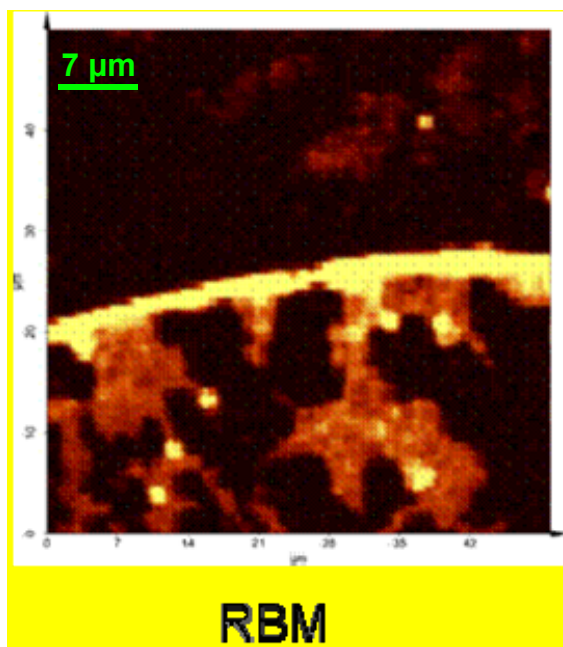
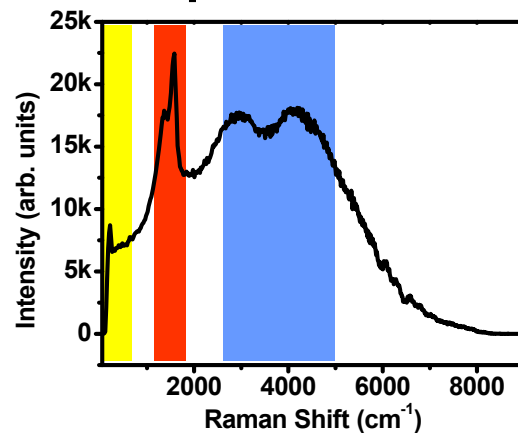
1. www.olympusmicro.com

2. E.H. Synge, *Phil.Mag.* **6**, 356 (1928)

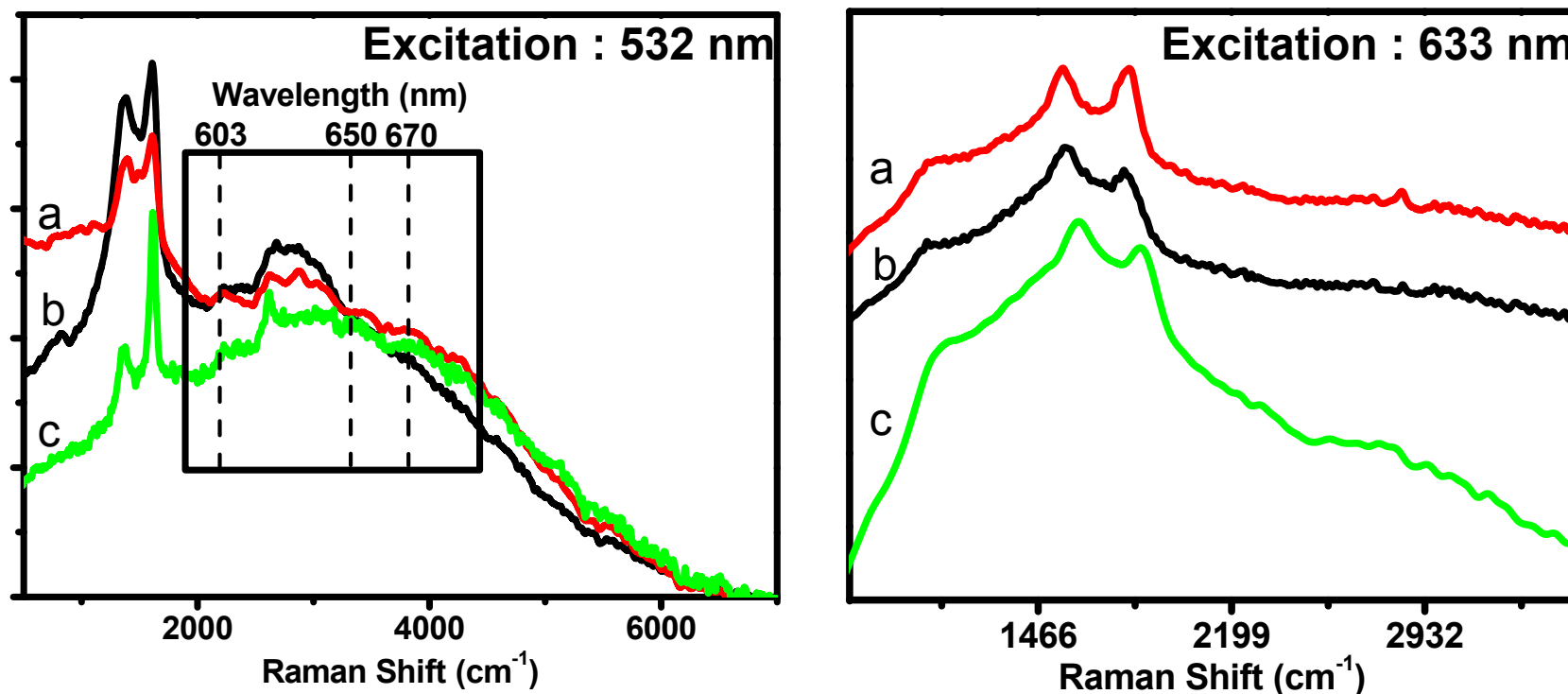


Raman Spectra of (a) Ag-SWNTs composite, (b) Au-SWNTs composite, (c) AuNR-SWNTs composite, (d) pristine SWNTs, (e) Pristine SWNTs treated with trisodium citrate and (f) Au nanorods.

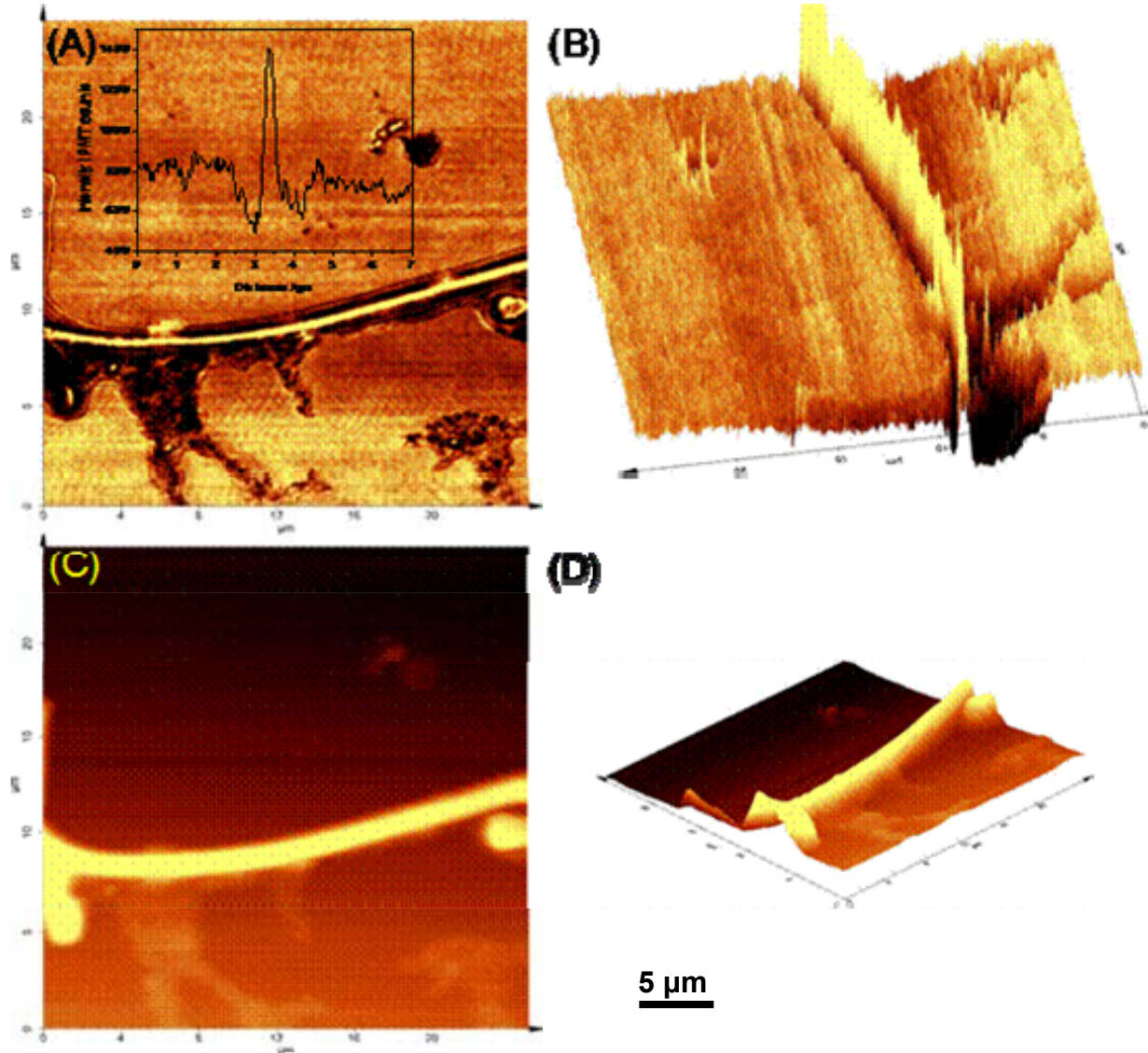
Raman Spectral imaging



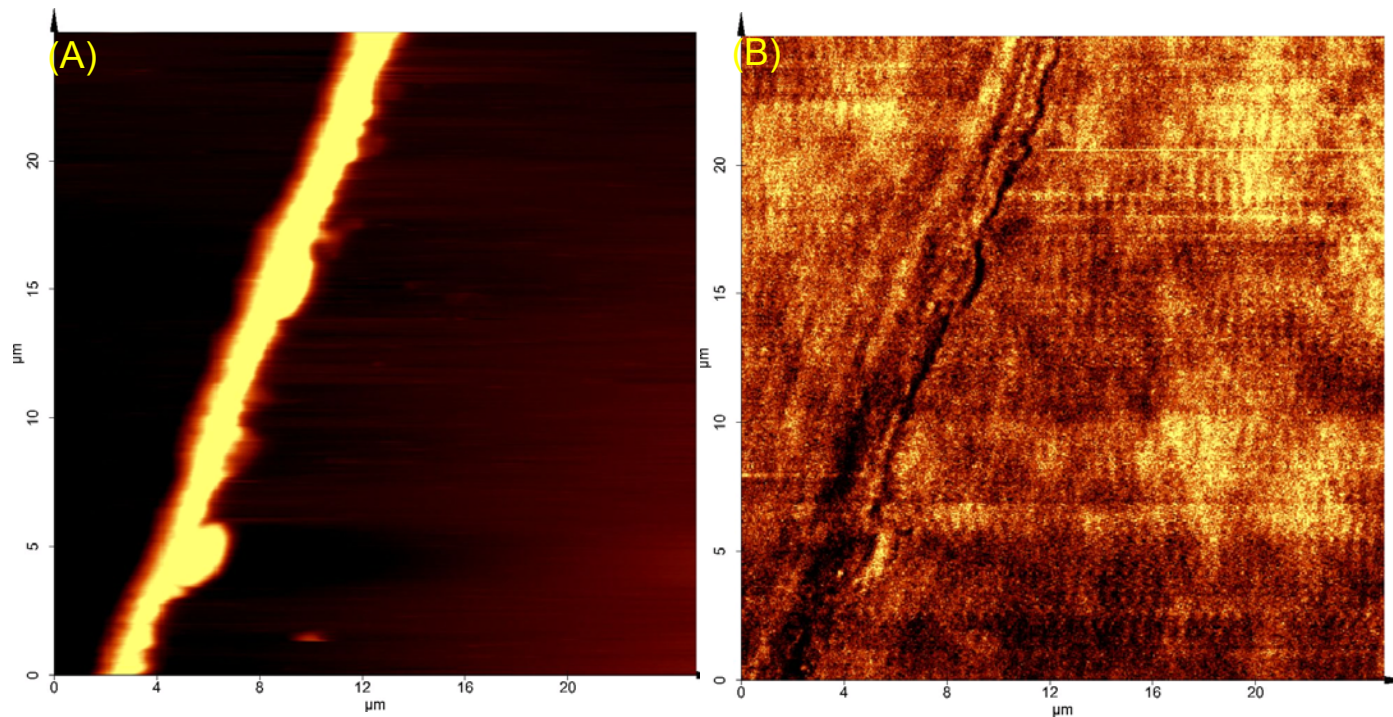
Varying excitation sources



Raman Spectra acquired with (A) 532 nm Nd-YAG and (B) 633 nm He-Ne as excitation sources. Traces (a), (b) and (c) correspond to Ag-SWNTs composite, Au-SWNTs composite and AuNR-SWNTs composite, respectively.

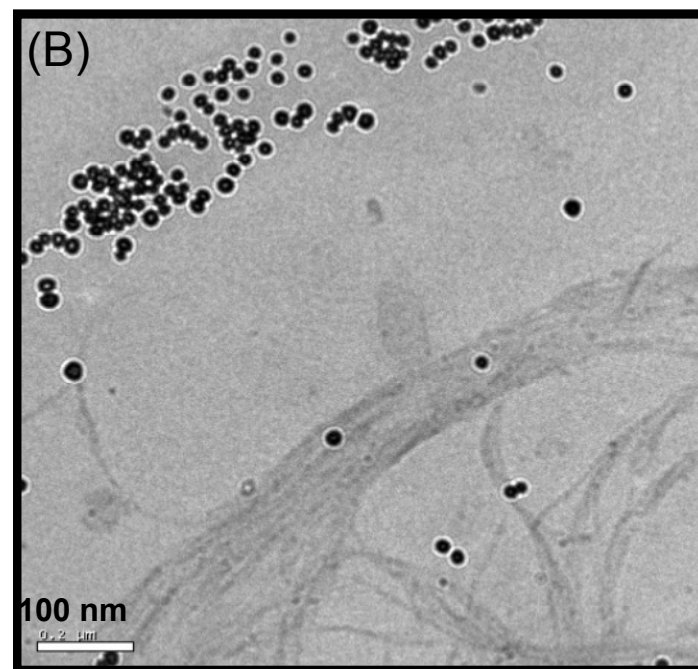
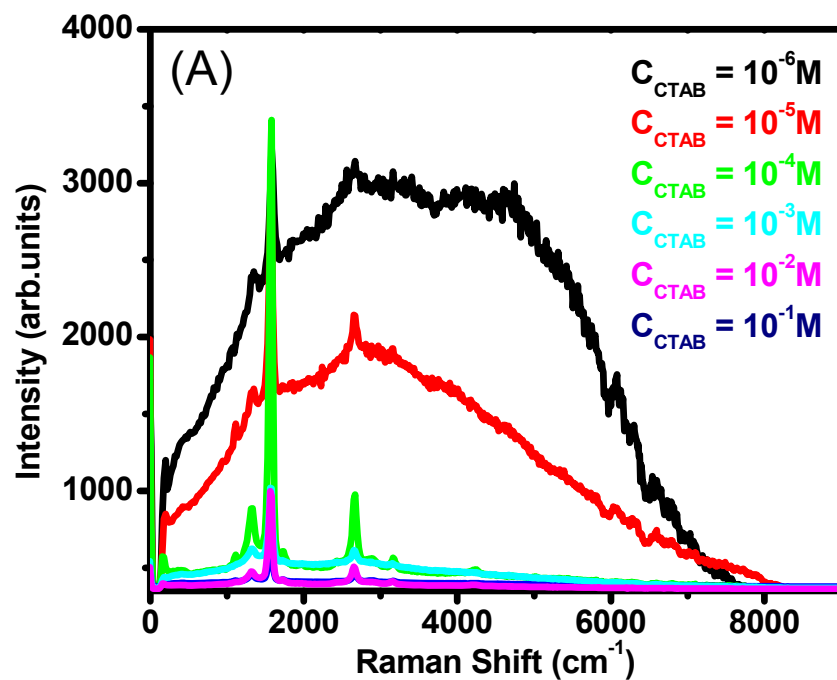


(A) SNOM images of Au-SWNT composite along with the (C) topography. (B) and (D) are their three dimensional representations.

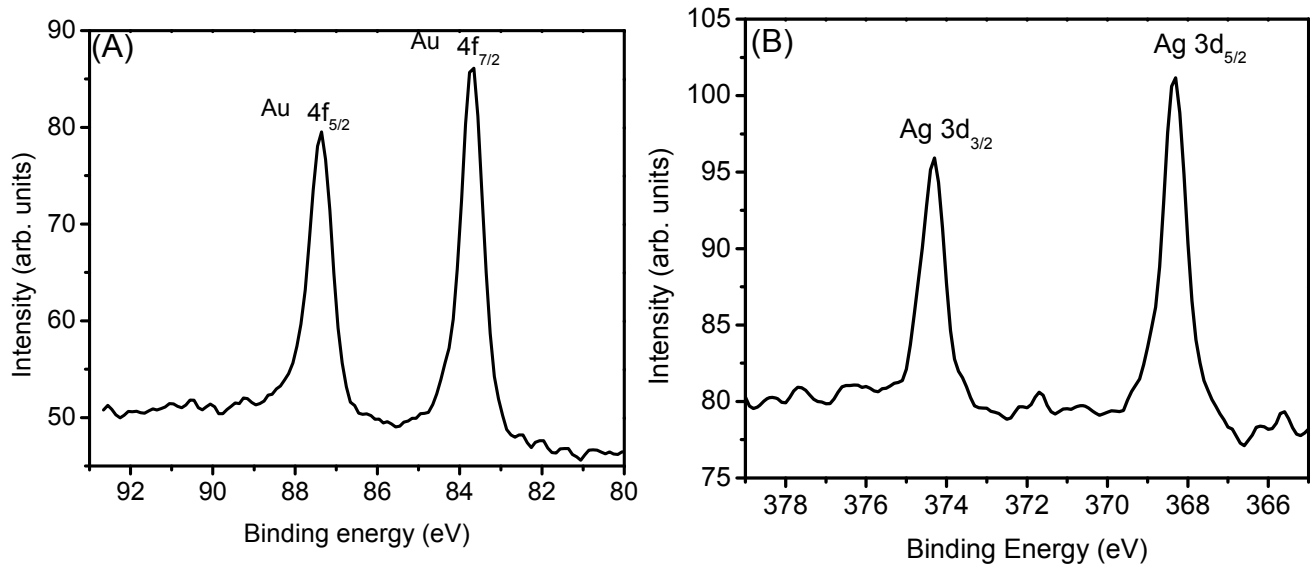


Transmission SNOM images of pristine SWNT based on (A) topography and (B) light intensity.

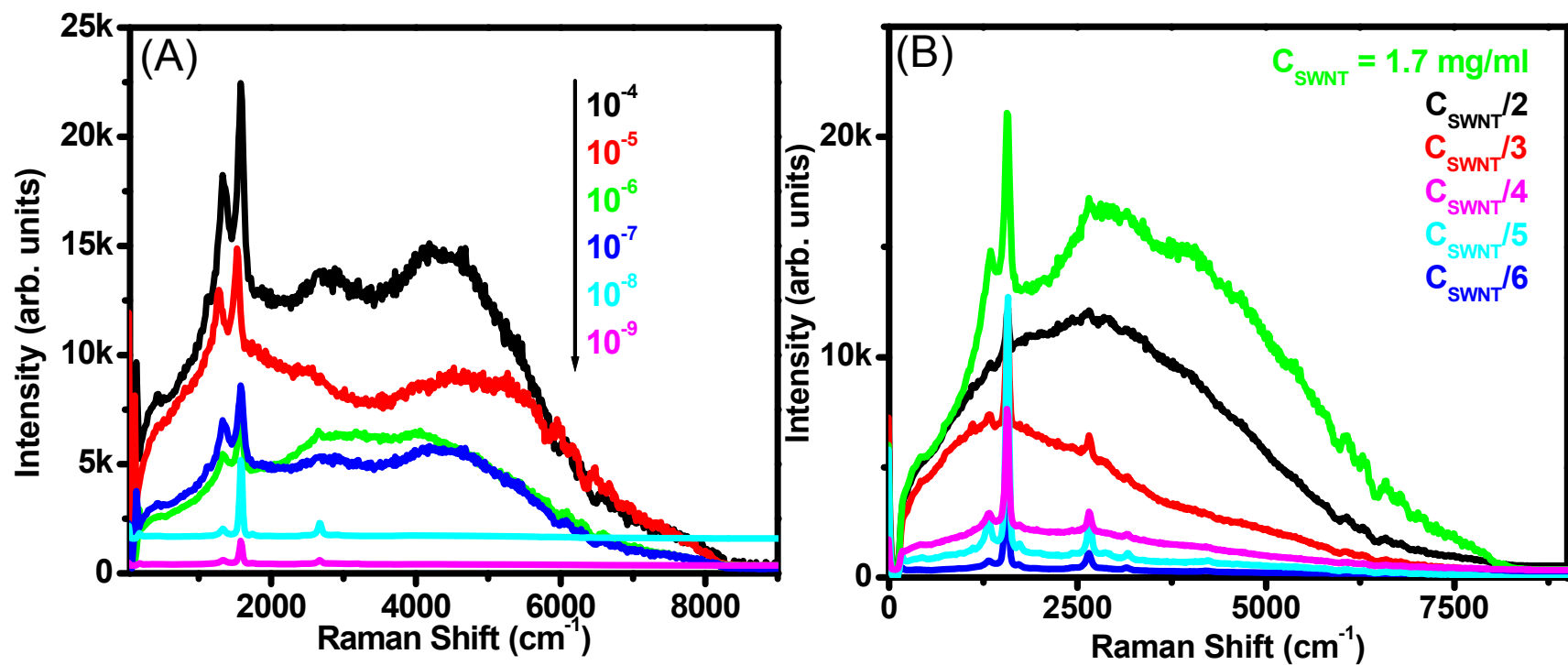
Supporting experiments



(A) Raman spectra of Ag-SWNT composite measured as a function of CTAB concentration. (B) TEM image of Au-CTAB-SWNT at $C_{\text{CTAB}} = 10^{-4} \text{ M}$



XPS spectra of (A) Au-SWNT and (B) Ag-SWNT composites in the Au 4f and Ag 3d regions, respectively



Raman spectra of Ag-SWNT composite, measured as a function of (A) concentration of Ag nanoparticles, (B) SWNT concentration.

(n,m) indexing

$$\omega_{RBM} = \frac{C_1}{d_t} + C_2, \text{ where } C_1 \text{ and } C_2 \text{ are constants}$$

$$d_t = \frac{\sqrt{3}a_{c-c}}{\pi} \sqrt{n^2 + nm + m^2}$$

(n,m)	RBM (cm^{-1} , Theoretical)	d_t (nm)	
(10,10)	175	1.37	} E_{11}^m
(18,0)	168	1.43	
(13,7)	172	1.40	
(17,0)	178	1.35	} E_{23}^s / E_{32}^s
(11,9)	175	1.37	
(12,8)	174	1.38	

What we know so far

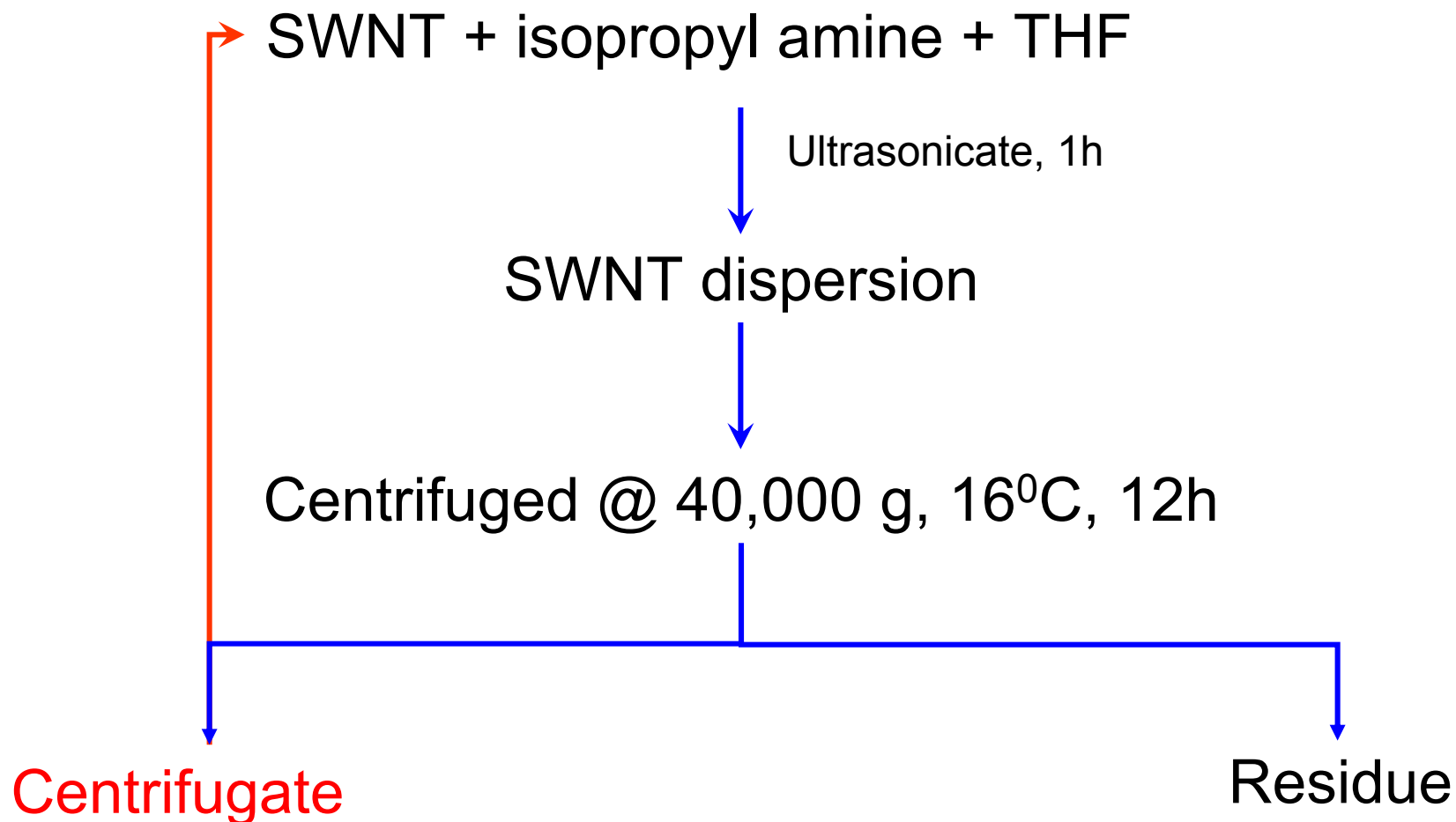
- ✓ Visible fluorescence from SWNTs is demonstrated.
- ✓ Raman spectral mapping is done to ascertain the origin of fluorescence.
- ✓ SNOM of SWNT structures is done using this fluorescence.

Origin of visible fluorescence

- ⊕ Near-infrared fluorescence in isolated SWNT is known.
- ⊕ This is not observed in bundles and metallic SWNTs.
- ⊕ Metallic SWNTs offer non-radiative decay channels.

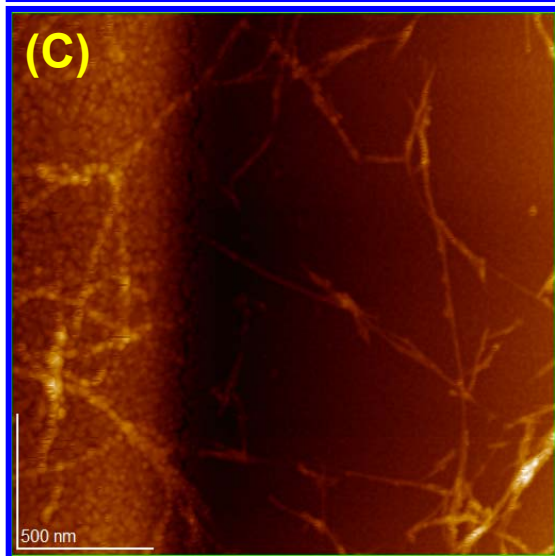
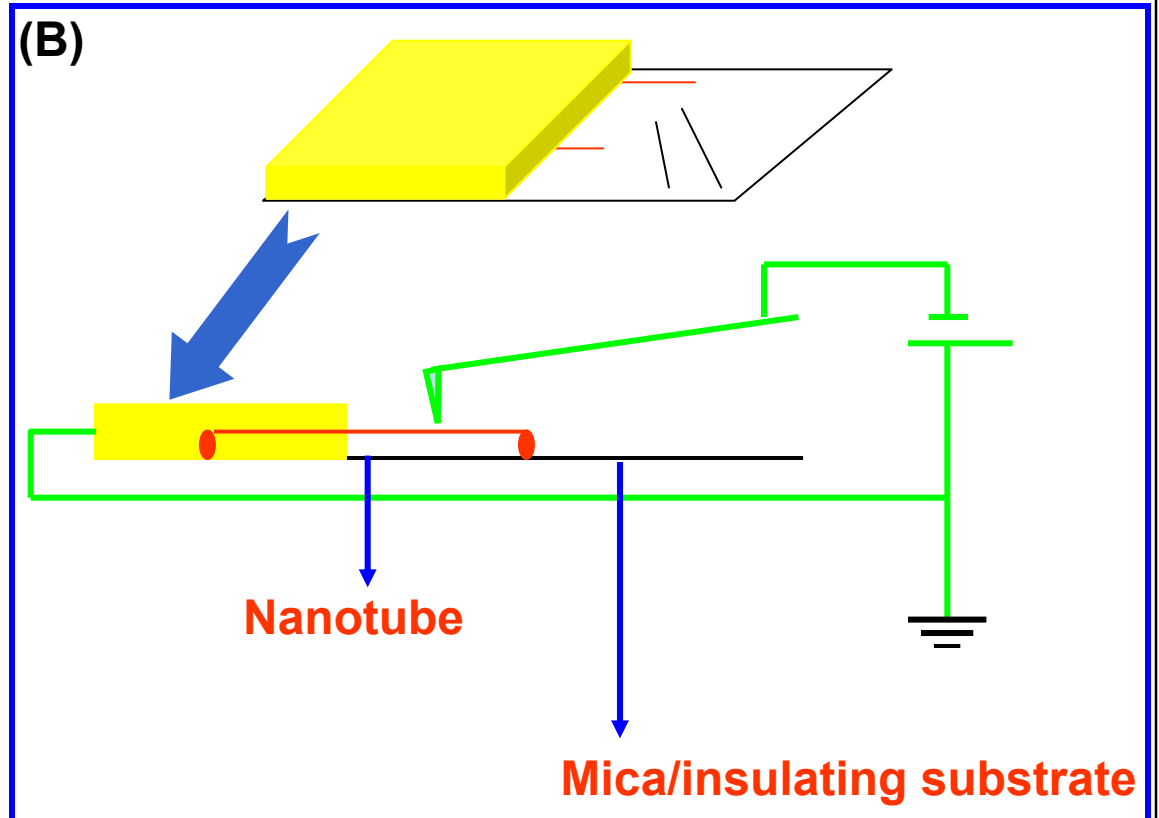
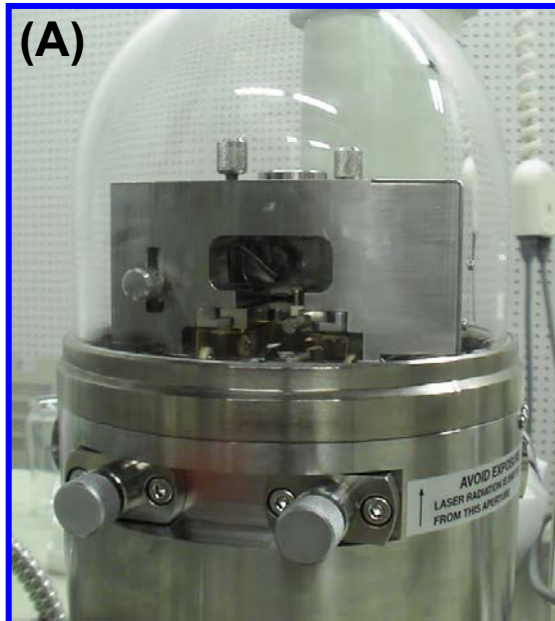
*So what happens to the metallic SWNTs
present in the composite?*

Separation protocol

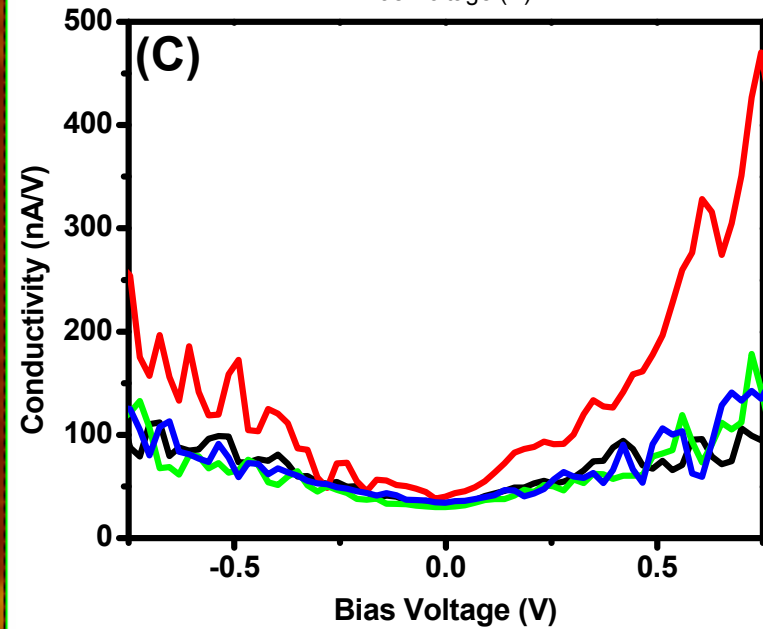
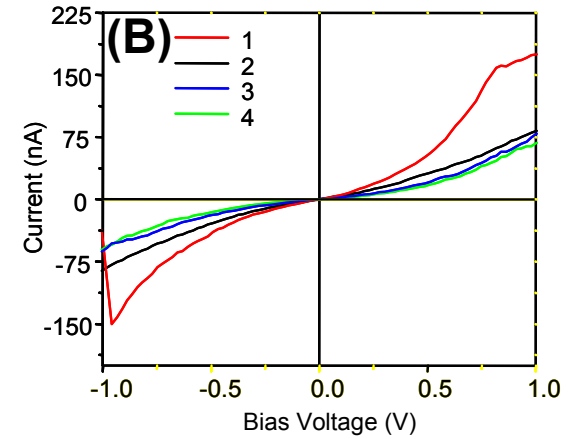
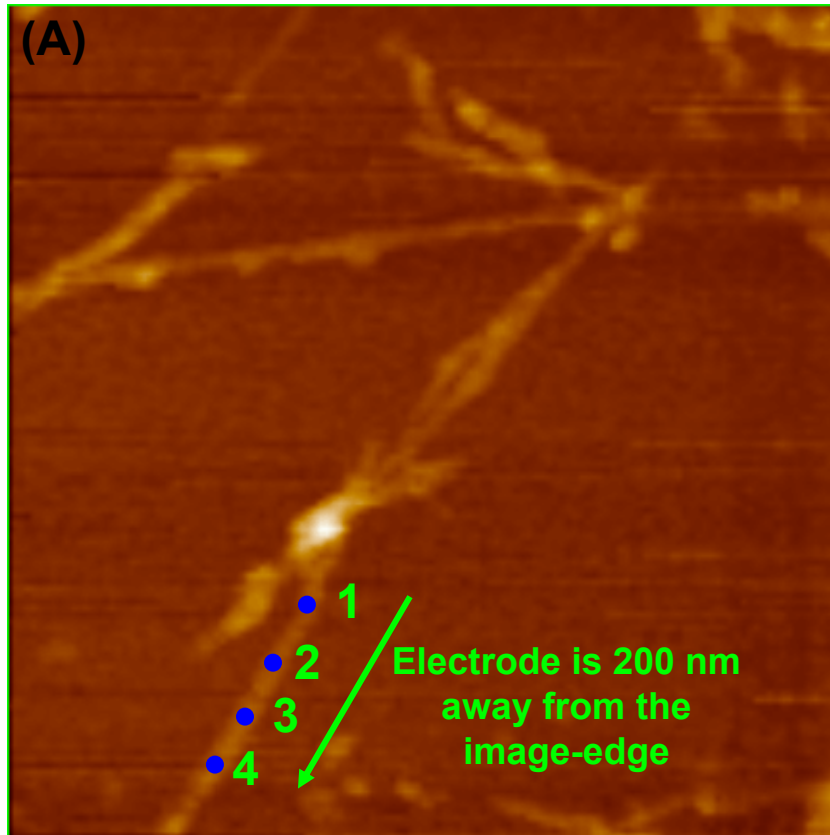


Alkyl amines stabilize metallic SWNT

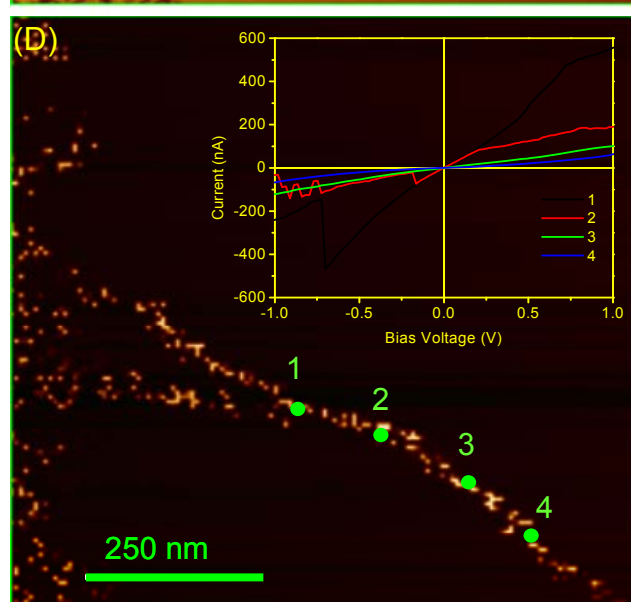
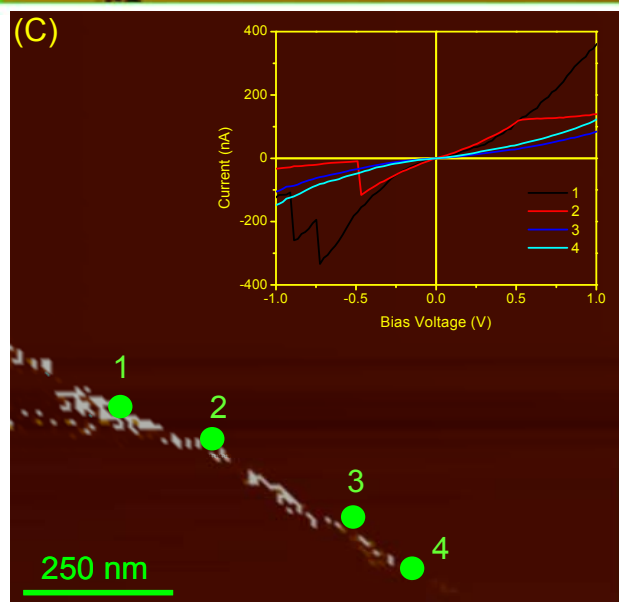
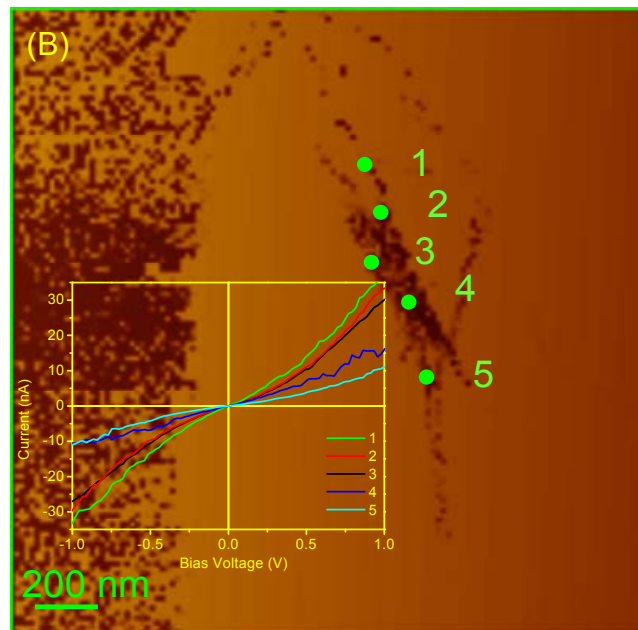
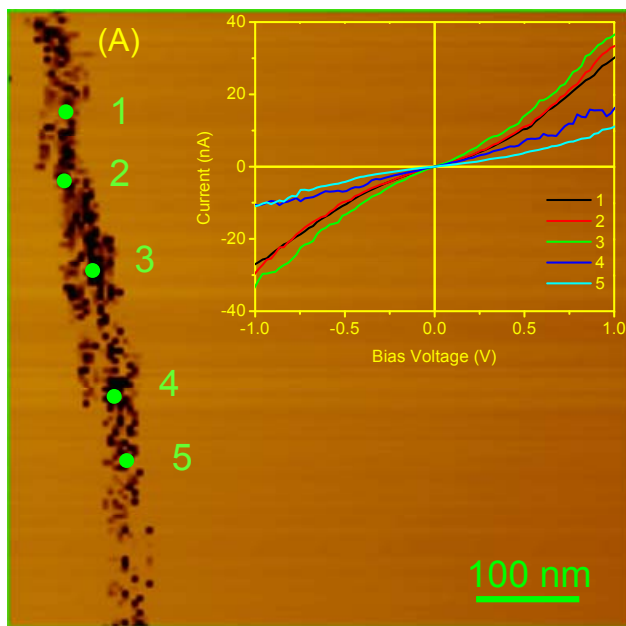
Measurement geometry

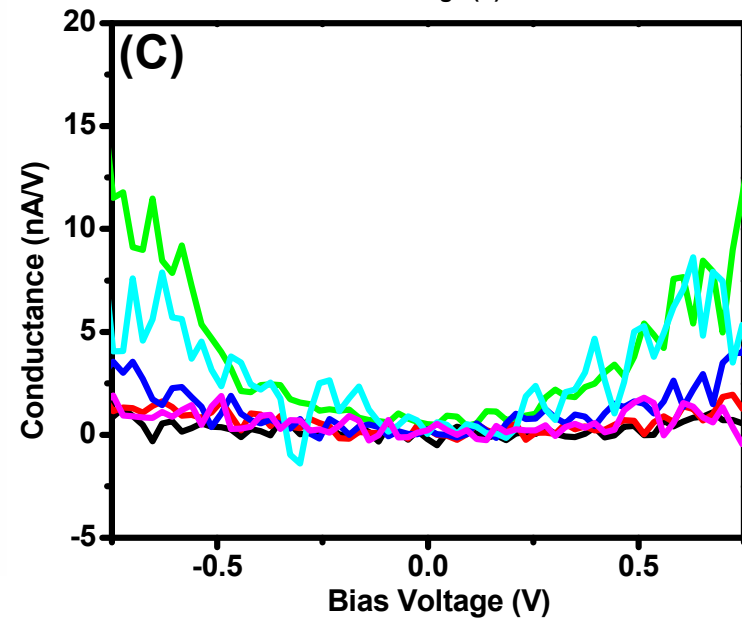
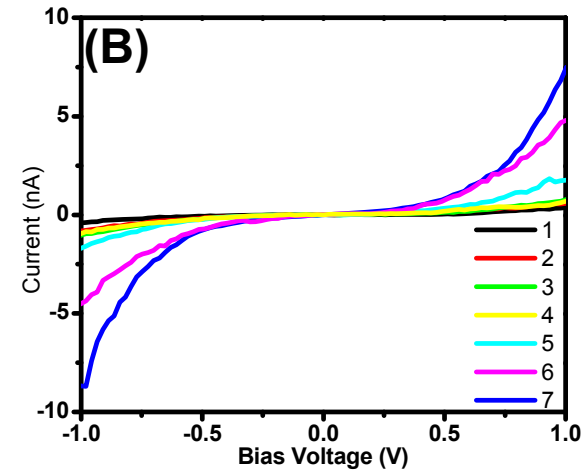
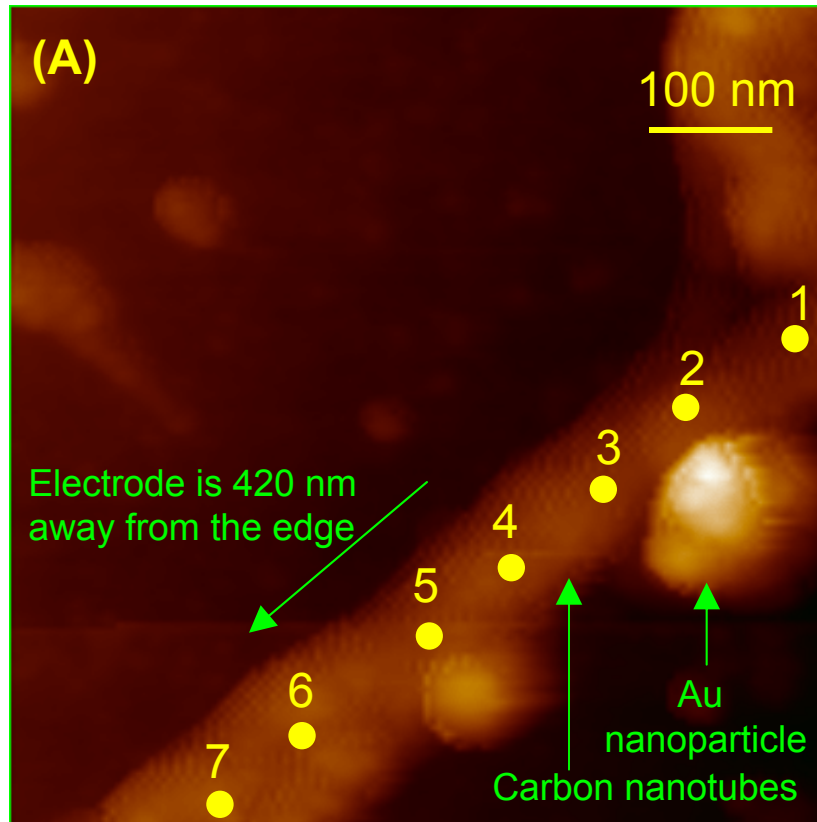


(A) Photograph of the scanning head, (B) schematic of the PCI-AFM measurement and (C) representative AFM image of pristine SWNTs

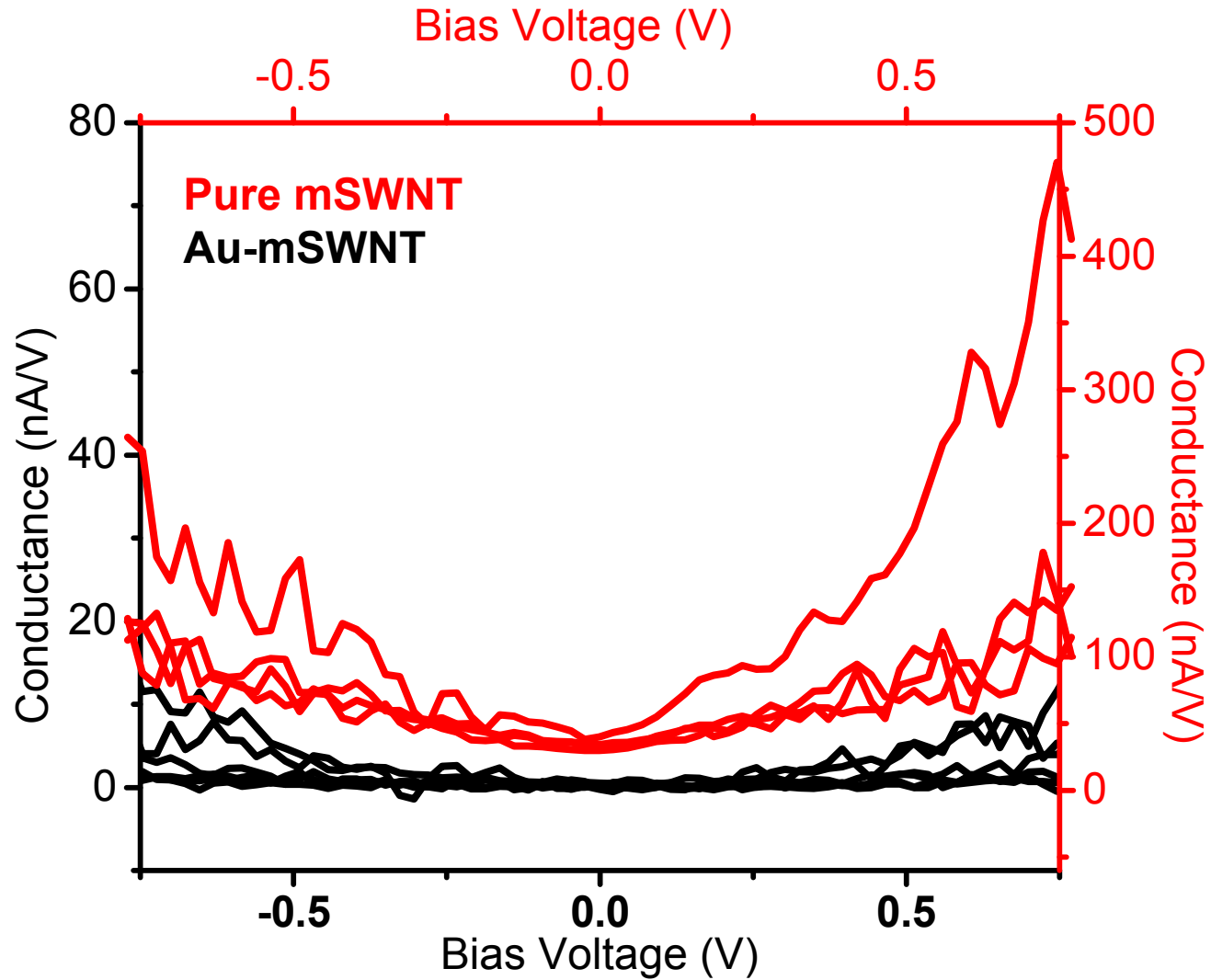


(A) PCI-AFM images of pure mSWNT with (B) I-V curves and (C) plot of conductance versus bias voltage.



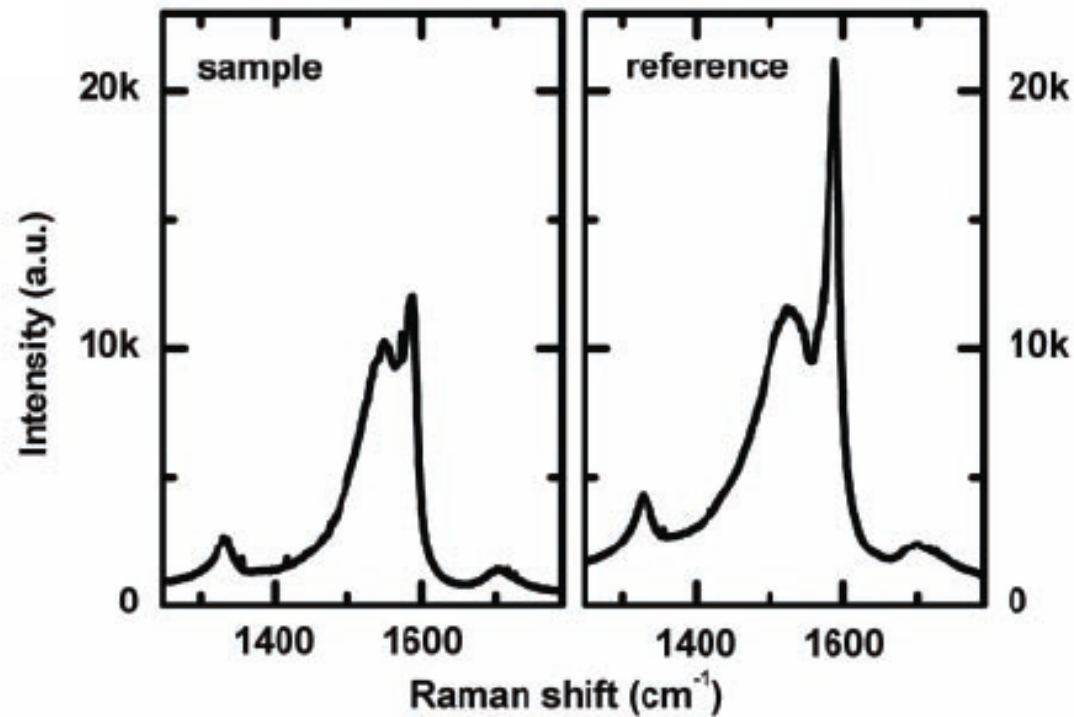


(A) PCI-AFM image of Au-mSWNT with (B) the corresponding I-V curves and (C) Plot of conductance versus bias voltage.



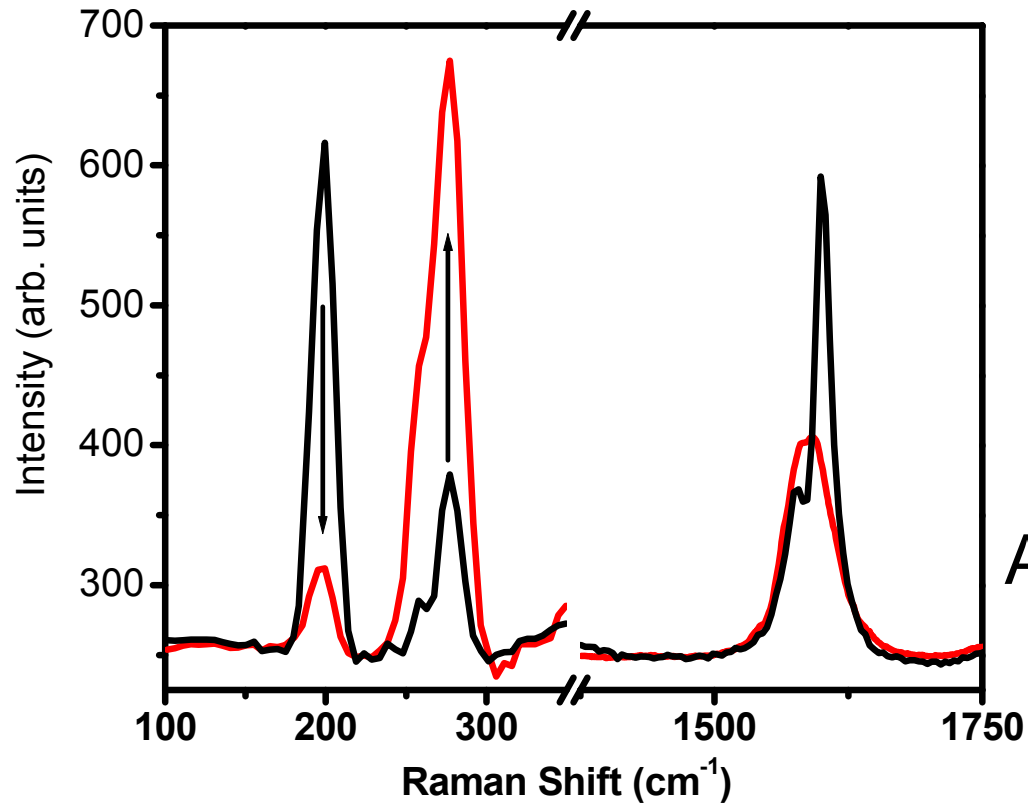
Comparison of conductance versus bias voltage for **pure mSWNT** and Au-mSWNT composite

G-band line shapes of metallic and semiconducting SWNT



Changes observed in G-band for metallic (left) and pristine (right) SWNT

➤ Confocal Raman investigations



$$A_s/A_m = 65.0$$

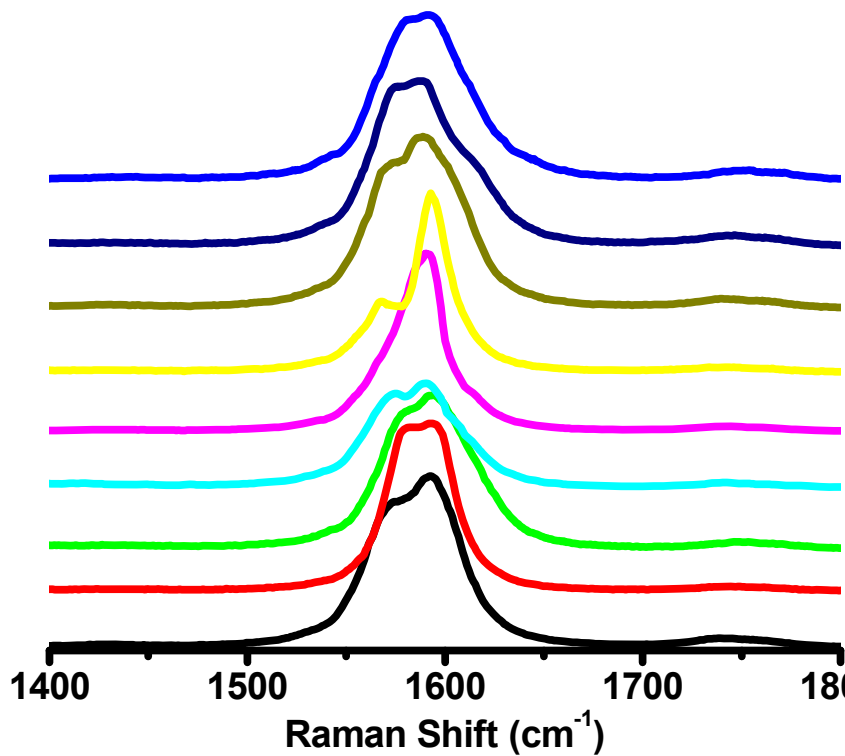
$$A_s/A_m = 0.14$$

Extraction efficiency

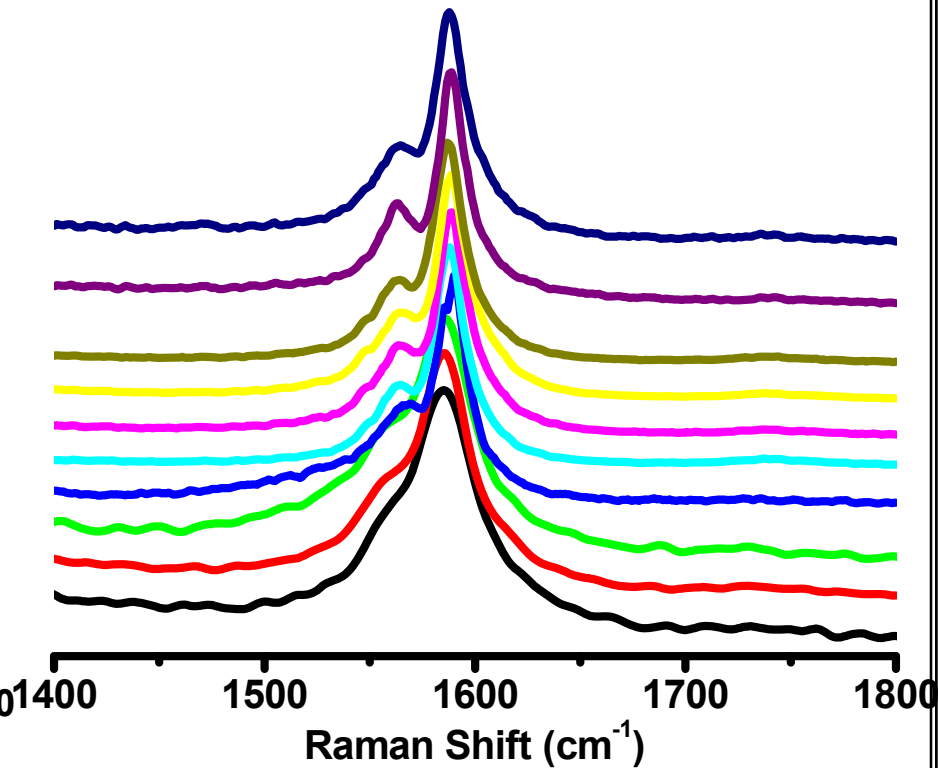
$$A_s/(A_s + A_m) * 100 = 88\%$$

Raman spectra in RBM and G-band regions of pristine SWNT (black) and **extracted mSWNT (red)**.

Pure mSWNT
FWHM = 48 cm^{-1}



Au- mSWNT
FWHM = 22 cm^{-1}



Comparison of G-band of pure mSWNT and Au-mSWNT

What we know:

Metallicity of SWNT is destroyed by interaction with nanoparticles.

PCI-AFM and confocal Raman confirm this M-S transition.

mSWNT fluoresce when their metallicity is destroyed.

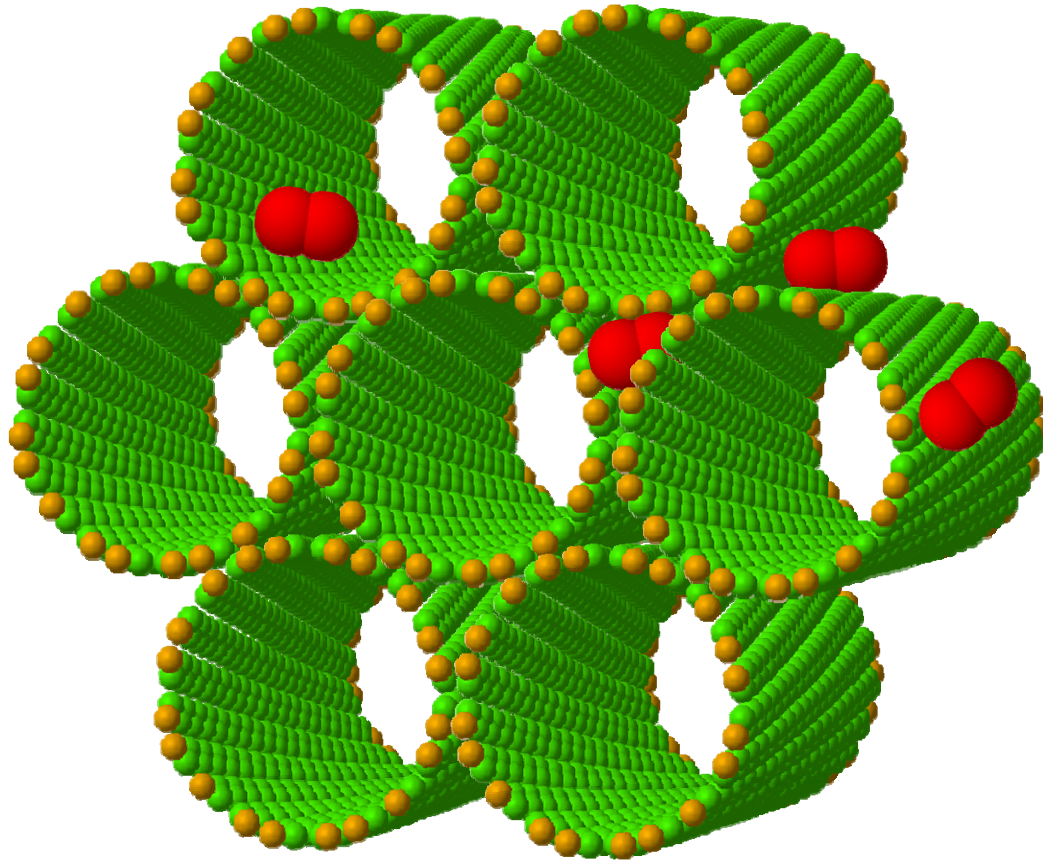
M-S transition has far reaching implication in nanoelectronics and design of nanodevices.

C. Subramaniam et al. Phys. Rev. Lett. (2007)

C. Subramaniam and T. Pradeep Patent applications 2006, 2007

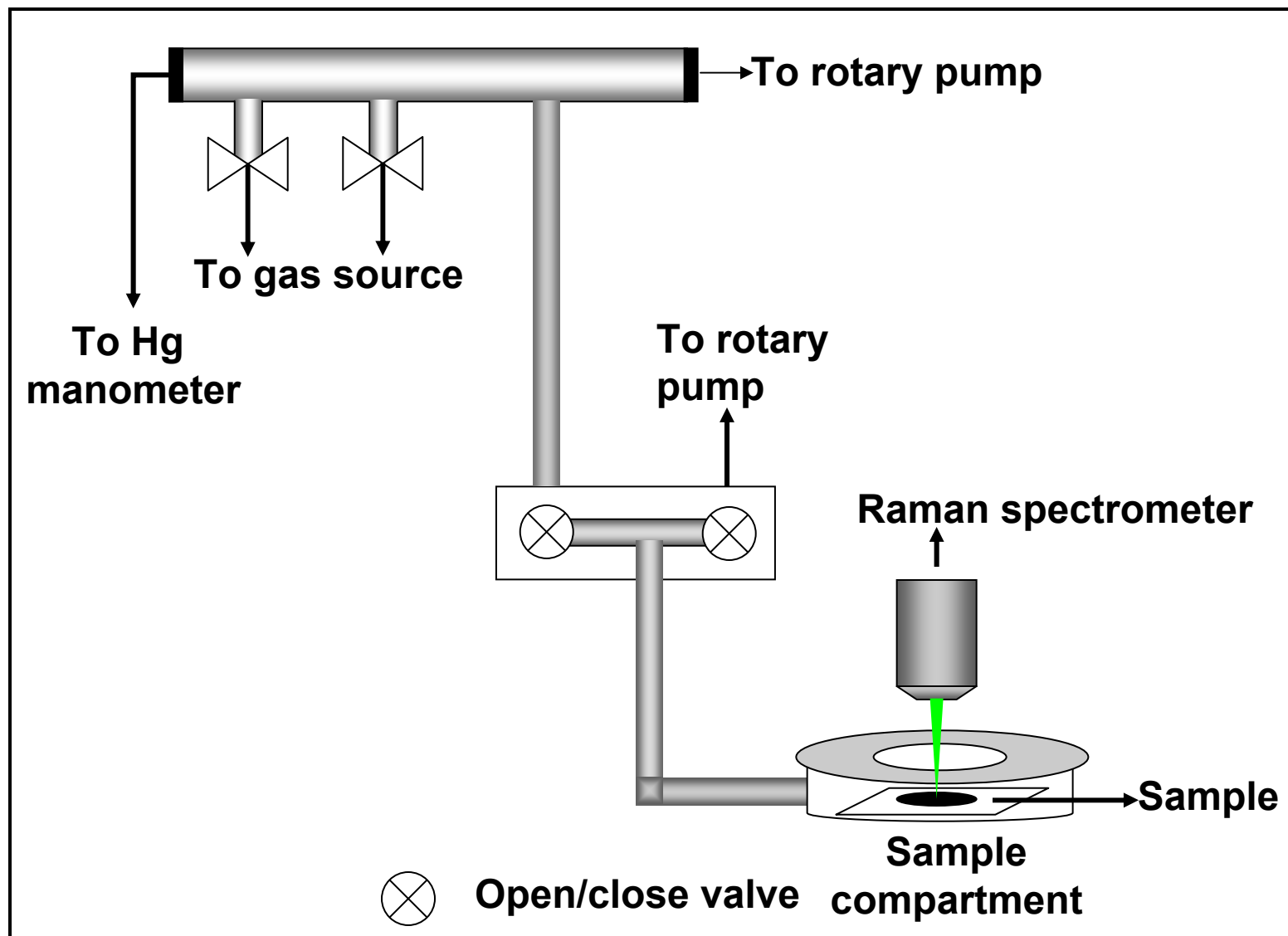
*Nanotube gas sensors using
fluorescence*

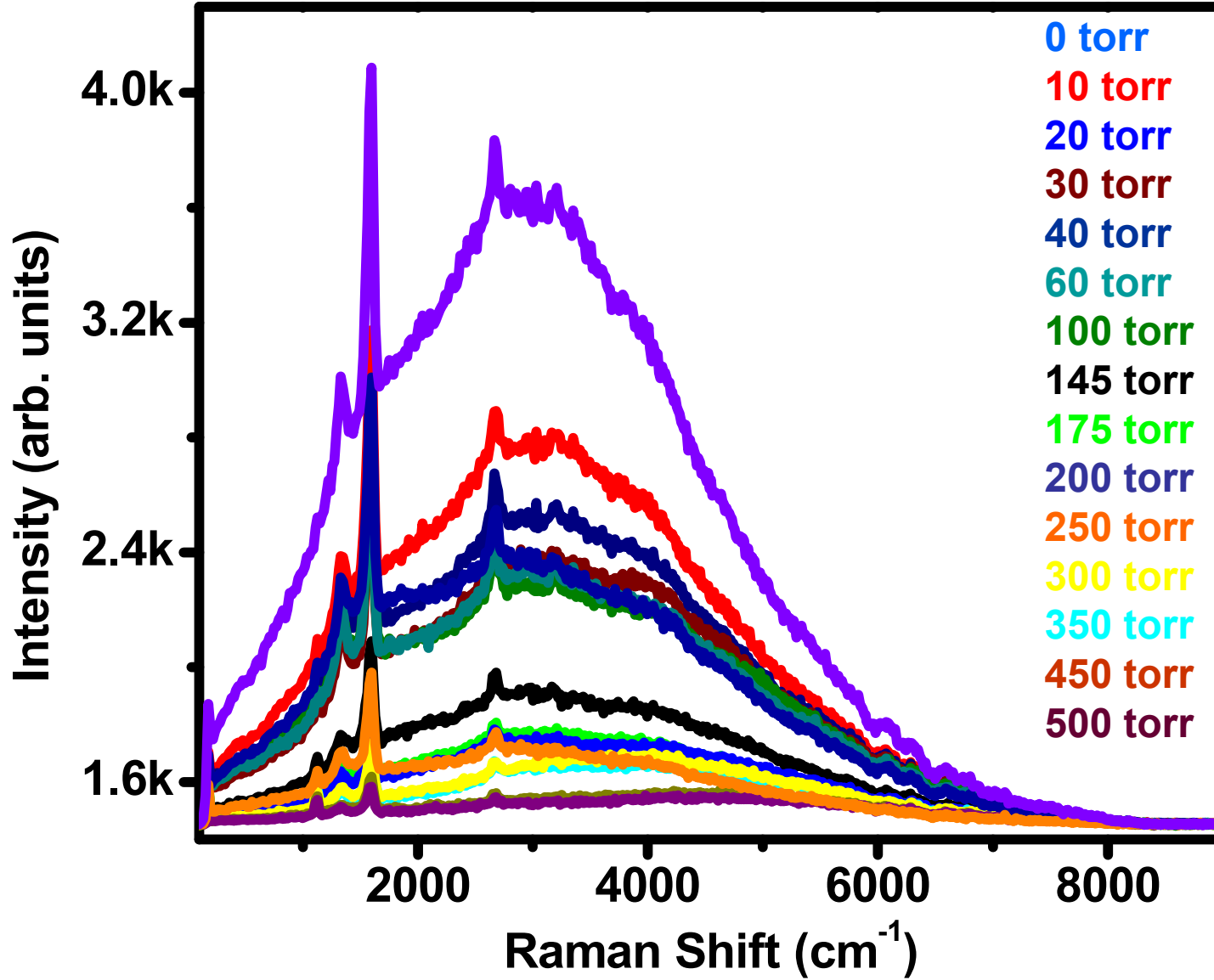
Fluorescence as a probe for studying gas-adsorption behavior



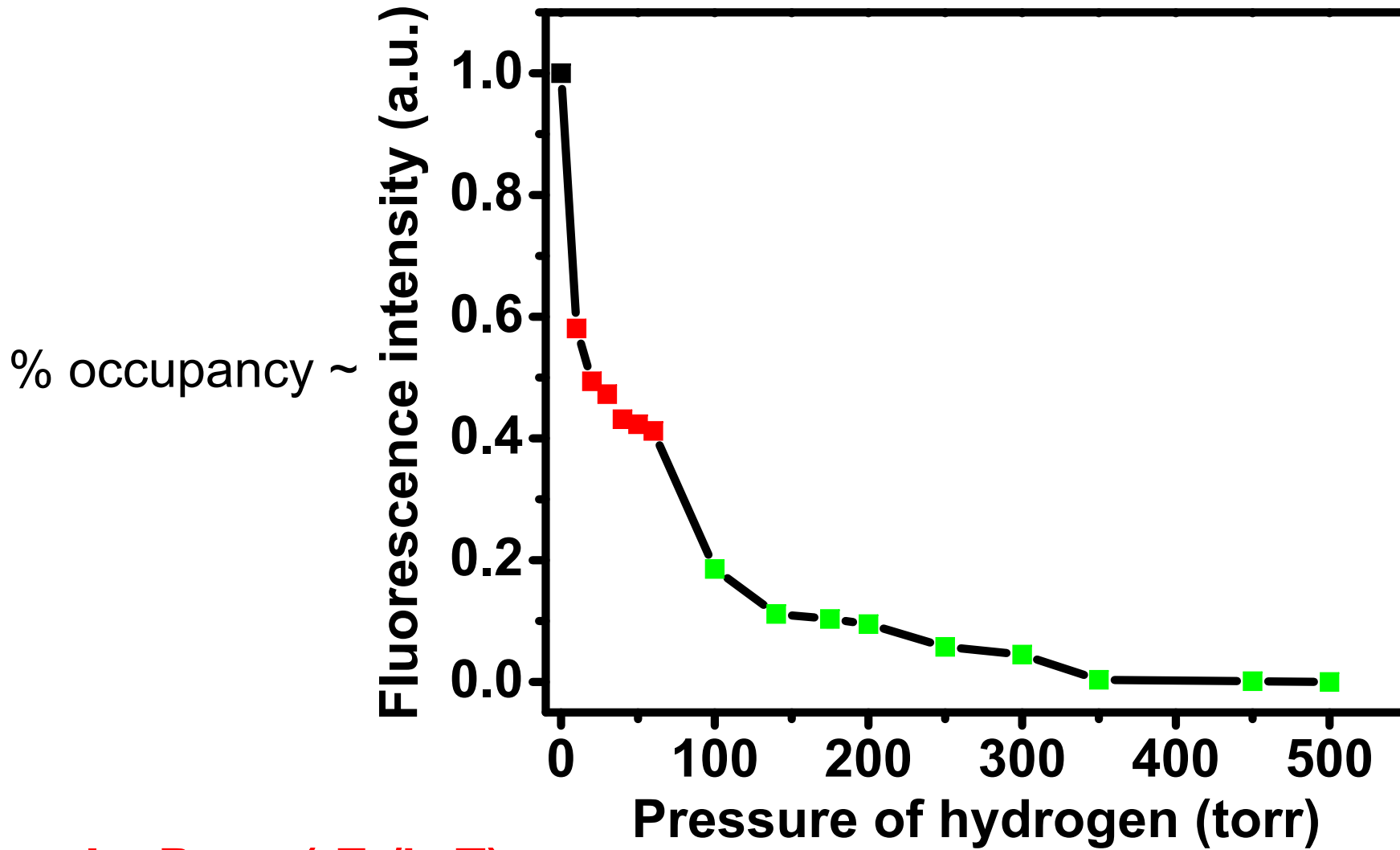
- Endohedral
- Interstitial
- Groove
- External

Instrumentation – Schematic of the gas-setup





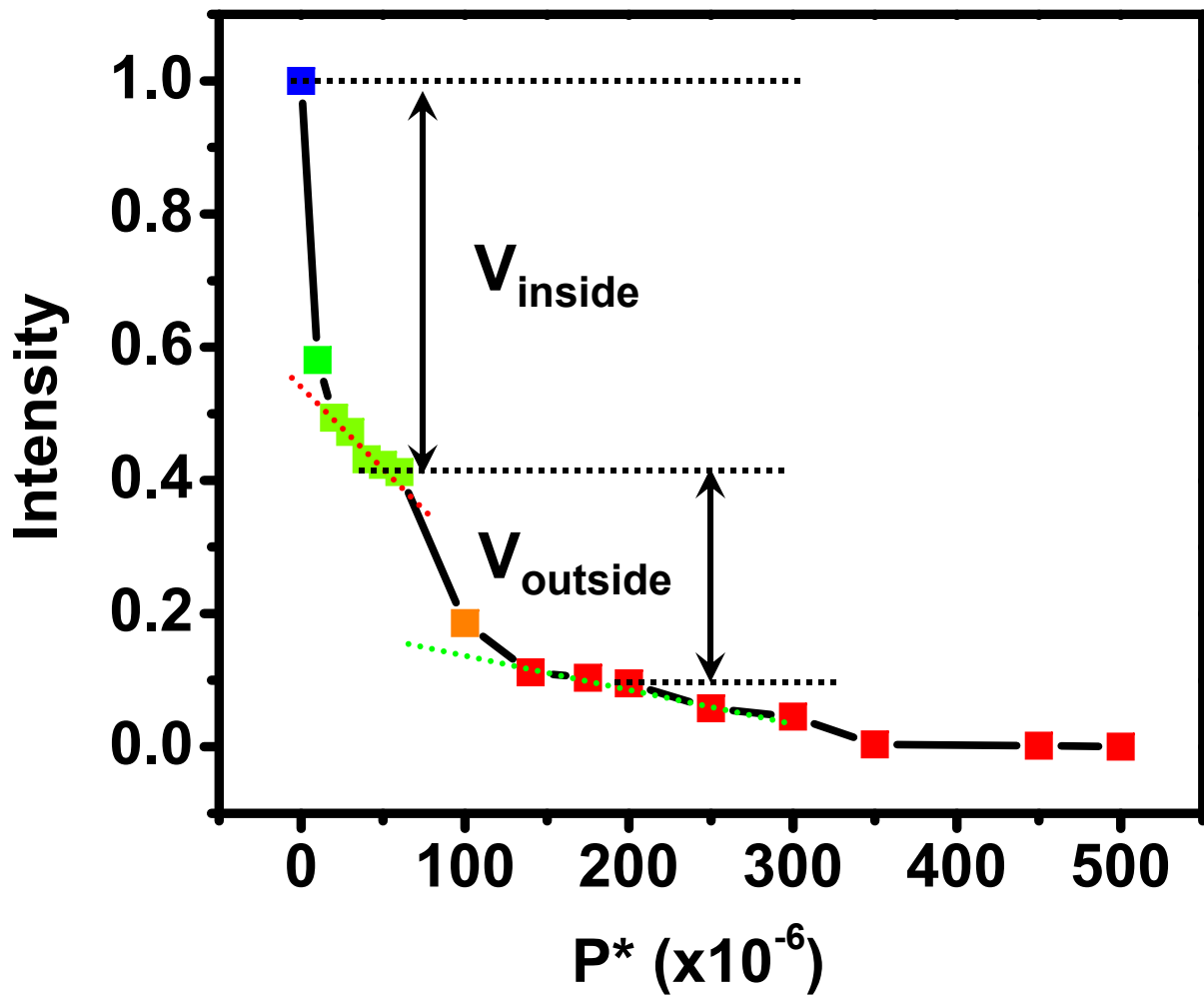
Au-SWNTs exposed to H₂ gas at various partial pressures.



$I = P_0 \exp(-E_a/k_B T)$

Slope, $m \sim E_a(\Delta H)$

Bulk pressure

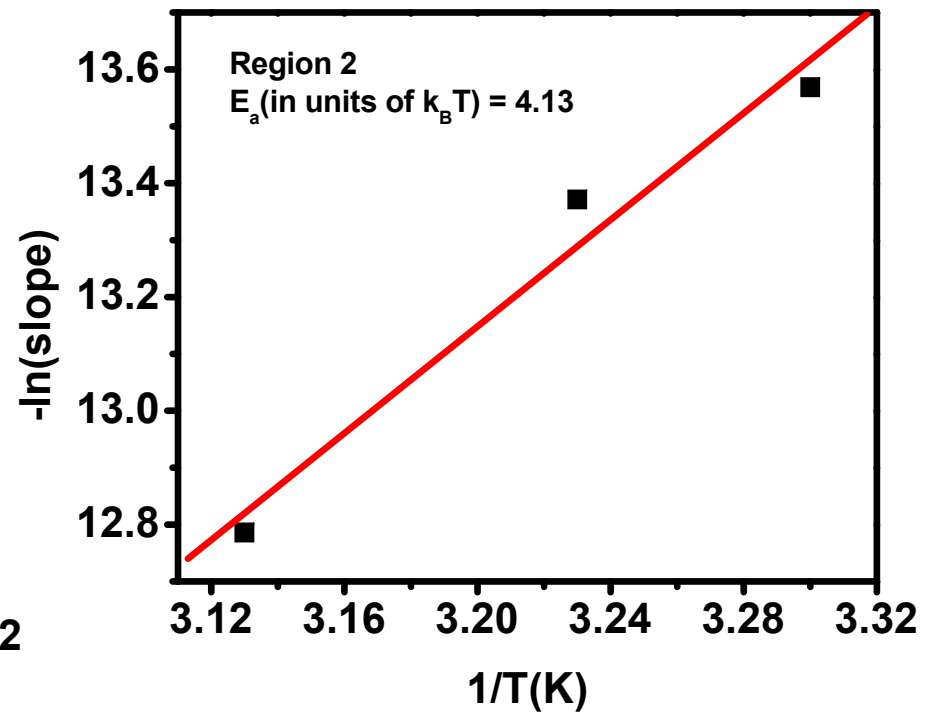
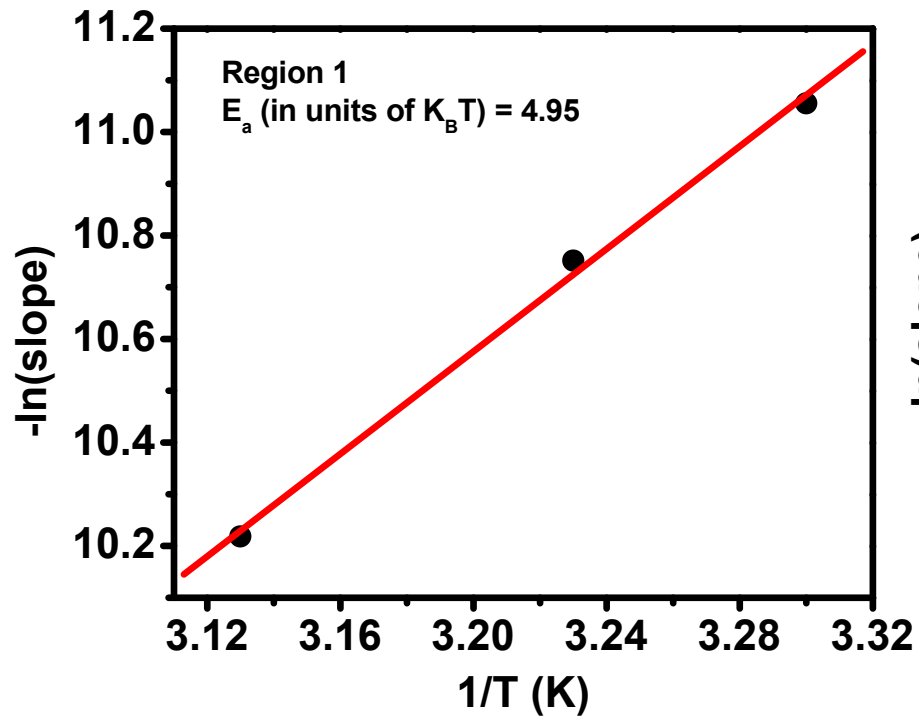


$V_{inside} = 59 \% (60\%)$

$V_{outside} = 32 \% (40\%)$

$m_{inside} = 8.6 (3.0)$

$m_{outside} = 6.9 (2.0)$

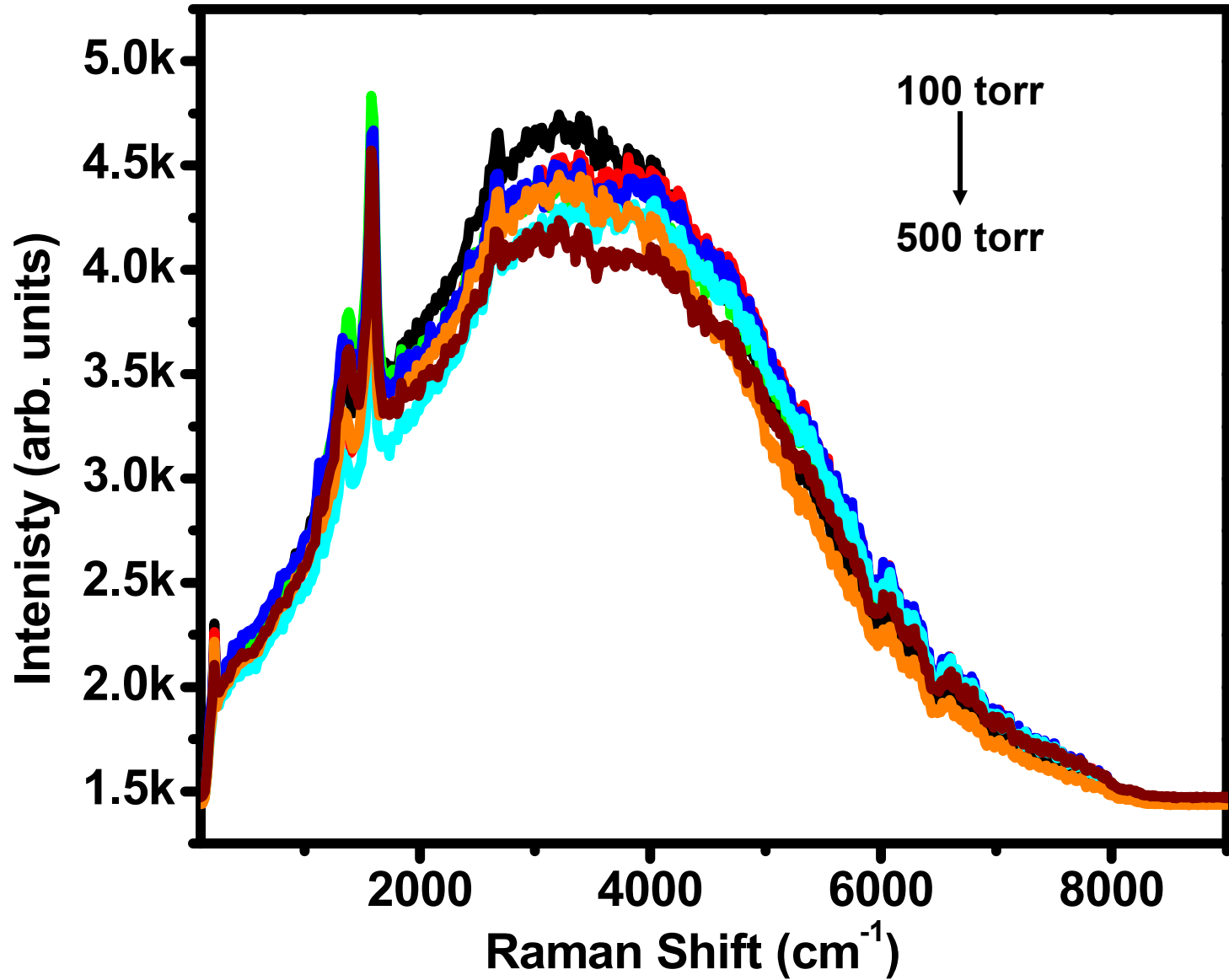


Arrhenius plot of $-\log(k)$ versus $1/T$ for two different regions where,

Region 1 : Interstitial and endohedral sites

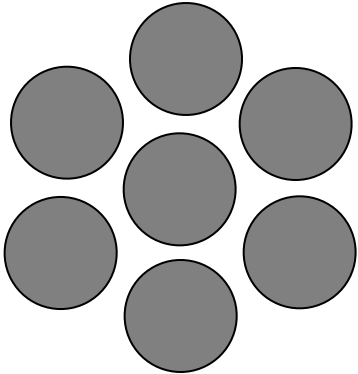
Region 2 : Groove and external sites

The slope, giving the value of E_a is given in the inset.



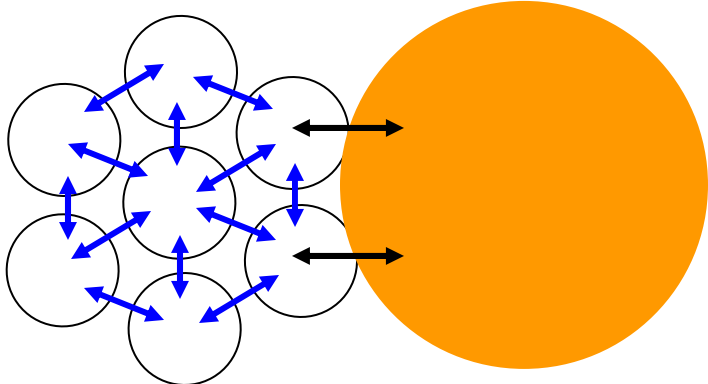
Au-SWNTs exposed to N₂ gas at various partial pressures.

Suggested mechanism



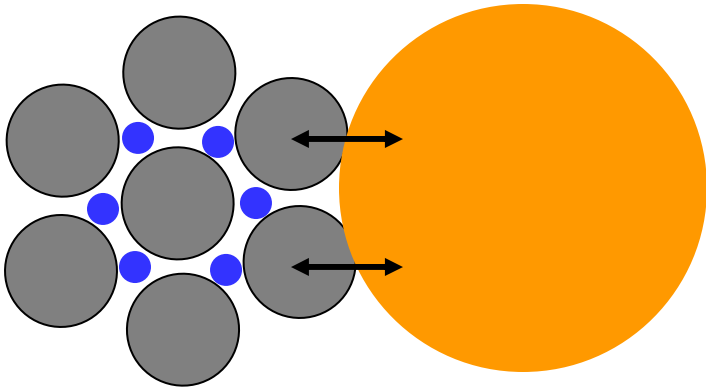
Metallic SWNT bundle

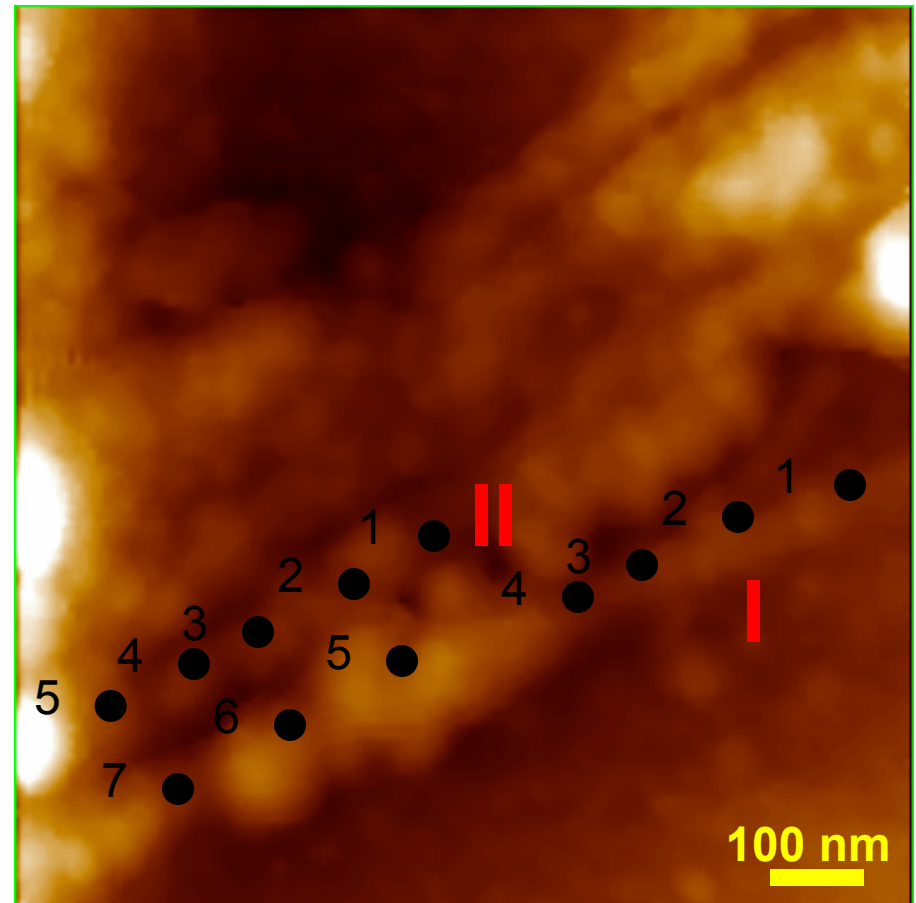
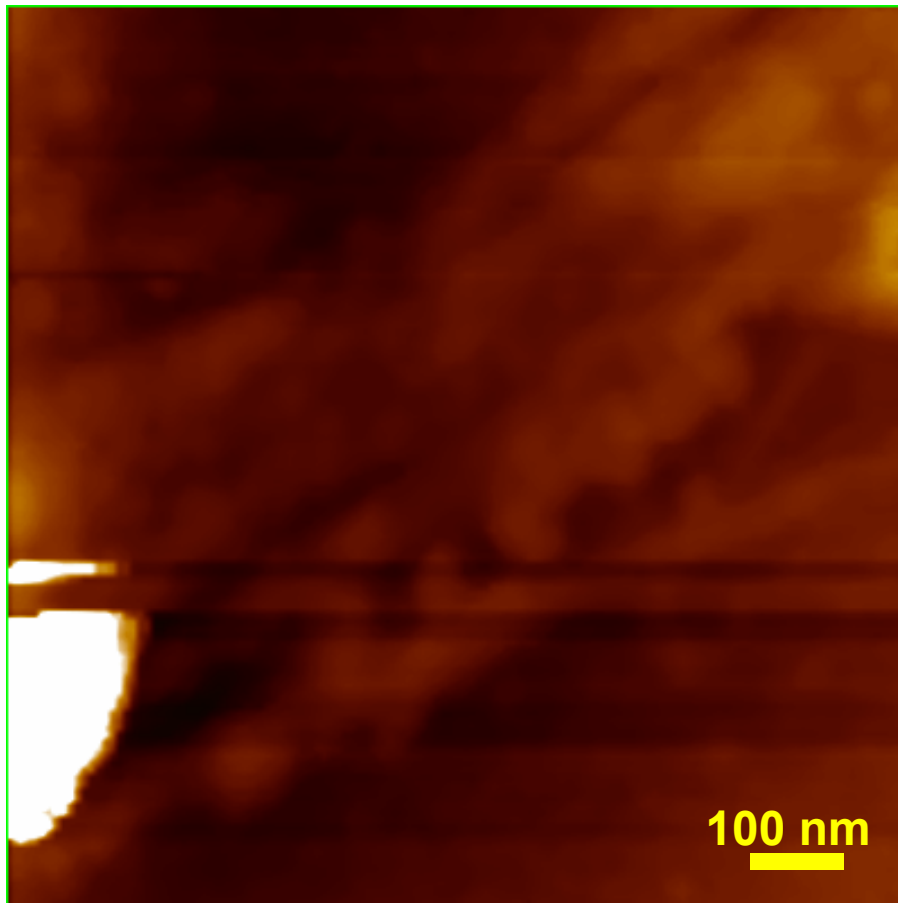
Composite



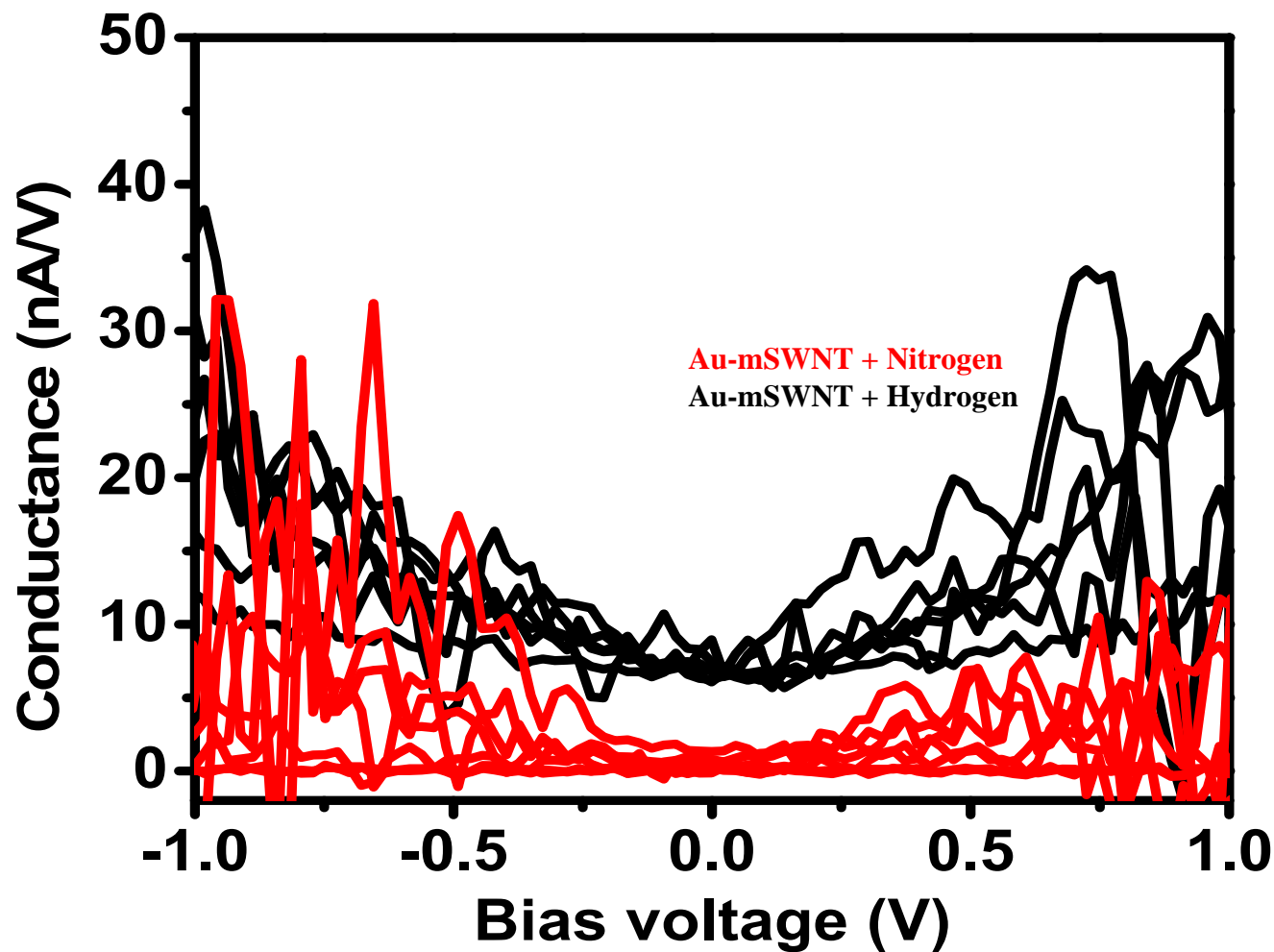
Semiconducting SWNT bundle

H₂/He

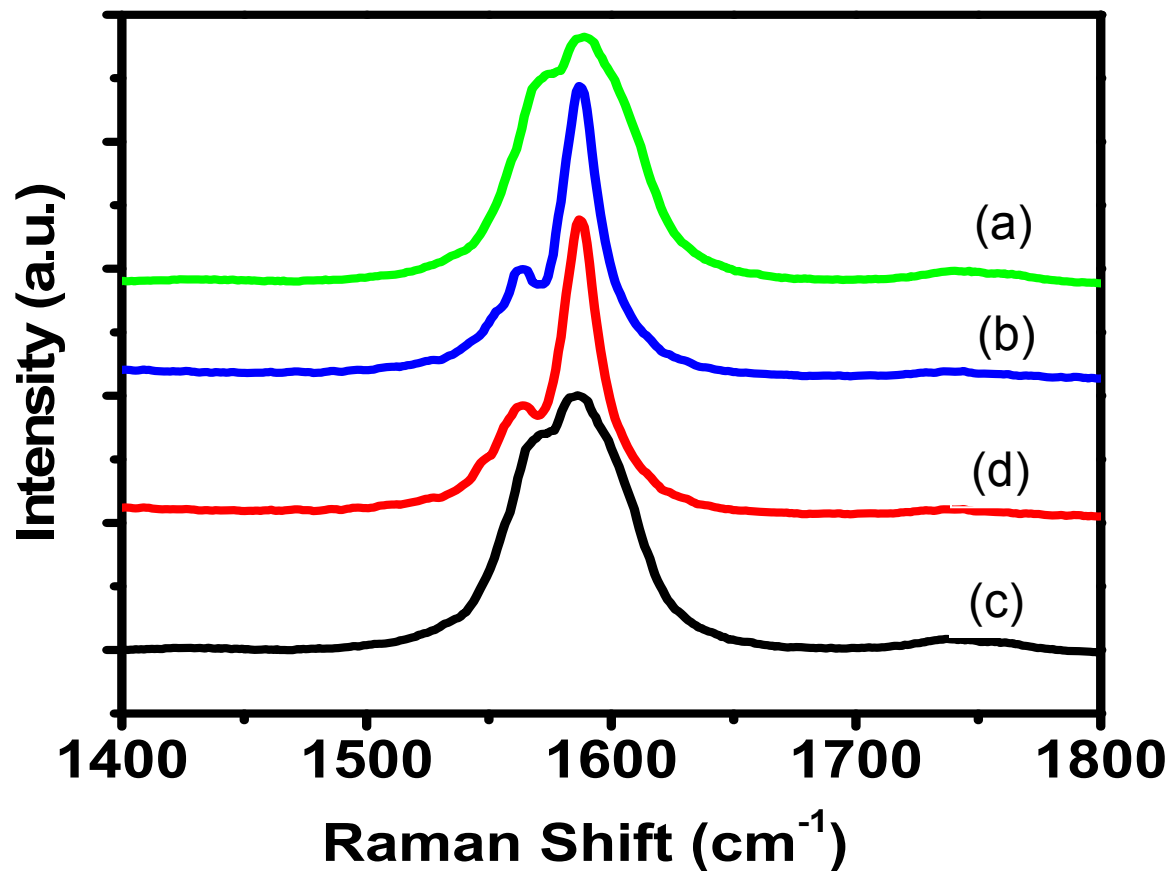




PCI-AFM images of Au-mSWNT composite. The points on the bundles considered for I-V characteristics have been marked, although all other bundles are also characterized.



Plot of conductance versus bias voltage constructed at various point of Figure 1A, under an atmosphere of nitrogen (red traces) and hydrogen (black traces).



Raman spectra of (a) purified mSWNTs, (b) Au-mSWNT composite, (c) Au-mSWNT upon exposure to 500 torr H_2 and (d) Au-mSWNT composite after pumping out H_2 exposed in (c). Spectra (a) to (d) are recorded at the same point on the composite sample.

Conclusions and future directions

Gas adsorption inside SWNT was studied using visible fluorescence from Au-SWNTs composite

Behavior was similar in case of Ag-SWNT and AuNR-SWNT composites.

In-situ gas storage detection

Observation of different adsorption sites

Gas separation

Understanding gas storage inside SWNTs

Probing electronic structure variation upon gas adsorption

Possibilities of isomer separation



IIT Madras

Thank you all